

7

**Anaesthetic effects in thalamocortical neurons**

by

Craig Robert Ries

MD, The University of Western Ontario, 1979  
FRCPC, Royal College of Physicians and Surgeons of Canada, 1986

A THESIS SUBMITTED IN PARTIAL FULFILLMENT OF

THE REQUIREMENTS FOR THE DEGREE OF

DOCTOR OF PHILOSOPHY

in

THE FACULTY OF GRADUATE STUDIES

(Department of Pharmacology and Therapeutics)

We accept this thesis as conforming to the required standard

THE UNIVERSITY OF BRITISH COLUMBIA

April 1997

© Craig Robert Ries, 1997

In presenting this thesis in partial fulfilment of the requirements for an advanced degree at the University of British Columbia, I agree that the Library shall make it freely available for reference and study. I further agree that permission for extensive copying of this thesis for scholarly purposes may be granted by the head of my department or by his or her representatives. It is understood that copying or publication of this thesis for financial gain shall not be allowed without my written permission.

Department of Pharmacologie Therapeutique

The University of British Columbia  
Vancouver, Canada

Date 28 April 1997

## ABSTRACT

The perturbation that is responsible for the anaesthetic-induced unconscious state remains undefined because of an incomplete understanding of awareness and the non-specific nature of anaesthetic actions. Recent investigations into sleep mechanisms show that thalamocortical neurons prevent throughput-gating of sensory information to the cerebral cortex, yet orchestrate oscillating cortical activity as part of consciousness. Extrinsic neuromodulation of membrane potential and intrinsic voltage-dependent firing patterns regulate this gating during wakefulness and sleep. The objective was to determine the effects of inhalational anaesthetics on intrinsic firing activities of thalamocortical neurons.

Investigations were carried out on ventrobasal neurons from thalamic brain slices of juvenile rats. The whole-cell patch-clamp method was used with current-clamp and voltage-clamp recording techniques. Aqueous applications of the inhalational anaesthetic, isoflurane (IFL), were studied in detail at 22°C to determine concentration-response relations, to approximate *in vivo* potencies at 31°C, to compare effects of IFL with halothane and enflurane, and to assess the universality of anaesthetic action in thalamic neurons.

IFL inhibited evoked tonic firing of action potentials (wakefulness mode) by increasing membrane conductance and inducing hyperpolarization in a reversible and concentration-dependent manner. IFL, halothane and enflurane were equipotent in producing similar effects, whereas IFL concentrations, that were proportionate to *in vivo* concentrations, increased conductance by 15-30%. Despite the hyperpolarization, IFL also suppressed burst firing (sleep mode). The inhibition of firing was mainly due to a shunt, as the increased conductance "short-circuited" the effectiveness of DC current injections which thereby reduced the spatial distribution of voltage responses. The increased conductance was direct (postsynaptic) and voltage-independent, reversing near the calculated equilibrium potential for K<sup>+</sup>. The IFL-induced conductance increase was dependent on the external [K<sup>+</sup>] and was suppressed by either external Ba<sup>2+</sup> or internal Cs<sup>+</sup> applications.

In summary, IFL inhibited thalamic relay neuron excitabilities by increasing a  $K^+$  leak conductance. Together with the thalamic roles in consciousness of cortical gateway and orchestrator, suppression of the activities of thalamocortical neurons may be critically important to the production of *in vivo* anaesthesia.

## TABLE OF CONTENTS

Abstract	ii
Table of Contents	iv
List of Figures	vii
Acknowledgements	ix
<b>1 Introduction</b>	<b>1</b>
1.1 Overview: the enigma of anaesthesia	1
1.2 What is anaesthesia?	2
1.2.1 Functional relevance of <i>in vivo</i> anaesthetic action	2
1.2.2 Spinal anaesthetic actions inhibit motor responses to noxious stimuli	4
1.2.3 Do general anaesthetics cause unconsciousness?	7
1.2.4 Auditory evoked potentials and anaesthetics	9
1.3 Consciousness: current views	10
1.3.1 Temporal mechanisms	10
1.3.2 Synchronized 40-Hz thalamocortical oscillations	11
1.4 Role of thalamus in consciousness and altered states of consciousness	12
1.4.1 Changing concepts of the brainstem's role in awareness and arousal	12
1.4.2 The gateway to our external and internal worlds	13
1.4.3 Slow thalamic oscillations in sleep and absence epilepsy	14
1.4.4 State-dependent firing properties are intrinsic to thalamic relay neurons	15
1.5 Evidence for a thalamic role in anaesthetic action?	16
1.5.1 A unified theory of state control	16
1.5.2 Investigation of central processing in <i>in vivo</i> anaesthesia	16
1.5.3 Anaesthetics are associated with EEG spindle and burst activity in the thalamus	17
1.5.4 Anaesthetics depress thalamic relay transmission	19
1.6 Objective and questions	20

<b>2 Methods</b>	<b>22</b>
2.1 Rat thalamic slice preparation	22
2.2 Whole-cell recording	23
2.3 Solutions, ionic channel antagonists and junction potentials	24
2.4 Volatile anaesthetic preparation	26
2.5 Experiments at a more <i>in vivo</i> relevant temperature	28
2.6 Statistical analysis	29
<b>3 Results</b>	<b>31</b>
3.1 Thalamocortical neurons	31
3.1.1 Experimental database	31
3.1.2 Electrophysiological firing properties	31
3.2 Inhibitory action of IFL at 22°C and 31°C	34
3.2.1 IFL hyperpolarized the membrane potential characteristic of wakefulness	34
3.2.2 IFL decreased input resistance, shunting current inputs and reducing the membrane time constant	36
3.2.3 The inhibitory effect of IFL was direct	37
3.2.4 The inhibitory effect of IFL was concentration-dependent	40
3.2.5 Temperature influence on IFL-induced inhibition	43
3.2.6 Analysis of IFL's inhibitory action	44
3.3 IFL and firing properties at 22°C and 31°C	46
3.3.1 IFL prevented the firing modes characteristic of wakefulness and sleep	46
3.3.2 IFL shunted tonic Na <sup>+</sup> -spike electrogenesis	49
3.3.3 IFL suppressed low-threshold Ca <sup>2+</sup> -spike electrogenesis	54
3.3.4 IFL suppressed depolarizing afterpotentials and high-threshold spikes	57
3.3.5 Analysis of IFL actions	60
3.4 Ionic basis of IFL-induced inhibition	62
3.4.1 IFL elicited an outward current at membrane potentials characteristic of the tonic firing mode	62
3.4.2 The principal ion of the IFL-evoked current was K <sup>+</sup>	64
3.4.3 The IFL-induced outward current became inward at potentials consistently positive to E <sub>K</sub>	66
3.4.4 IFL increased steady-state conductance through nongated "leak" channels	71
3.4.5 IFL decreased inward rectification	76
3.4.6 IFL did not increase steady-state conductance through the ATP-sensitive K <sup>+</sup> channel that is suppressed by glibenclamide	79
3.4.7 IFL's effect on non-spiking cells was consistent with leakage of K <sup>+</sup> from spiking cells	81
3.4.8 Analysis of IFL-induced increase in K <sup>+</sup> conductance	84

	vi
3.5 Mechanism of IFL-induced burst suppression	85
3.5.1 IFL-induced burst suppression appeared related to a dendritic shunt	85
3.5.2 IFL suppressed T-current by changing the spatial distribution of imposed voltages	90
3.5.3 IFL-induced spatial block of T-window current did not affect $E_{IFL}$	95
3.5.4 Analysis of IFL-induced burst suppression	95
3.6 Other inhalation anaesthetics	98
4 Discussion	100
4.1 Summary of results	100
4.2 Comparison with other studies	101
4.2.1 $K^+$ -mediated anaesthetic-induced inhibition	101
4.2.2 Anaesthetic reduction of $Ca^{2+}$ -current	104
4.3 Functional significance	105
4.3.1 Reconciling <i>in vitro</i> experimentation and <i>in vivo</i> MAC values	105
4.3.2 Anaesthetic-induced thalamic shunt	105
Nomenclature	107
Bibliography	108

## LIST OF FIGURES

Fig. 1. Voltage-gated firing modes of wakefulness and sleep	33
Fig. 2. Inhibitory effect of isoflurane (IFL) on thalamic relay neurons	35
Fig. 3. Effect of IFL on passive membrane properties	38
Fig. 4. Direct action by IFL	39
Fig. 5. Concentration-dependent effect of IFL	42
Fig. 6. Effect of IFL on conductance at 31 °C	45
Fig. 7. Effect of IFL-induced hyperpolarization on firing modes	47
Fig. 8. Effect of IFL-induced shunt on firing modes	48
Fig. 9. Effect of IFL on repetitive tonic firing	50
Fig. 10. Effect of IFL on repolarization during repetitive tonic firing	51
Fig. 11. Effect of IFL on tonic firing at 31 °C	53
Fig. 12. Effect of IFL on rebound LTS: de-inactivation of the underlying T-current	55
Fig. 13. Effect of IFL on burst firing: time-dependent aspects	56
Fig. 14. Effect of IFL on burst firing at 31 °C	58
Fig. 15. Effect of IFL on postspike depolarizing afterpotentials (DAPs)	59
Fig. 16. Effect of IFL on high-threshold $\text{Ca}^{2+}$ -spike (HTS) electrogenesis	61
Fig. 17. Effect of IFL on steady-state currents	63
Fig. 18. Effect of changes in the extracellular concentration of potassium on $E_{\text{IFL}}$	65
Fig. 19. Concentration-dependent effect of IFL	67
Fig. 20. $E_{\text{baclofen}}$ as a biological assay for $E_{\text{K}}$	69
Fig. 21. $E_{\text{tacrine}}$ as a biological assay for $E_{\text{K}}$	70
Fig. 22. Voltage-dependent gating of $\text{K}^{+}$ -mediated inward rectification and $E_{\text{K}}$	72
Fig. 23. Effect of barium on IFL-induced current	73
Fig. 24. Effect of internal $\text{Cs}^{+}$ on $E_{\text{IFL}}$	74
Fig. 25. Effect of resting membrane potential on $E_{\text{IFL}}$	77
Fig. 26. Effect of IFL on inward rectification	78
Fig. 27. Effect of IFL on steady-state conductance during blockade of inward rectification	80
Fig. 28. Effect of IFL on non-spiking cells	82

Fig. 29. Effect of Cs <sup>+</sup> on IFL-induced current in non-spiking cells	83
Fig. 30. Effect of IFL on LTS in an acutely "dissociated" neuron	87
Fig. 31. Effect of IFL washin and washout on leak conductance and T-current	89
Fig. 32. Effect of IFL on voltage-dependence of T-current activation	91
Fig. 33. Effect of IFL on steady-state T-current inactivation	92
Fig. 34. Effect of IFL on recovery from T-current inactivation	94
Fig. 35. Effect of IFL on T-current in the presence of internal Cs <sup>+</sup>	96
Fig. 36. Effect of blocking T-window current on E <sub>IFL</sub>	97

## ACKNOWLEDGEMENTS

The Canadian Anaesthetists' Society with Janssen Pharmaceutica (Dr. Paul Janssen Canadian Research Fellowship in Anaesthesia), the Medical Research Council of Canada (Fellowship) and the Department of Anaesthesia of The University of British Columbia provided financial support.

Drs. Ernie Puil (Departments of Pharmacology & Therapeutics and Anaesthesia), Bernie MacLeod (Departments of Anaesthesia and Pharmacology & Therapeutics), Robert Miura (Departments of Mathematics and Pharmacology & Therapeutics) and Michael Walker (Department of Pharmacology & Therapeutics) supervised this thesis.

Mr. Lance Corey contributed computer support which included design of the leak subtraction software. Mr. Christian Caritey built various components of the recording setup.

## 1 INTRODUCTION

### 1.1 Overview: the enigma of anaesthesia

Although the revolutionary nature of inhalational anaesthetics in permitting surgery has long passed since the first public demonstration of ether (Oct 16, 1846), the mechanism of anaesthesia remains uncertain. This uncertainty is compounded by a difficulty in describing the state of anaesthesia in scientific terms. In addition, the lack of conscious experience and perception during anaesthesia makes it an obscure concept that is remote from day to day experiences. The result is illustrated by the following clinical and scientific paradoxes. Because clinical anaesthesia permits the injury of surgery to occur, the "miracle" of anaesthesia and the injurious aspects of surgery are ignored in the astonishing claim that surgery heals (Fox 1992). And, in scientific investigations of sensory processing in animals where anaesthetics again permit invasive procedures, the impact of anaesthesia on brain function is sometimes overlooked.

Research into anaesthetic action is important not only because of what these drugs permit, but because of their potential for significant adverse outcomes. Anaesthetics are among medicine's most dangerous drugs since the ratio of the median lethal dose to the median effective dose ( $ED_{50}$ ) is small (Wolfson *et al.* 1978). Therefore, the principal factor that determines the clinical utility of an anaesthetic is the incidence of adverse effects. In fact, an assessment of hemodynamic control is used to determine the adequacy of anaesthesia since an appropriate monitor for the depression of brain activity does not exist. Unfortunately, traditional pharmacology takes a reductionist approach to anaesthesia by focusing on the brain in isolation. Holistic concepts, however, need to be integrated in the education of both medical researchers and practitioners, so as to bridge the gap between science and patient care (Ries, Sutter and Sutter 1997).

Perhaps to hide the unknown and the inherent dangers, popular culture has made anaesthesia ordinary. This is done by anaesthetists and patients when the induction of anaesthesia is

compared to sleep, as in "you are going to sleep now."<sup>1</sup> This is also done by society: "dear child, we will put our pet to sleep so that (s)he will not suffer." In contrast, society does not refer to a death penalty by lethal injection as putting criminals to sleep.

But what about the sleep metaphor? Are anaesthesia and sleep mechanisms similar, or is anaesthesia really different from sleep? This mystery will now be explored. First, this thesis will present a review of the functional relevance of anaesthetic action as well as current concepts of consciousness. This will then lead to a review of the role of the thalamus in consciousness and altered states of consciousness. The introduction will conclude with a review of the evidence for a thalamic role in anaesthetic action.

Please note that nomenclature derived from abbreviations is listed following Section 4.

## 1.2 What is anaesthesia?

### 1.2.1 Functional relevance of *in vivo* anaesthetic action

The state of anaesthesia involves the use of drugs to prevent psychological and somatic responses to surgical trauma (Kissin 1993). This means that the word anaesthesia<sup>2</sup> is much more than its Greek translation, insensibility to objects of touch (Miller 1927). Indeed, a spectrum of functional components exists during anaesthesia. These elements include analgesia, anxiolysis, amnesia and unconsciousness, as well as suppression of somatic motor, cardiovascular and hormonal responses to surgical injury (Woodbridge 1957). The central neural mechanisms of these functional components, however, are also unknown.

Inhalational anaesthetics best provide this spectrum of functional components. Although inhalational anaesthetics are also preferred because of rapid emergence, they are combined with intravenous sedatives, analgesics and muscle relaxants to ease induction and reduce

---

<sup>1</sup>"We watch closely those who sleep" is the motto of the Canadian Anaesthetists' Society.

<sup>2</sup>The word "anaesthesia" was introduced in 1846 less than a month following the use of ether as an "anaesthetic" agent.

cardiovascular depression as an adverse effect. Concomitant use of multiple drugs from differing pharmacological classes is generally superior to single-agent therapy in terms of side effects because of synergistic drug interactions. During a so-called "balanced" anaesthetic, the dose of each drug is limited in order to diminish adverse effects but at the same time maintain or increase desired effects.

Single intravenous agents without inhalational anaesthetics can produce a state of anaesthesia but with varying efficacy in terms of the above spectrum of functional components. For example, high-dose opioids are given for heart surgery so as to avoid cardiac depression. Despite profound analgesia, however, the occasional patient will experience intraoperative awareness. In contrast to inhalational agents, intravenous anaesthetics are known to act on specific receptors, meaning that some of their effects can be reversed by specific antagonists.

Other features of *in vivo* anaesthesia may provide valuable information concerning its mechanism. For example, the autonomic nervous system requires higher doses for depression when compared to the somatic nervous system. In addition, neuroexcitation occurs frequently during induction of anaesthesia with either inhalational anaesthetics or low doses of intravenous anaesthetics such as barbiturates or propofol, and occasionally during recovery from anaesthesia. Although these inconsistencies are generally neglected in mechanistic studies of anaesthesia, propofol related neuroexcitation has received some attention. In addition to rapid anaesthetic emergence with dreaming and hallucinations, propofol is associated with muscular hypertonus, such as opisthotonos (Ries, Scoates and Puil 1994), muscular jerking (Bevan *et al.* 1997) and restlessness.<sup>3</sup> A possible withdrawal mechanism involving acute tolerance at  $\gamma$ -aminobutyric acid (GABA) and glycine receptors has been postulated (Ries, Scoates and Puil 1994).

Inhalational anaesthetics, however, are thought to share a nonspecific (i.e., not receptor mediated) yet unified mechanism of action. Despite a wide range of anaesthetic molecular structure, a unitary site of action in lipid membranes has been popularized since the turn of the century by the correlation between lipid solubility and anaesthetic potency (Meyer 1899; Overton

---

<sup>3</sup>Bevan JC, Ries CR, Blackstock D, Macnab AJ, Kokatailo E. An evaluation of propofol as a factor in restlessness in the pediatric post anesthesia care unit. Submitted to Journal of Peri-Anesthesia Nursing.

1901). A physico-chemical mechanism was further supported in the 1970's with the reporting of anaesthesia reversal by elevations in hydrostatic pressure (Lever *et al.* 1971). Over the years, the unitary theory has explored various possibilities such as membrane volume expansion, membrane fluidity and more recently action on protein channels within lipid membranes (Little 1996).

A unitary anaesthetic action seems both doubtful and insignificant to some (Kissin 1993; Collins, Kendig and Mason 1995; Little 1996). For example, potency ratios between movement and righting vary for inhalational anaesthetics (Deady *et al.* 1981; Kissin 1983). This observation suggests then that inhalational anaesthetics have multiple pharmacological actions and not a unified mechanism that produces a spectrum of effects. Even so, investigating the molecular site of action does not speak to the more difficult problem of how the state of anaesthesia takes place. Similarly, cellular investigations do not always consider the relationship between *in vivo* and *in vitro* anaesthetic action.

So, in contrast to a traditional reductionist approach, a top-down approach would address the importance of the functional goals of anaesthesia (Kissin 1993). The two most significant effects are unconsciousness and suppression of motor responses to noxious stimulation. Both result from a depression of neuronal excitability in the central nervous system (CNS).

### 1.2.2 Spinal anaesthetic actions inhibit motor responses to noxious stimuli

Investigators assume that anaesthesia involves changes in cortical activities. However, there is evidence that the suppression of pain-evoked activity by inhalational anaesthetics partly involves the spinal cord.

The evidence comes in three parts. First, the electroencephalogram (EEG) does not predict movement in response to noxious stimulation during anaesthesia. Second, neither parietal cortical lesions, decerebration nor spinal cord transection change the effective dose of inhalational anaesthetic necessary to block motor responses in rats. And third, preferential brain anaesthesia increases, whereas preferential spinal cord anaesthesia decreases the effective dose for movement blockade in the goat.

The EEG evidence will now be probed further. To begin, it is important to appreciate that the clinical adequacy of general anaesthesia is simply based on maintaining hemodynamic control without purposeful movement (Stanski and Shafer 1995). A potential problem occurs, however, as cardiovascular variables do not predict movement to noxious stimuli (Dutton, Smith and Smith 1990). Since cortical electrical activity changes during anaesthesia in a dose-dependent manner, the EEG has been extensively examined as a clinical anaesthetic monitor.

Unfortunately, EEG parameters do not correlate with the cardiovascular and respiratory indicators of anaesthetic "depth." Even in studies investigating single-agent rather than multi-agent anaesthesia, the EEG does not predict responses such as movement to noxious stimuli. For example, a recent investigation in 18 patients found a dose-dependent decrease in EEG activity but was unable to predict movement in response to surgical incision at one MAC<sup>4</sup> isoflurane (Dwyer *et al.* 1994).

It is difficult to find fault with this study. Because of the clinical difficulty in inducing anaesthesia with a pungent volatile agent, all patients received nitrous oxide and some patients received small amounts of intravenous propofol to ease the inhalation of the anaesthetic, isoflurane (IFL). The muscle relaxant, vecuronium bromide, was administered to facilitate tracheal intubation and hence mechanical ventilation. This in turn allowed for the control of anaesthesia-induced respiratory depression and permitted accurate end-tidal IFL determinations. In attempting to study just IFL, the investigators reasonably allowed a 30 min period to elapse between discontinuation of the supplemental anaesthetics and surgical incision; neuromuscular function was also monitored to ensure that pharmacological paralysis had resolved. Additional EEG analysis showed no differences between the 8 patients who had received propofol (of which 50% moved on incision) and the 10 patients who had not.

In other studies, even almost complete depression of cortical electrical activity by isoflurane in rats (Rampil and Laster 1992) or thiopental in humans (Hung *et al.* 1992) does not ensure that movement will not occur in response to a noxious stimuli. Taken together, these EEG

---

<sup>4</sup>The acronym MAC represents the minimum alveolar concentration of an inhalational anaesthetic that in 50% of subjects prevents movement with a noxious stimuli, i.e., surgical incision (Eger 2d, Saidman and Brandstater 1965). This measure is useful since the alveolar concentration reflects the partial pressure of anaesthetic at its site of action, i.e., the CNS.

investigations suggest that anaesthetic blockade of pain-induced movement is a subcortical or spinal cord effect.

The second piece of evidence for spinal cord involvement comes from three investigations in rats using CNS lesion techniques. In the first example, a recent, minor injury of the parietal cortex was reported not to alter MAC for the inhalational anaesthetic, halothane (Todd, Weeks and Warner 1993). Although this would be expected if the injury does not cause neurological or behavioural changes (i.e., sedation), even acute removal of the cortex and thalamus does not alter IFL's potency for movement blockade (Rampil, Mason and Singh 1993). In an attempt to further localize the neural structures that mediate the motor response to pain, the latter group of investigators found that an acute spinal cord transection, performed in a manner that prevented spinal shock, does not change IFL's MAC (Rampil 1994). These studies suggest then that the CNS site for MAC determinations is in the spinal cord.

The third piece of evidence comes from experiments designed to identify the CNS site of anaesthetic inhibition of pain-induced movement in the goat. The purpose of using the goat was not to use another mammal that may or may not be more highly developed. Rather the goat has a unique cerebral circulation that permits preferential delivery of anaesthetic to either the brain or spinal cord in isolation by cardiopulmonary bypass methods. In these experiments, nonpulsatile bypass was unlikely to be a factor as bypass does not change MAC in dogs (Antognini and Kien 1992). During preferential delivery of IFL to the cortex, thalamus, pons, midbrain and cerebellum in goats, MAC increases to 240% of the control value (Antognini and Schwartz 1993). During preferential delivery to the caudal medulla, spinal cord and periphery, however, IFL's MAC decreases to 60% of the control value (Borges and Antognini 1994). Together, these investigations confirm that the principal site of drug action for movement blockade is the spinal cord. In addition, it would appear that the awake brain influences pain perception. Possible explanations include descending inhibition and stress-induced analgesia involving serotonergic, monoaminergic, enkephalinergic and/or adrenocorticoid mechanisms (Akil, Mayer and Liebeskind 1976).

MAC, then, reflects dose-response relationships in the spinal cord. In contrast, IFL's potency for amnesia and responsiveness to oral command is 25-40% MAC (Dwyer *et al.* 1992). Although

there may or may not be a unitary anaesthetic action throughout the CNS, it would appear that anatomical and physiological factors are critical in determining both pharmacological actions and sensitivities. This again means that mechanistic studies in anaesthesia may be better served by functional considerations rather than reductionist investigations of molecular action.

Furthermore, the relationship between *in vitro* concentrations and so-called "clinically relevant" concentrations for inhalational anaesthetics is uncertain. For example, the solubility of inhalational anaesthetics is temperature-dependent. This factor presumably affects the *in vitro* concentration that is proportionate (not "relevant") to the *in vivo* concentration at 37°C.

Do anaesthetic actions at the spinal cord relate to unconsciousness? Although these actions may contribute to analgesia, it is unlikely that they directly affect wakefulness (cf. patients with quadriplegia).

### 1.2.3 Do general anaesthetics cause unconsciousness?

Different anaesthetic potencies in the spinal cord for movement blockade, and the brain for amnesia, are reflected by clinical practice. For example, paralyzing drugs keep patients immobile for surgery, permitting a lighter depth of inhalational anaesthetic and hence less cardiovascular toxicity. The development of paralyzing drugs has removed the need for "deep" anaesthesia and therefore increased the safety of anaesthetics<sup>5</sup>. With the more recent development of potent short-acting opioids, as well as concerns for local and environmental pollution, anaesthetists are using even lower concentrations of inhalational anaesthetics. Pharmacological paralysis and opioids, however, remove the possibility of detecting conscious awareness through somatic and autonomic responses, respectively.

Despite the overall improvements in modern anaesthesia, the seemingly low existence of postoperative recall of intraoperative awareness is very intriguing to popular culture<sup>6</sup> (Anonymous 1995). Long before the modern recognition of awareness during anaesthesia,

---

<sup>5</sup>The lethal concentration for inhalational anaesthetics is only three times the "therapeutic" concentration.

<sup>6</sup>Dateline Television Show, National Broadcasting Corporation October 27, 1996.

however, Claude Bernard graphically described the effects of curare on the fully conscious subject: "Can you imagine a more dreadful agony than that of a mind conscious of the loss of control over those organs designed to serve it and finding itself fully alive entombed in a corpse?" As a result, litigation for awareness during surgery is said to be on the increase. Presumably "when patients are no longer surprised by surviving anaesthesia, they perhaps understandably begin to criticize the quality of the experience" (Heneghan 1993).

Anaesthetics do block explicit recall of the intraoperative experience (Cormack 1993). But, do these drugs actually cause unconsciousness (Kulli and Koch 1991)? This question is difficult to address since patients cannot orally describe their experiences while anaesthetized. However, the isolated-forearm technique has been useful in detecting awareness when paralyzing drugs are used with anaesthetics. In this technique, a blood pressure cuff is used as a tourniquet to isolate the forearm from the circulation and thereby prevent paralysis. Hand responses are then elicited from the patient in response to orally presented questions. In clinical investigations with combinations of opioids and either volatile anaesthetics (Tunstall 1979) or benzodiazepines (Russell 1993), the clinical signs of light anaesthesia (i.e., high blood pressure, tachycardia, sweating and lacrimation) do not predict which patient will respond. Interestingly, responders rarely experience pain during surgery and rarely recall intra-operative events. However, patients who do not respond may have intra-operative recall (Bogod *et al.* 1990). Although the isolated-forearm test would appear to monitor auditory perception, it is less certain if it monitors conscious awareness (Jessop and Jones 1991). Despite methodological difficulties, the psychological literature has devoted much interest in learning and memory during anaesthesia. "Implicit" memory for intraoperative events is argued as being a separate type of memory that does not require conscious awareness during anaesthesia (Ghoneim and Block 1992; Kihlstrom and Couture 1992).

The clinician's inability to detect patient awareness during surgery exposes an inability to determine the adequacy of the brain's anaesthetic state. An experimental monitor using auditory evoked potentials, however, is showing much promise as both a research and clinical tool.

#### 1.2.4 Auditory evoked potentials and anaesthetics

Since auditory evoked potentials have identifiable anatomical significance, and perhaps since this sensory system dominates the research in intra-operative learning and memory, auditory information processing during anaesthesia has received much recent attention. Two responses are used: mid-latency auditory evoked potential (MLAEP, Schwender *et al.* 1993) and the 40-Hz auditory steady state response (40-Hz ASSR, Plourde 1993; Plourde and Villemure 1996).

The MLAEP is an auditory evoked potential elicited by repeated clicks. The stimuli are presented at a frequency sufficiently slow ( $\sim 10/s$ ) such that each transient response is over before the next stimulus. Averaged responses consist of a series of positive and negative voltage deflections that reflect sensory transmission through the anatomical components of the auditory pathway. Early waves are from the brainstem, mid-latency waves involve the thalamus and auditory cortex, and late latency waves arise from the frontal cortex and association areas. The mid-latency potentials have a periodic waveform with a maximal power spectrum in the 30- to 40-Hz frequency range. In contrast, the 40-Hz ASSR is a sustained sinusoidal auditory evoked potential elicited by repeated auditory stimuli at a frequency of 40/s. The 40-Hz stimulating frequency is harmonically related to the measured power spectrum of the MLAEP. As a result, the responses of successive stimuli overlap to create a steady-state response.

During anaesthesia with either inhalational agents or the intravenous induction agents (e.g., thiopental or propofol), the brainstem response remains largely unchanged (Schwender *et al.* 1993). However, the MLAEP, its power spectrum, and the 40-Hz ASSR change markedly with these anaesthetics: the MLAEP shows marked dose-dependent increases in latencies and decreases in amplitudes; the power spectrum of the MLAEP shows a shift from 30- to 40-Hz activity to low-frequencies; and the amplitude of the 40-Hz ASSR is attenuated (Plourde 1993). In contrast to the 40-Hz ASSR, the MLAEP is difficult to use during emergence from anaesthesia as reflex muscle responses are not removed on averaging and therefore contaminate the signal with artifacts (Stark 1993; Plourde and Villemure 1996). Because of a low signal-to-noise ratio, it takes at least 3 min to average an adequate MLAEP waveform, whereas the 40-Hz ASSR takes approximately 20 s (Munglani and Jones 1992). During emergence, the 40-Hz ASSR remains attenuated when patients react to pain, such as coughing induced by an endotracheal tube, and

returns just as patients respond to oral commands (Plourde *et al.* 1996).

During "anaesthesia" with the intravenous sedatives (e.g., benzodiazepines or ketamine, a so-called "dissociative" anaesthetic) or high-dose opioids, the MLAEP is unchanged from wakefulness. This is not surprising. Investigations of the relationship between MLAEP and recall have been performed during caesarean section (Schwender *et al.* 1995) and cardiac surgery (Schwender *et al.* 1994). Typically, these surgeries are more frequently associated with intra-operative awareness. During caesarean section, the mother is "lightly" anaesthetized with thiopental, nitrous oxide and an inhalational anaesthetic, usually IFL, until the fetus is delivered. During cardiac surgery, high-doses of opioids are administered as the principal agents so as to avoid impairment of the cardiovascular system. Supplemental propofol, benzodiazepines, or IFL are used as required during the sternotomy to maintain hemodynamic control. In the caesarean investigation, 12 of 20 patients exhibited movement and/or had "explicit" recall of intraoperative events, whereas 7 of 45 cardiac patients had implicit recall for details of an audiotape played after sternotomy. Only the patients with movement or recall had unchanged MLAEP.

Pharmacologically, the preservation of the 40-Hz auditory evoked response and the risk of intra-operative awareness with benzodiazepines, ketamine or opioids is perhaps consistent with the specific receptor-mediated (i.e., restricted) action of these drugs. During anaesthesia with inhalational anaesthetics, thiopental or propofol, however, brainstem auditory processing is intact but cortical processing is suppressed. Does the 40-Hz auditory evoked response relate then to awareness and consciousness?

### 1.3 **Consciousness: current views**

#### 1.3.1 Temporal mechanisms

Because of the difficulty in describing consciousness in scientific terms, a metaphor such as "information processing" may be useful in determining possible mechanisms (Shafer 1995). But is information processing a conscious process? Consider the following. Individuals with a

disorder of brain function known as blindsight<sup>7</sup> can respond to simple visual stimuli but deny seeing things since they do not know what they can see (Crick 1993). In other words, visual perception in these individuals is dissociated from conscious experience. Blindsight then may represent a dissociation between a processing system and a consciousness system (Frith 1992).

Unconscious sensory processing probably involves the multitude of sensory inputs that an individual is receiving at any given moment. Remember the popular psychological pictures that can be viewed as one of two visual patterns. Although the visual input to our brains is constant, the pattern that we are consciously aware of can change (Horgan 1994). The phenomenon of attention then allows us to be aware of various aspects of our unconscious processing that are all in progress at any given moment (Andrade 1993). What neural activity might correspond to changes in attention? Where and how in the brain do perceptions come together?

This is where the 40-Hz activity may fit in (Koch 1993). Neurons in different regions of the visual cortex produce coherent 40-Hz oscillations in response to a visual stimulus (Eckhorn *et al.* 1988; Gray and Singer 1989). It may be that the 40-Hz activity temporally binds the spatially disparate information into a unified perception. Synchronized 40-Hz oscillations may phase-lock the firing of these neurons and thereby both unite them into conscious perception and distinguish them from background information processing.

Unfortunately scientific progress does not yet explain more difficult problems such as how physical processes in synchronized neurons lead to a conscious experience (Chalmers 1995). Anaesthetic suppression of temporal binding, however, may be relevant to the change in the level of consciousness. Where then are the neural generators and circuits for the 40-Hz activity?

### 1.3.2 Synchronized 40-Hz thalamocortical oscillations

Morphological considerations for the information processing metaphor involve synaptic connections between the periphery and the cerebral cortex. Sensory signals from the cranial and peripheral nerves with the exception of the olfactory system all make a final synapse in the

---

<sup>7</sup>A child exhibited this syndrome transiently during recovery from propofol anaesthesia at B.C. Children's Hospital, Vancouver a few years ago according to anaesthetist Derek Blackstock.

thalamus before further transmission to the cortex. Indeed, metaphors for this thalamic function include "gateway" and "relay" to the forebrain. However, the connectivity between the thalamus and the cortex is bi-directional since these two brain areas are reciprocally linked (Llinás and Paré 1991). After receiving thalamocortical inputs, cortical pyramidal neurons project their axons as corticothalamic fibers back to the same area in the thalamus. As synchronization of neuronal activity has been observed in the cortex and thalamus (Singer 1993; Sillito, Jones, Gerstein and West 1994), 40-Hz oscillations in thalamocortical-corticothalamic circuits may be involved in temporal binding and consciousness.

An inter-dependent relationship between the thalamus and the cerebral cortex appears to be critical for awareness and arousal. The thalamic gateway metaphor has been further described as a "searchlight" in directing neuronal traffic to attended cortical areas (Crick 1984). A searchlight role, however, may be more directly related to corticothalamic feedback (Singer 1994). This view is supported by two findings: thalamic synchronization emerges during the late phases of sensory processing; and corticothalamic projections outnumber thalamocortical fibers. But where exactly do the 40-Hz oscillations originate? Abnormal MLAEP and abnormal "40-Hz" responses are reported in humans with CNS disorders involving a sub-cortical site such as the midbrain or thalamus (Harada *et al.* 1994). Whether the thalamus or cortex serves as the 40-Hz generator may not be too relevant, however, if circuitry is not intact.

#### 1.4 **Role of thalamus in consciousness and altered states of consciousness**

##### 1.4.1 Changing concepts of the brainstem's role in awareness and arousal

The roles of the thalamus in information processing and attention have been dramatized by the recent reporting of the autopsy findings of the brain of Karen Ann Quinlan (Kinney *et al.* 1994). Quinlan was a highly publicized American who survived nine years following the withdrawal of life-sustaining treatment for an overdose-related cardiopulmonary arrest with severe brain damage. In a persistent vegetative state, she had intact sleep-wake cycles without signs of awareness or cognition. To everyone's surprise, however, her autopsy showed that she had suffered injury to her thalamus instead of her cerebral cortex. These findings support the important inter-dependence of the thalamus and the cerebral cortex in awareness and cognition.

The thalamus not only plays a role in sensory (and motor) relay but in sensory analysis. Positron emission tomography studies show that thalamic metabolism increases during sensory stimulation when receptive fields of cortical neurons change (Picton and Stuss 1994; Posner and Dehaene 1994). Presumably, the thalamus filters out non-targets and amplifies attended stimuli.

Recent research has also refined our understanding of arousal. A thalamic role is illustrated by humans who lack both full wakefulness during the day and complete sleep at night following paramedian thalamic strokes (Guilleminault, Quera-Slava and Goldberg 1993; Bassetti *et al.* 1996). Thalamic function is now known to be modulated by the brainstem reticular formation. This extrinsic influence involves multiple ascending transmitter systems that project to both the thalamus and the cerebral cortex (Marrocco, Witte and Davidson 1994). These ascending activating systems are located in the upper brainstem, posterior hypothalamus, and basal forebrain and the transmitters include acetylcholine, norepinephrine, serotonin, histamine and glutamate. During arousal, the transmitters modulate thalamic relay by inducing a prolonged depolarization. The depolarization involves suppression of a  $K^+$  leak current which is coupled to muscarinic ACh and  $\alpha_1$ -adrenergic receptors by means of G-proteins that are insensitive to pertussis toxin (McCormick 1992). A descending corticothalamic system involving excitatory amino acid receptors also reinforces the activation (McCormick and van Krosigk 1992). By modulating thalamic function, arousal systems then are responsible for the transition from sleep to wakefulness. In addition, state-dependent changes are influenced by intrinsic properties at the single cell level in the thalamus.

#### 1.4.2 The gateway to our external and internal worlds

During ascending arousal by the reticular formation, the transition from sleep to wakefulness is associated with a voltage-dependent increase in the thalamic transfer ratio of sensory information (McCormick and Bal 1994). This increase in sensory relay to the cerebral cortex is due to extrinsic and intrinsic thalamic factors. Extrinsic synaptic influences from the brainstem affect the membrane potential of thalamic neurons (see above). Intrinsic voltage-dependent membrane properties in turn determine state-specific firing modes and hence the change in the thalamic transfer ratio (see below). Together with descending modulation by corticothalamic systems during wakefulness, sensory relay leads to fast 40-Hz oscillations with sensory analysis and

external cognition. During nonREM (rapid-eye-movement) sleep, however, ascending extrinsic influences become inactive and slow spontaneous oscillations arise in thalamic neurons (see next section). These slow waves synchronize in the thalamus, thereby filtering out sensory interference from the external world for the sleeping brain.

Not only do coherent 40-Hz oscillations in thalamocortical-corticothalamic loops characterize wakefulness, but also REM sleep (Llinás and Paré 1991; Llinás and Ribary 1993). REM sleep may simply be a result of a stimulation-free environment where a reduction in sensory impulses may not be sufficient to produce awareness of the external world. Dreaming and even day-dreaming then may be internal equivalents to cognition when external inputs are replaced by the brain's own outputs. This closed-loop property is suggested by the fact that very little of the reciprocal connectivity between the thalamus and the cortex is devoted to sensory input. Presumably the cortical neuronal activity of REM sleep is important in functions such as the processing of information and memory that accumulates during wakefulness (Winson 1993; Steriade, Contreras and Amzica 1994).

#### 1.4.3 Slow thalamic oscillations in sleep and absence epilepsy

In the flow of sensory impulses towards the brain during sleep, the thalamus is the first synapse at which signals are functionally blocked. The block is due to slow synchronized oscillations that arise from neuronal activity in thalamic and cortical networks (Steriade 1993; Steriade, McCormick and Sejnowski 1993; Steriade, Contreras and Amzica 1994). The mechanism of the synchronization involves the thalamic reticular nucleus that is located within the thalamic network. As we fall asleep, the thalamic reticular nucleus acts like a pacemaker and thereby controls the flow of traffic through thalamic relay neurons to the cerebral cortex. EEG spindles (episodic oscillations at 7- to 14-Hz) reflect this periodic thalamic activity arriving in the cortex and serve as an electrographic landmark for the loss of awareness during the transition from wakefulness to sleep. As sleep progressively deepens, delta oscillations (1- to 4-Hz) and then slow waves (<1-Hz) occur, reflecting activity in corticothalamic and intra-cortical networks, respectively. In contrast to spindles, delta waves and slow waves are not always reflected at the global EEG as they are generally not synchronized.

The thalamic mechanisms that underlie spindle generation can also account for generalized absence epilepsy. In absence or petit-mal, individuals exhibit a few seconds of staring while a synchronous slow oscillatory rhythm occurs in thalamocortical circuits (Snead 1995). Although positron emission tomography studies of regional blood flow show that thalamic perfusion selectively increases during an absence seizure (Prevett 1995), a thalamic origin has not been confirmed in humans. However, animal models strongly suggest that the thalamic reticular nucleus is involved.

Intracellular recordings from thalamic relay neurons show that periodic high frequency bursts of action potentials occur during spindles, delta oscillations and slow waves of nonREM sleep.

#### 1.4.4 State-dependent firing properties are intrinsic to thalamic relay neurons

State-dependent firing activities result from an interaction between extrinsic brainstem influences and intrinsic membrane properties of thalamic relay neurons (McCormick and Bal 1994; McCormick 1992). During wakefulness and REM sleep, extrinsic modulation depolarizes the membrane potential and tonic firing of action potentials occurs with sensory stimulation. During nonREM sleep when extrinsic modulation of membrane potential is absent, spontaneous rhythmic burst firing of action potentials occurs.

Burst firing during nonREM sleep involves an interplay in the thalamic circuit between thalamic reticular neurons and thalamic relay neurons (von Krosigk, Bal and McCormick 1993). When extrinsic modulation is absent, both of these neuron groups exhibit rhythmic burst firing. During the burst firing activity, thalamic relay neurons activate the GABA-ergic neurons of the thalamic reticular nucleus, which in turn, burst and activate the relay neurons. In this recurrent interaction, the intrinsic bursting property involves the "transient" low-threshold  $\text{Ca}^{2+}$ -current known as T-current. Hyperpolarization of relay neurons through a  $\text{GABA}_A$ -mediated increase in  $\text{Cl}^-$ -conductance and a  $\text{GABA}_B$ -mediated increase in  $\text{K}^+$ -conductance results in the removal of inactivation of T-current (Crunelli and Leresche 1991). As the GABAergic inhibitory postsynaptic potential (IPSP) decays and causes a "relative" depolarization, T-current is in turn activated and a low-threshold  $\text{Ca}^{2+}$ -spike (LTS) is paradoxically excited (Llinás and Jahnsen 1982). In addition, a burst of  $\text{Na}^+$ -dependent action potentials appear on the rising "crest" and

"crown" of the LTS. These bursts excite thalamic reticular neurons and thereby facilitate their oscillation, beginning the cycle again. During wakefulness and REM sleep, burst firing is suppressed since the inactivation of T-current is not removed when extrinsic modulation depolarizes thalamic relay neurons.

## 1.5 Evidence for a thalamic role in anaesthetic action?

### 1.5.1 A unified theory of state control

A new constructionist approach to anaesthetic action looks for a unified theory of state control with involvement of a critical brain region (Lydic and Biebuyck 1994). Although the brainstem reticular formation has been implicated in the past (Rhines and Magoun 1946; Keifer *et al.* 1994), the thalamus would also be an obvious candidate in view of its role in altered states of consciousness (Munglani and Jones 1992). Anaesthetic perturbation of thalamic state control should have significant effects on thalamocortical-corticothalamic circuitry and function. Blockade of conscious information processing, awareness and dreaming would occur, consistent with the functional observations in human anaesthesia. What is known then about thalamic actions of anaesthetics?

### 1.5.2 Investigation of central processing in *in vivo* anaesthesia

Although human investigations show that anaesthetics block 40-Hz oscillations, it is difficult to make the same conclusion from animal studies (Picton and Stuss 1994). Investigation of auditory pathways and awake-sleep electrophysiology using acutely implanted electrodes are conducted under anaesthesia for obvious ethical reasons. Even in chronic experimentation, anaesthetic drugs are used to decrease movement artifact during the recordings. Surprisingly, very few investigators use anaesthetic drugs as pharmacological probes in the investigation of consciousness and state-control (Ghoneim and Block 1992).

Since these animals are assumed to be anaesthetized, a cause and effect relationship between 40-Hz rhythms and consciousness has not been proven as yet. But are the animals actually unconscious during these experiments on 40-Hz activity? In contrast to humans, animals cannot

complain about the quality of their "anaesthetic" experience. On the other hand, we can never be absolutely certain that animals experience either consciousness or anaesthetic-induced unconsciousness in human terms. However, there are at least five reasons why the adequacy of anaesthesia is uncertain in animal experiments. First, animal experiments do not employ hemodynamic monitoring to determine the adequacy of the anaesthesia state. Second, movement is removed as an indicator of spinal cord anaesthesia since the animals are often pharmacologically paralyzed (Drummond 1996). Third, intravenous agents are generally used rather than inhalational anaesthetics. Fourth, the intravenous agents are often given as intramuscular or intraperitoneal boluses without further consideration for steady-state concentrations and duration of action. And fifth, local anaesthetics are given to counteract surgical stimulation during the electrophysiological recordings. A recent publication reporting 40-Hz rhythms in "anaesthetized" cats illustrates these points (Steriade, Amzica and Contreras 1996): no blood pressure monitoring; paralysis with gallamine; intramuscular ketamine and xylazine, an  $\alpha_2$ -agonist; and an unspecified local anaesthetic and dose prior to surgical incision. Of course, toxic administrations of local anaesthetic are associated with central stimulation.

### 1.5.3 Anaesthetics are associated with EEG spindle and burst activity in the thalamus

Sleep-like EEG spindles are generated in the thalamus during barbiturate anaesthesia (Contreras and Steriade 1996). One spindle represents a sequence of neuronal oscillatory activity at 7- to 14-Hz that characteristically waxes and wanes and recurs at a frequency  $< 1$ -Hz. EEG spindle activity depends on intrinsic properties of thalamocortical cells (i.e., the LTS) and network pacing by the thalamic reticular nucleus. Multiple simultaneous *in vivo* intracellular recordings with barbiturate anaesthesia show that spindle activity occurs in phase among thalamic reticular, thalamocortical and corticothalamic neurons. During depolarizing plateaus in thalamic reticular neurons, rhythmic spike activity leads to synchronous GABA-ergic IPSPs in thalamocortical cells, which in turn lead to synchronous excitatory postsynaptic potentials (EPSPs) in the cortical neurons. Rebound spike bursts occur following the IPSPs and action potentials occur with the EPSPs. The waxing pattern consists of a progressive increase in synaptic potentials during the first part of the spindle sequence. Waxing depends on a progressive recruitment and synchronization of thalamic and cortical cells. The waning pattern at the end of the spindle occurs due to a progressive desynchronization of the thalamocortical afferent input to

corticothalamic neurons such that the EEG oscillation fades.

Spindle activity is reported with other anaesthetics such as ketamine, urethane (Contreras and Steriade 1996) and halothane (Avramov 1991; Keifer *et al.* 1994). Prolonged membrane hyperpolarization precedes each spindle sequence in cortical, thalamic reticular and thalamocortical neurons (Contreras and Steriade 1996). A decrease in stimulation during anaesthesia as in sleep would lead to a decrease in the release of arousal neurotransmitters, hyperpolarization and thalamic oscillation. Additional pharmacological properties of anaesthetics presumably facilitate the oscillation. For example, intracellular recordings from thalamic brain slices indicate that low concentrations of pentobarbital increase the LTS amplitude whereas higher concentrations decrease the LTS amplitude (Puil *et al.* 1996).

As anaesthetic depth is increased, the spindle activity changes to EEG burst-suppression (Steriade, Amzica and Contreras 1994). In contrast to a spindle sequence, the burst-suppression pattern consists of abrupt bursts of oscillatory activity interspersed with periods of electrocortical silence (Angel 1991). The burst duration decreases and the periods of suppression increase in a dose-dependent manner until electrical silence occurs. Intracellular recordings show that thalamic reticular, thalamic relay and cortical neurons exhibit bursts and silences in synchrony with the EEG (Steriade, Amzica and Contreras 1994). However, the bursting activity is greatest in the thalamus (Akrawi *et al.* 1996) and many of the thalamic neurons continue to burst during periods of cortical and global electrical silence (Steriade, Amzica and Contreras 1994). At the cellular level, intracellular recordings indicate that thalamic and cortical neurons exhibit membrane hyperpolarization and a decrease in input resistance during the burst-suppression stage of anaesthesia, suggesting an increase in  $K^+$  conductance. In addition, the synaptic responsiveness of cortical neurons to stimulation of thalamic relay nuclei is eliminated at this time.

A study of auditory processing in gerbils showed that pentobarbital increases brainstem metabolism while reducing thalamic and cortical metabolism (Wang, Ryan and Woolf 1987). Do anaesthetics then prevent the transmission of sensory impulses at a postsynaptic thalamic level during anaesthesia?

#### 1.5.4 Anaesthetics depress thalamic relay transmission

Anaesthetic depression of thalamic relay transmission was first reported 40 years ago in awake, paralyzed cats (King, Naquet and Magoun 1957). Following surgery and recovery from ether anaesthesia, somatosensory evoked potentials in response to electrical stimulation of the radial nerve were recorded simultaneously from electrodes placed in the medial lemniscus and internal capsule. The capsular responses to radial stimulation were also compared to lemniscal stimulation.<sup>8</sup> Presumably, EEG monitoring distinguished ascending and descending evoked potentials, but this was not specified. Control measurements were obtained during mechanical ventilation and curarization. Intravenous pentobarbital and thiopental increased the latency to peak capsular responses but did not increase lemniscal responses, suggesting that barbiturates delay thalamic transmission without affecting the medullary sensory relay. Depression of the thalamic relay, however, could have been mediated presynaptically via ascending and descending projections to the thalamus.<sup>9</sup> These experiments cannot be repeated because of current ethical standards prohibiting pain and suffering in awake animals. Unfortunately, the adequacy of hemodynamic control and hence O<sub>2</sub> delivery and anaesthesia was not monitored.

A similar study was performed with cardiovascular monitoring in cats during background anaesthesia with nitrous oxide and/or halothane (Marshall and Murray 1980). Electrical stimulation of the optic tract evoked field potentials in the visual thalamic nucleus and stimulation of either deep cerebellar nuclei or the precruciate cortex evoked responses in a somatosensory thalamic nucleus. Intravenous pentobarbital during nitrous oxide inhalation or an increase in concentration of halothane depressed the amplitude of evoked potentials in both thalamic nuclei. A postsynaptic thalamic mechanism seems likely since the anaesthetic depression involved three anatomically separate afferent pathways.

Simultaneous multi-site extracellular recordings of somatosensory transmission in the rat confirm that anaesthetics depress thalamic transfer without affecting medullary transfer, and suggest that

---

<sup>8</sup>The medial lemniscus contains the ascending thalamic input from the medullary sensory relay. The internal capsule contains the ascending cortical input from the thalamic relay.

<sup>9</sup>Presynaptic influences could arise from the thalamic reticular nucleus as well as the brainstem reticular activating, cerebellothalamic and corticothalamic systems.

the thalamic depression may be postsynaptic (Angel 1991; Clarke and Djourhi 1991). These studies were performed with a background of intraperitoneal urethane at a depth of anaesthesia that just abolishes the motor response to a pinch. (However, the motor response to electrical stimulation of the forepaw was not discussed.) Although the adequacy of the cardiovascular system during urethane was only inferred from previous studies, a thalamic anaesthetic effect due to inadequate brain perfusion seems unlikely as the medullary relay was affected only by near fatal levels of anaesthesia. In contrast, extracellular thalamic recordings showed a dose-dependent increase in latency and a dose-dependent decrease in probability of response with either IFL or further administrations of urethane. The cortical response decreased along with the decrease in thalamic response, consistent with a thalamic effect at the thalamocortical-corticothalamic synapse. A thalamic effect was suggested by further experiments using electrical stimulation of thalamocortical efferents to the cortex. In these experiments, there were no changes in either amplitude or latency of cortical responses with increasing levels of anaesthesia.

In investigating anaesthetics at a thalamic level, *in vitro* intracellular recordings would be helpful in distinguishing presynaptic from postsynaptic actions. However, only one investigation has examined this question. In a study of intralaminar thalamic nuclei presumably involved in relaying nociceptive information,<sup>10</sup> halothane induced a hyperpolarization in 50% of neurons (Sugiyama, Muteki and Shimoji 1992). Spontaneous firing was blocked and both EPSPs and IPSPs were decreased. The hyperpolarization involved a postsynaptic K<sup>+</sup>-mediated mechanism.

## 1.6 Objective and questions

In view of the role of the thalamus in consciousness and altered states of consciousness, and the probable role of the thalamus in anaesthesia, the experimental objective was to determine if inhalational anaesthetics inhibit the excitabilities of thalamic relay neurons. The investigations therefore were organized to address the following questions:

- i. Does a concentration of the modern inhalational anaesthetic, IFL, that is proportionate to

---

<sup>10</sup>Intralaminar neurons are part of the so-called "nonspecific" (i.e., diffuse projection) thalamocortical system. Their function is less clear than relay neurons in the "specific" thalamocortical system (Groenewegen and Berendse 1994).

*in vivo* concentrations, inhibit the passive membrane properties of rat thalamic relay neurons *in vitro*?

- ii. Does this concentration of IFL inhibit the intrinsic firing patterns characteristic of both wakefulness and sleep *in vitro*?
- iii. What are the ionic mechanisms of IFL inhibition in *in vitro* thalamic relay neurons?
- iv. Do equipotent concentrations of other inhalational anaesthetics (i.e., halothane and enflurane) have actions in *in vitro* thalamic relay neurons similar to IFL?

## 2 METHODS

### 2.1 Rat thalamic slice preparation

At the beginning of each experiment, a juvenile (range 9 to 22 days old) Sprague-Dawley rat was placed at room temperature under an inverted glass funnel (3" diameter) so as to provide a small gas-tight induction chamber. In order to maximize neuronal survival during the slice preparation, the rat was pre-oxygenated with 100% O<sub>2</sub> administered at 500 ml/min for ~30 s. Rapid anaesthesia was administered by injecting halothane 0.25 ml into a compressed cotton ball suspended under a rubber stopper at the "top" of the inverted funnel. After ~30 s, the immobile but still breathing rat was quickly removed from the anaesthetic chamber and decapitated with a large steel scalpel. The scalp was removed with steel scissors and a dorsal skull cap was reflected, starting at the foramen magnum and extending rostrally on both sides being careful not to damage the brain. The brain was moistened with a few ml of cold, aerated (95% O<sub>2</sub>, 5% CO<sub>2</sub>) artificial cerebrospinal fluid (aCSF) that had been maintained at <2°C in an ice bath. Next, the cranial nerves were transected from the olfactory bulb with a flat steel ribbon, and the brain was gently eased from the cranial vault and submerged in aerated, cold aCSF in a chamber on top of an ice bath. The brain harvesting took about 1 min.

The cold brain immersion<sup>11</sup> was used to rapidly decrease O<sub>2</sub> consumption so as to improve neuronal survival, as well as increasing rigidity for ease of sectioning. After about 30 sec, the chilled brain was placed on a moistened dissection platform and quickly trimmed. Two vertical cuts were made with a steel razor blade to remove the brain anterior and posterior to the thalamus. The thalamic block was placed "nose up," the brainstem was removed with a third cut, and the cube was returned to the cold, aerated aCSF.

---

<sup>11</sup>A comparison of the decrease in brain temperature by cold immersion was made between a decapitated head and a harvested brain. Although the onset of cooling of the brain within the intact head presumably started earlier, the temperature of this brain took 5 min to drop from 37 to 10°C, whereas the harvested brain took <1.5 min.

A vibroslicer (Campden Instruments Ltd, London, UK) with a fresh steel razor blade (VWR Scientific, Media, PA) was then used for sectioning. The block of brain containing both hemispheres was gently blotted, then glued (Lepage's Limited Accu-flo Super Glue Automatic Pen, Brampton, ON) "nose up" onto the specimen holder. 400 or 500  $\mu\text{M}$  slices were sectioned, from rostral to caudal, while submerged in cold aerated aCSF. Slices containing the ventral posterior nucleus were retained (Palkovits and Brownstein 1988) and the hemispheres within each submerged slice were divided with a steel scalpel. The slices were then quickly transferred with a moistened steel surgical scoop to a holding chamber with aerated aCSF at room temperature.

## 2.2 Whole-cell recording

After ~60 min, an attempt at whole-cell recording was made at room temperature.<sup>12</sup> The slice was first debulked so as to maximize the slice surface area to volume ratio and thereby increase the rate of IFL uptake and washout as well as maximizing  $\text{O}_2$  supply and  $\text{CO}_2$  buffering. The hippocampus and cerebral cortex lying superior to the thalamus were trimmed with a steel scalpel from each slice, leaving a 3 x 5 mm rectangular slice containing first thalamus, then internal capsule and finally parietal and entorhinal cortex. The trimmed slice was orientated with the thalamus upstream towards fresh solution in the recording chamber. The recording chamber consisted of a plexiglass 1 x 5 cm cutout with rounded ends, a depth of 5 mm, and a glass bottom made from a microscope slide. Multiple aCSF reservoirs using 60 ml plastic syringes were suspended above the recording chamber to provide a flow rate of 2.5 ml/min with Teflon micro-tubing and a plexiglass manifold (total lag time of 30 s). Low continuous suction was used to aspirate aCSF from the distal end of the recording chamber, leaving a constant bath volume of 1.6 ml. Lens paper was placed in the bottom of the recording chamber followed by the slice, while a nylon screen and polypropylene mesh overlay were used to both retain the slice and presumably promote turbulent flow. Turbulent flow thereby ensured rapid mixing for the equilibration of new solutions.

The recording chamber was inside a Faraday cage on a "floating" recording table to minimize

---

<sup>12</sup>Although some recordings were made at a more *in vivo* relevant temperature (see Section 2.4), this was not done routinely because of greater difficulty as well as time constraints.

electrical and mechanical interference, respectively. Whole-cell patch-clamp recordings were performed from an Axopatch-1C patch-clamping amplifier (Axon Instruments, Inc., Foster City, CA) using thin-walled borosilicate glass tubing (outer diameter 1.5 mm, World Precision Instruments, Inc., Sarasota, FL) pulled on a Narashige PP83 puller. Electrode and initial series resistances were ~6 and ~20 M $\Omega$  respectively, and series resistance compensation was routinely used and adjusted before each data acquisition. The membrane currents were low pass filtered (-3 dB) at a frequency of 2000 Hz, but whole-cell capacitance was not compensated as currents were not measured during voltage-clamp recordings until after the capacitive transient.

Data were collected >10 min following whole-cell access to allow the electrode solution to equilibrate with the neuron. Current and voltage protocols were applied using pCLAMP software (MS-DOS version 5.5, Axon Instruments, Inc.) and data were digitized and stored in a computer as well as on a chart recorder. Following current-clamp recordings, input resistance and membrane time constants were estimated by fitting an exponential to the membrane response elicited by a small hyperpolarizing current pulse near resting membrane potential (RMP). Leak subtraction was also performed following voltage-clamp recordings using software created in this laboratory. During voltage-clamp recordings, current responses were evoked near RMP with small amplitude hyperpolarizing voltage commands for leak subtractions as well as for later calculation of resting conductance. During some experiments using cumulative IFL concentrations, the peak amplitude of T-currents did not recover completely to control values. This was assumed to be due to rundown, so drug effects were measured relative to the extrapolated slope between control and maximal recovery.

Each neuronal recording session lasted ~60 min. Following pullout of the electrode from the slice, the absolute membrane potential was determined by measuring any electrode offset in aCSF. A new slice was used whenever drugs had been applied in the previous neuronal recording.

### **2.3 Solutions, ionic channel antagonists and junction potentials**

The aCSF contained the following in mM: NaCl 124, KCl 4, KH<sub>2</sub>PO<sub>4</sub> 1.25, CaCl<sub>2</sub> 2, MgCl<sub>2</sub> 2, dextrose 10, NaHCO<sub>3</sub> 26. This composition gave a measured osmolarity of 310 mOsmoles.

Bubbling with a compressed gas mixture of 95% O<sub>2</sub> and 5% CO<sub>2</sub> (Praxair Canada Inc., Mississauga, ON) at a flow rate of 500 ml/min through Teflon micro-tubing gave a pH<sup>13</sup> of 7.32 ± 0.05 at 22 ± 2°C (*n* = 284). Gas-dispersion tubes were not used because their high resistance reduced gas flow to < 500 ml/min which was insufficient for proper function of the anaesthetic vaporizers (Scurr and Feldman 1982). Gluconate patch-clamp solutions contained the following in mM: KOH 140, NaCl 15, ethylene glycol-bis(β-aminoethylether) N,N,N',N'-tetraacetic acid (EGTA) 10, CaCl<sub>2</sub> 1, Na-(N-[2-hydroxyethyl]piperazine-N'-[2-ethanesulfonic acid]) (NaHEPES) 10, Mg adenosine 5'-triphosphate (Mg ATP) 2, Na guanosine 5'-triphosphate (Na GTP) 0.3, and balanced with D-gluconic acid to a pH of 7.30 at 22°C. Using the Nernst equation (Nernst 1888), calculated equilibrium potentials for Na<sup>+</sup> (*E*<sub>Na</sub>), K<sup>+</sup> (*E*<sub>K</sub>), Ca<sup>2+</sup> (*E*<sub>Ca</sub>) and Cl<sup>-</sup> (*E*<sub>Cl</sub>) at 25°C (*RT/ZF* = 26 mV, Koester 1991) were as follows in mV: +46, -85, +159 (based on a calculated free internal Ca<sup>2+</sup> concentration of 10<sup>-8</sup> M, Max Chelator for Windows version 1.2, Pacific Grove, CA) and -54 respectively.

The composition of the aCSF was changed in ion substitution experiments. The external K<sup>+</sup> concentration was changed to 1.25, 2.45 and 9.25 mM by adjusting KCl and NaCl concentrations, thereby changing calculated *E*<sub>K</sub> as follows in mV: *E*<sub>K</sub> -123, -106 and -71, respectively at 25°C. In these different K<sup>+</sup> solutions, the NaCl was adjusted so as to maintain the same concentration of Cl<sup>-</sup>, thereby changing *E*<sub>Na</sub> by only +0.9, +0.7 and -0.5 mV, respectively. In other experiments, choline Cl was substituted for some of the NaCl, changing external Na<sup>+</sup> to 26 mM and thereby shifting *E*<sub>Na</sub> to 0 mV. In addition, occasionally some of the NaCl was replaced by Na isethionate, changing external Cl<sup>-</sup> to 12 mM and thereby shifting *E*<sub>Cl</sub> to +10 mV.

Ionic channel blockers as well as drugs with known ionic actions were sometimes added to the external solutions as follows: tetrodotoxin (TTX) 300 nM; tetraethylammonium (TEA) 10 mM; 4-aminopyridine (4-AP) 3 mM; Cs<sup>+</sup> 5 mM; Ba<sup>2+</sup> 100 μM; Cd<sup>2+</sup> 50 μM; and Ni<sup>2+</sup> 0.5 mM. In other experiments, substitutions for Ca<sup>2+</sup> were made with Ba<sup>2+</sup>, Co<sup>2+</sup> and Mg<sup>2+</sup>. The GABA<sub>B</sub> agonist, baclofen (racemic mixture, 10 μM), as well as the anticholinesterase agent, tacrine (100

---

<sup>13</sup>With cooling, hibernating mammals maintain a pH of 7.40 when measured at the animal's temperature. In contrast, the blood pH of cold-blooded animals changes with temperature, even though at 37°C their blood pH is the same as warm-blooded animals. Whether temperature correction to 37°C should be used in hypothermic humans (e.g., during heart-lung bypass procedures) is unknown.

$\mu\text{M}$ ), were administered to some neurons. In addition, the ATP-sensitive  $\text{K}^+$  channel blocker, glibenclamide, was prepared in dimethyl sulfoxide (final concentration for neuron of 0.5%; Erdemli and Krnjević 1994).

The patch-clamp solutions also were altered in three types of experiments. First, in experiments with intracellular  $\text{Cs}^+$ ,  $\text{CsOH}$  was substituted for  $\text{KOH}$ . Second, internal  $\text{Cl}^-$  was increased to 50 mM by substituting  $\text{KCl}$  for some of the  $\text{KOH}$ , thereby shifting  $E_{\text{Cl}}$  to -26 mV. And third, 1,2-bis(2-aminophenoxy)ethane  $\text{N,N,N',N'}$ -tetraacetic acid (BAPTA) 10 mM was substituted for the slower  $\text{Ca}^{2+}$  chelator, EGTA. In the BAPTA experiments,  $\text{CaCl}_2$  was decreased to 0.5 mM in order to maintain the same internal free  $\text{Ca}^{2+}$ .

In contrast to intracellular electrodes, the solution used in whole-cell patch-clamp electrodes introduces a junction potential. For example, the gluconate anion, being larger and less mobile than intracellular anions (Zhang and Krnjević 1993), makes the recorded membrane potential appear more positive than the true membrane potential. To compensate, a measured junction potential of 12 mV was subtracted from all recorded voltages.

#### 2.4 Volatile anaesthetic preparation

As it was important to investigate a concentration of IFL that was proportionate to *in vivo* anaesthetic concentrations, some introductory comments regarding inhalation anaesthetics will be made. During continuous administration of an inhalational anaesthetic, the partial pressure of drug in the lung is equal to the partial pressure in the brain. As end-tidal concentrations approximate alveolar gas concentrations, experimental concentration-response measurements using MAC are a routine part of every clinical anaesthetic. Even though MAC probably reflects a spinal cord site of action, the anaesthetizing concentration for a given inhalational anaesthetic is similar from *Drosophila* to humans, despite 300 million years of presumed evolution (Allada and Nash 1993). All of these aspects of inhalational anaesthetics, however, are in contrast to all other drugs used in brain research. For example, the mg/kg dose of oral or parenteral sedatives, hypnotics and anticonvulsants varies widely across animal species, and serum concentrations do not necessarily reflect brain concentration. Inhalational anaesthetics then are ideal drugs to investigate in an *in vitro* system.

The inhalational anaesthetic IFL (Anaquest, Mississauga, ON) was selected as the prototype anaesthetic in these preliminary investigations into the cellular actions of anaesthetics. IFL was administered by perfusion using aCSF equilibrated with IFL vapour at specified gas concentrations. Fluotec 3 halothane vaporizers (Cyprane Limited, Keighley, UK) that had been previously dry aerated were calibrated for IFL using an infra-red anaesthetic gas analyzer (Ohmeda Respiratory Gas Monitor 5250, Murray Hill, NJ). The carrier gas was the compressed mixture of 95% O<sub>2</sub> and 5% CO<sub>2</sub>, and the flow rate was standardized at 500 ml/min. IFL vapour was scavenged (i.e., removed from the room) by a fume hood placed over the reservoir syringes; IFL vapour from the recording bath was partially scavenged by the bath suction. Since the solutions required bubbling for 10 to 15 min for equilibration (Miu and Puil 1989; Kress *et al.* 1991), three vaporizers were used simultaneously to prepare separate solutions for cumulative concentration-response experiments. The order of IFL concentrations employed in these experiments was both ascending and descending.

In determining a concentration of IFL that was proportionate to *in vivo* anaesthetic concentrations, age and temperature factors were considered. At normothermic temperatures, the MAC for IFL in 9 week old Sprague-Dawley rats, corrected for inspired-to-alveolar differences, is 1.46% (Mazze, Rice and Baden 1985). Consistent with MAC differences in children and adults, halothane MAC is 30% higher in 15 day old compared to 60 day old Sprague-Dawley rats (Cook *et al.* 1981). Since MAC is useful in potency comparisons, the relevant IFL MAC was calculated to be 1.9%. However, as the solubility of inhalational anaesthetics is ~2-fold greater at 22°C compared to 37°C, the *in vitro* proportionate IFL gas concentration would be about 1%. In the experiments, a variety of IFL concentrations (0.5, 1, 2 and 4%) were used to determine concentration-dependence. These gas percentages correspond theoretically to the following bath concentrations at 22°C in mM: 0.29, 0.61, 1.2 and 2.4<sup>14</sup> (Halsey 1980; Bosnjak, Supan and Rusch 1991). Although bath concentrations were not measured, some degree of evaporation would presumably take place from the tubing as well as the open recording bath. As a result, actual IFL concentrations at the neuronal level would be lower.

IFL 1% was also applied at a temperature of 31°C (see below), which corresponds to a calculated

---

<sup>14</sup>Although the IFL gas concentrations are strongly temperature-dependent, aqueous concentrations are relatively temperature-insensitive (Franks and Lieb 1996).

[IFL] of ~0.24 (Miu and Puil 1989). In addition, halothane 0.5% (Wyeth-Ayerest Canada, Inc., Montreal, PQ; calibrated Fluotec 3 vaporizer, Cyprane Limited, Keighley, UK) and enflurane 1.5% (Ohio Medical Canada Inc., Toronto, ON; calibrated Ohio Enflurane Vaporizer, Airco, Inc., Madison, WN) were used during room temperature experiments to determine an anaesthetic potency ratio for inhalational anaesthetics. These gas concentrations correspond theoretically to the following bath concentrations at 22°C in mM: halothane, 0.3; and enflurane, 1.

## 2.5 Experiments at a more *in vivo* relevant temperature

Limitations arise in interpreting *in vitro* results for *in vivo* anaesthesia. For example, the potency of inhalational anaesthetics increase with decreasing temperature as their solubilities increase. Although temperature is said not to impair consciousness until <30°C (Halsey 1980), anaesthetics are not required at 22°C in the prevention of movement with painful stimuli in goats maintained on life-support (Antognini 1993). Intuitively then, one might think that a marked decrease in temperature should prevent all cellular excitabilities. However, ionic channel conductances decrease only weakly as temperature drops (Hille 1992). To shed light on this difficulty, IFL experiments were also performed at temperatures >30°C (Miu and Puil 1989).

Experiments at an elevated temperature were performed with a heating apparatus consisting of three separate heaters. This involved heating the solution reservoirs so that IFL would equilibrate at the intended experimental temperature. In contrast, a perfusion line and recording bath heater distal to the site of room temperature IFL equilibration would have led to a concentration ~2-fold greater. This error is probably made in many investigations of inhalational anaesthetics at elevated temperatures (Eger 2d 1986).

Three "resistive" heaters were used to heat the reservoir solutions, the perfusion lines and the recording bath. The heating method can be likened to the filament in an incandescent lamp: a high resistance wire releases heat when electric current is applied. A recycled computer power supply was used to provide DC current and thus avoid 60 Hz interference. Electrical current was continuously applied with manual rheostat adjustments of current output to maintain constant temperatures. A feedback servo-loop was not used so as to avoid electrical transients due to line switching. For the reservoir heater, an aluminum block, with heat-sink resistors, was bored with

multiple holes for each inverted 60 ml syringe. Then, the perfusion lines were placed inside a brass rod along with a separate heated Nichrome wire.

In order to ensure steady-state heating in the reservoirs for long experiments, a room temperature reservoir was attached by a sump line to an initial heating reservoir, which was attached by a second sump line to a second heating reservoir. A separate solution system was used for IFL. Dilution of gas concentrations ( $O_2$ ,  $CO_2$  and IFL) was avoided by bubbling all of the reservoirs. In order to avoid mixing solutions with different temperatures and different IFL concentrations, the second sump line (between the first and second heating reservoirs for IFL) was clamped during slice perfusion with anaesthetic. During recovery, the sump line again was opened to replenish the second heated IFL reservoir. A mercury glass thermometer was placed in the second heated IFL reservoir.

For maintaining the elevated temperature of the solutions in the recording bath, a bath "interface" heater was constructed<sup>15</sup>. The interface heater consisted of a gas hood, made from a disposable plastic 10-ml syringe, placed over the recording bath. The gas hood then was flushed with moist, heated gases ( $O_2 + CO_2 \pm$  IFL vapour) by inserting a plastic-coated heating wire inside thick plastic tubing that connected an IFL vaporizer directly to the gas hood. As the interface heater did not work when the heated gases were dry, humidity was supplied by slowly and continuously injecting drops of distilled water into the heated gas tubing with an electric syringe injector.

During these experiments, the slices in the holding chamber were slowly heated and maintained at the same temperature as the recording bath. Before slice placement in the bath, an electrical thermometer using a thermocouple was attached to a micromanipulator and immersed at various depths and positions to ensure a constant bath temperature. Immediately following a recording session, the temperature was measured again to verify that the temperature had not changed.

## 2.6 Statistical analysis

Statistical analysis was performed using SPSS (Windows version 6.0, Chicago, IL) and

---

<sup>15</sup>When a heated aluminum plate was placed below the glass bottom of the recording bath, the temperature of the bath varied with depth. The heating plate therefore was not used.

GraphPad Prism (version 2.0, San Diego, CA) software. Results were expressed as means  $\pm$  SD. The distribution of data was examined with the boxplot. Appropriate data transformation was determined by power estimation, and homogeneity of variance was assessed with the Levene test. The difference between means for paired samples was evaluated by the *t*-test, and the comparison of multiple means from independent samples was made with the one-way analysis of variance. In addition, regression lines were plotted using the method of least squares, linear associations were assessed with the Pearson correlation coefficient, and slopes were compared using 95% confidence intervals. Statistical tests were considered significant when  $P < 0.05$ .

### 3 RESULTS

#### 3.1 Thalamocortical neurons

##### 3.1.1 Experimental database

The results were obtained from 284 thalamic relay neurons (postnatal age  $14 \pm 3$  days) in the ventral posterior nucleus<sup>16</sup> of the thalamic slice preparation (Palkovits and Brownstein 1988). Using the whole-cell configuration and a gluconate-based patch solution, resting membrane potentials (RMPs) were stable and action potentials were overshooting ( $>0$  mV). Average RMPs and input resistances were  $-67 \pm 5$  mV and  $220 \pm 94$  M $\Omega$ , respectively. Following neuronal recordings at an average temperature of  $22 \pm 2^\circ\text{C}$ , the average electrode offset was  $+1.1 \pm 1.8$  mV.

These neurons were assumed to be thalamic relay neurons, although intracellular staining was not performed during these experiments. Reportedly, there are "insignificant" numbers of GABA-ergic interneurons in the ventral posterior nucleus of the rat in contrast to the cat and monkey (Ohara and Lieberman 1993). However, interneurons may comprise 25% of the total population of cells in the lateral geniculate nucleus of the thalamus (Pape and McCormick 1995; Williams *et al.* 1996).

##### 3.1.2 Electrophysiological firing properties

Thalamic firing modes during wakefulness and sleep arise from intrinsic membrane properties that are voltage-dependent. Even when the thalamus is isolated from extrinsic brainstem influences, these modes persist during current-clamp recordings in neurons from *in vitro* thalamic slice preparations. For example, from a depolarized holding potential of about -50 mV,

---

<sup>16</sup>The ventral posterior nucleus is important for relaying somatic sensation, receiving afferent connections by way of lemniscal and spinothalamic inputs (Jones 1985). In addition, corticothalamic connections terminate in the ventral posterior nucleus.

intracellular injection of a constant depolarizing pulse elicited a tonic firing pattern of action potentials, the so-called "wakefulness" mode (see Fig. 1A, left). When the membrane potential was held at about -60 mV, a similar depolarization by the same current pulse would not trigger any firing. However, from a membrane potential near rest of about -75 mV, a similar depolarization would elicit an LTS, as in the so-called "sleep" mode (See Fig. 1A, right). *In vitro* properties were assumed to correlate with *in vivo* relay function.

The LTS exhibited the typical electrophysiological features reported for the underlying T-current. For example, from a hyperpolarized holding potential of about -75 mV, depolarizing current pulse injections elicited the LTS in a near all-or-none manner once a critical voltage was reached in the neuron (see Fig. 1B). Burst (i.e., phasic) firing occurred as a "bursting" of 2 to 5 fast action potentials at a frequency of about 300 Hz on the rising "crest" or "wave" of the LTS. The bursting occurred only if the LTS was of sufficient amplitude to reach the Na<sup>+</sup>-spike threshold. Application of 4-AP (3 mM) increased the LTS amplitude, presumably by blocking a K<sup>+</sup>-dependent transient A-current (Huguenard, Coulter and Prince 1991). When TTX was perfused, the same depolarizing pulses elicited a slow, transient spike without the characteristic burst of Na<sup>+</sup>-dependent action potentials (see Fig. 1B). The Ca<sup>2+</sup>-dependence of the LTS was readily demonstrated by removing external Ca<sup>2+</sup> ( $n = 6$ ; see Fig. 1C) or applying a Ca<sup>2+</sup>-channel blocker, Ni<sup>2+</sup> (0.5 mM;  $n = 4$ ).

These two voltage-dependent firing modes could be elicited from the same holding potential with depolarizing and hyperpolarizing current pulses. From an imposed depolarized potential positive to about -65 mV, depolarizing pulses of increasing magnitude elicited first subthreshold voltage responses and then tonic firing once a critical voltage was reached. Delayed firing was not seen and little if any accommodation in firing frequency occurred, suggesting the functional absence of the slowly inactivating K<sup>+</sup>-dependent slow A-current (Huguenard and Prince 1991; McCormick 1991). As the size of the current step was increased, the tonic firing frequency would steadily increase in a nearly proportionate manner. Then, when hyperpolarizing pulses were applied from this depolarized holding potential, an LTS could be elicited at the offset of a pulse, i.e., as a "rebound" depolarization (see Fig. 1D). Three factors, however, were important in eliciting the rebound LTS. First, the LTS occurred only if the hyperpolarizing pulse reached a critical voltage, presumably removing T-current inactivation (see Fig. 1D). Second, the

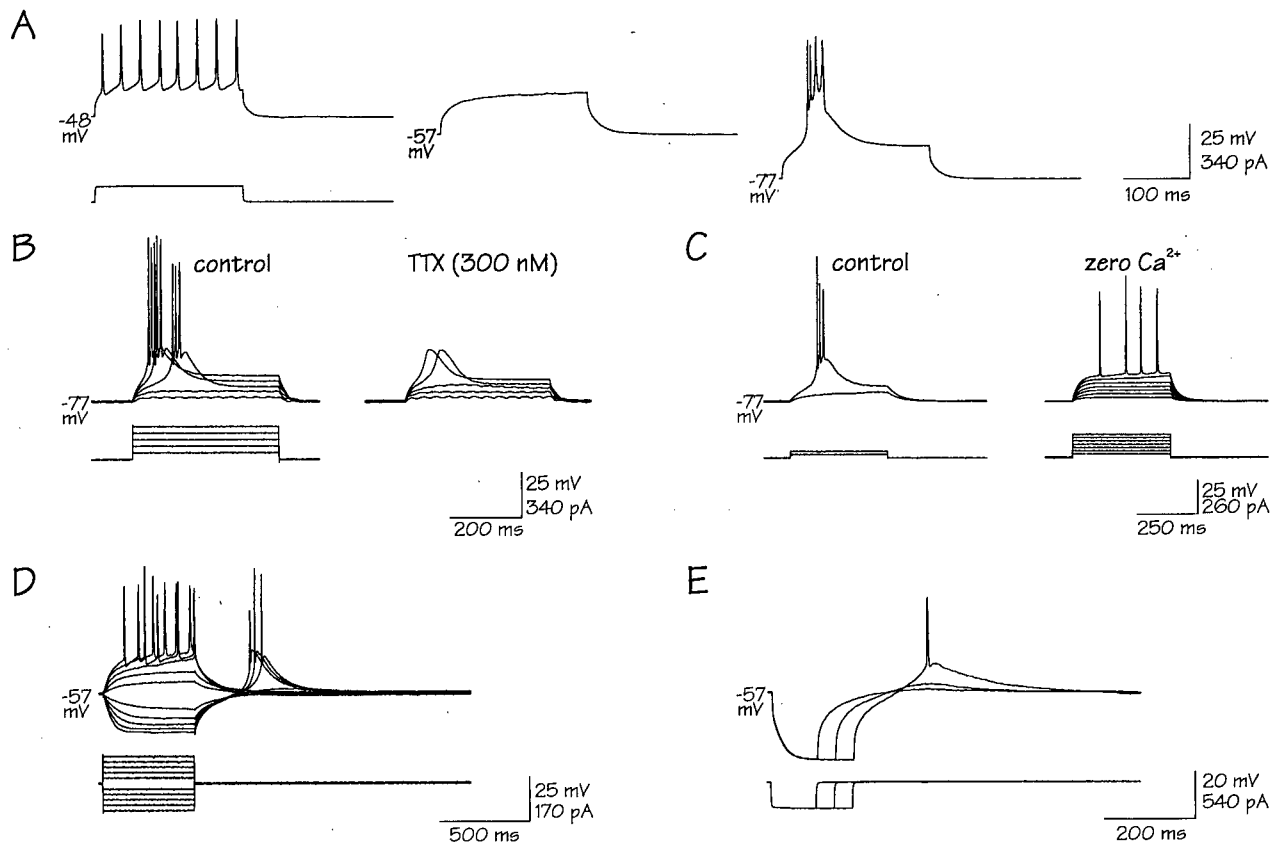


**Fig. 1. Voltage-gated firing modes of wakefulness and sleep.**

**A:** voltage-gated modes of firing (upper traces) elicited by the same depolarizing current pulse (lower trace) at 3 different holding potentials. Voltage response at depolarized potential shows tonic firing of action potentials without accommodation (wakefulness mode) whereas response at hyperpolarized potential shows burst firing of action potentials due to the  $\text{Ca}^{2+}$ -dependent low-threshold spike (LTS; sleep mode); the middle panel is the response at a potential intermediate between the 2 active modes. **B:** voltage-dependent activation of LTS elicited from a hyperpolarized holding potential with superimposed depolarizing current pulses of increasing amplitude before and after TTX. Note the slow spike that underlies the action potentials. **C:** superimposed depolarizing current pulses of increasing amplitude from a hyperpolarized holding potential with and without external  $\text{Ca}^{2+}$  showing  $\text{Ca}^{2+}$ -dependence of LTS. Note that in zero  $\text{Ca}^{2+}$ , tonic firing was elicited. **D:** tonic and burst firing modes elicited from the same depolarized holding potential with superimposed depolarizing and hyperpolarizing current pulses of increasing amplitude (simulating excitatory and inhibitory postsynaptic potentials). Note the rebound LTS and its dependence on the amplitude of the hyperpolarizing pulse (indicating voltage-dependent removal of inactivation of the underlying T-current). Note also the presence of hyperpolarization-activated inward rectification, i.e., saturation of hyperpolarizing pulses and the absence of hyperpolarization-activated depolarizing sag. **E:** superimposed hyperpolarizing pulses of increasing duration eliciting the rebound LTS. Note that the LTS was dependent on the duration of the hyperpolarizing pulse (indicating time-dependent removal of inactivation of T-current). In **D** and **E**, note that activation of the rebound LTS is additionally dependent on the voltage of the depolarized holding potential, as shown in **B** and **C**. Each panel is a different neuron.

hyperpolarizing pulse also had to be of sufficient duration to remove the T-current inactivation (see Fig. 1E). And third, the rebounding membrane potential had to reach a critical voltage for T-current activation (see Fig. 1B and C).

A hyperpolarization-activated depolarizing "sag" response was infrequently observed (cf. McCormick and Pape 1990), which can account for an absence of spontaneous rhythmic burst firing in these preparations. The failure to observe a sag in the hyperpolarizing responses may be related to the intracellular buffering of  $\text{Ca}^{2+}$  with EGTA in the patch-clamp solution, as the sag response appeared only with quite negative hyperpolarizations (Hagiwara and Irisawa 1989). In contrast to much thalamic research (intracellular recordings, McCormick 1992; cf. whole-cell recordings, Ramoa and McCormick 1994), a fast and persistent inward rectifier (presumably  $\text{K}_{\text{ir}}$ -current; see Section 3.4.3) was usually present with hyperpolarizing current pulses (see Fig. 1D). However, blockade of this fast inward rectifier with a low concentration of  $\text{Ba}^{2+}$  exposed a hidden sag response (see Section 3.4.5).

## 3.2 Inhibitory action of IFL at 22°C and 31°C

### 3.2.1 IFL hyperpolarized the membrane potential characteristic of wakefulness

IFL, being an anaesthetic, was initially tested at membrane potentials characteristic of neurons firing during wakefulness. As spontaneous firing was not observed in resting thalamic relay neurons *in vitro*, action potentials were elicited with DC current injection during current-clamp experiments. In initial investigations, continuous DC was injected to depolarize the membrane potential until the spike threshold was reached. Application of IFL (2%, gas concentration) by continuous perfusion curtailed the firing in 1 to 2 min in all neurons tested ( $n = 9$ ; see Fig. 2A). During this time, IFL also hyperpolarized the membrane potential by 2 to 4 mV. The membrane potential recovered during IFL washout, but firing resumed only occasionally (3 of 9 neurons). In neurons where firing did resume, recovery was partial, i.e., the frequency of firing was reduced compared to the pre-IFL period.

Because neurons generally became unstable when current was applied to elicit firing for more than 1 to 2 min, intermittent DC injections were employed in the next set of experiments. During

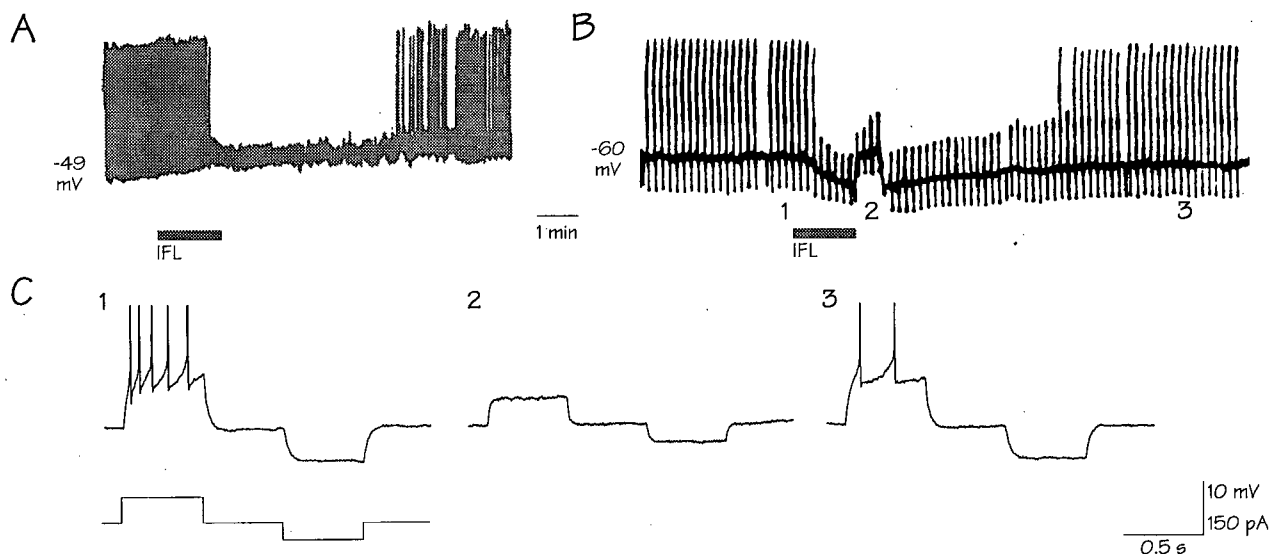


**Fig. 2. Inhibitory effect of isoflurane (IFL) on thalamic relay neurons.**

**A:** chart recording of membrane potential depolarized by continuous injection of positive DC current to elicit repetitive action potentials (upward deflections). IFL 2% (gas concentration) application for 1.5 min resulted in cessation of firing and a 2 mV hyperpolarization with partial reversibility during washout. Note that the recovery time was significantly longer than the onset time. **B:** chart recording of membrane potential depolarized by continuous injection as well as intermittent injection of DC current so as to avoid premature instability. Repetitive upward deflections of membrane voltage include action potentials initially whereas regular downward deflections show passive membrane responses to hyperpolarizing current pulses. In addition, smaller hyperpolarizing pulses were used intermittently to monitor series resistance. IFL 2% application for 1.5 min led to cessation of firing, membrane hyperpolarization of approximately 6 mV and a reduction in membrane resistance (holding current was increased briefly by 253% to manually clamp voltage again at -60 mV). Note that a maximal response was not achieved with a 1.5 min IFL application, as well as the slower but prompt recovery. **C:** expanded traces of the neuron in *B*, showing responses to the depolarizing and hyperpolarizing pulses before (1), during (2) and after (3) IFL application. Note that besides stopping firing by membrane hyperpolarization, IFL shunted current inputs. Spikes in *A* and *B* are submaximal due to chart recording limitations, and in *C* are truncated.

this protocol, a background injection of continuous DC injection was used to depolarize the membrane potential positive to the voltage range for burst firing, i.e., at membrane potentials where the T-current was inactivated (Hernández-Cruz and Pape 1989). Then, short depolarizing current steps were applied repetitively to elicit intermittent tonic firing. As a result of the greater stability, assessment of the time to first IFL effect and recovery onset was possible. Under these circumstances, the application of IFL (1% or 2%) induced a hyperpolarization within 30 s and suppressed firing shortly thereafter ( $n = 5$ ; see Fig. 2B). Although these applications produced up to 7 mV hyperpolarization, a steady-state effect was not apparent within the 1.5-3 min application, suggesting a less than maximal effect. During IFL washout, the membrane potential began to recover within 1 min, and recovery was extended over a period approximately 2 to 3 times longer than the application of IFL itself (see Fig. 2B). The slower recovery reflects differences in rates of IFL diffusion to the neuron and elimination from its environment, as a steady-state partial pressure at the site of action would not have been achieved. For example, continued partitioning of IFL probably occurred within the slice during the initial washout. After washout, the hyperpolarizing effect was reproducible on repeated IFL applications.

### 3.2.2 IFL decreased input resistance, shunting current inputs and reducing the membrane time constant

Intermittent DC pulses also were used to monitor input resistance during the IFL-induced hyperpolarization. Small hyperpolarizing pulses were repeatedly injected so as to minimize activating voltage-gated channels. During IFL application, the amplitude of voltage deflection in response to the hyperpolarizing current pulses progressively decreased, indicating a decrease in resistance ( $n = 5$ ; see Fig. 2B). Since the decrease in resistance could have been an indirect result of the hyperpolarization, the membrane potential was restored to the control value by re-adjusting the initial depolarizing holding current. At the control holding potential, input resistance was found to be decreased since the voltage deflection in response to the hyperpolarizing current pulse during IFL application was less than the control deflection. The required positive holding current also increased, providing another indication that the hyperpolarization was due to an increase in outward membrane current. An increase in outward membrane conductance has important mechanistic implications; the ion channel responsible for the hyperpolarization must have had an equilibrium potential negative to the voltage range characteristic of wakefulness (see

Section 3.4). During further experiments, a manual voltage clamp was maintained throughout the IFL application by increasing the positive holding current.

While compensating for the IFL-induced hyperpolarization, the amplitude of voltage deflection in response to the intermittent depolarizing current injections also decreased. In addition, control action potentials were not elicited during IFL application, presumably since their threshold could not be reached (see Fig. 2C). In other experiments with subthreshold depolarizations from a manual voltage clamp, the pulsed current was increased during IFL application to compensate for the reduction in voltage response (see Fig. 3A). For the same voltage response during control and IFL conditions, the relative increase in current reflected the IFL-induced increase in conductance (see Fig. 3B and C). The increase in membrane conductance, therefore, inhibited thalamic relay neurons in two ways. First, by increasing the conductance of an ion whose equilibrium potential was negative to the depolarized voltage range for tonic firing, IFL application moved the membrane potential away from the threshold for action potential generation. And second, by increasing membrane conductance, the effectiveness of injected current was "short-circuited" or "shunted," also preventing the membrane potential from reaching spike threshold.

Further analysis of the voltage responses to current pulses during IFL application included assessment of IFL effects on the membrane time constant. IFL application affected the rate of change in the membrane potential subjected to current pulse injection (see Fig. 3A and D). The decrease in input resistance was associated with a decrease in membrane time constant, suggesting that input capacitance was unchanged. Application of IFL reduced the voltage response then in both amplitude and time.

### 3.2.3 The inhibitory effect of IFL was direct

The IFL-induced increase in conductance could have been through a direct postsynaptic effect or an indirect effect involving the release of neurotransmitter. Three types of experiments were performed to assess contributions of possible presynaptic actions of IFL to the voltage responses. First, IFL decreased input resistance in current-clamp recordings during concomitant application of TTX (300 nM;  $n = 7$ ; see Fig. 4A). Because TTX blocks action potential related release, this

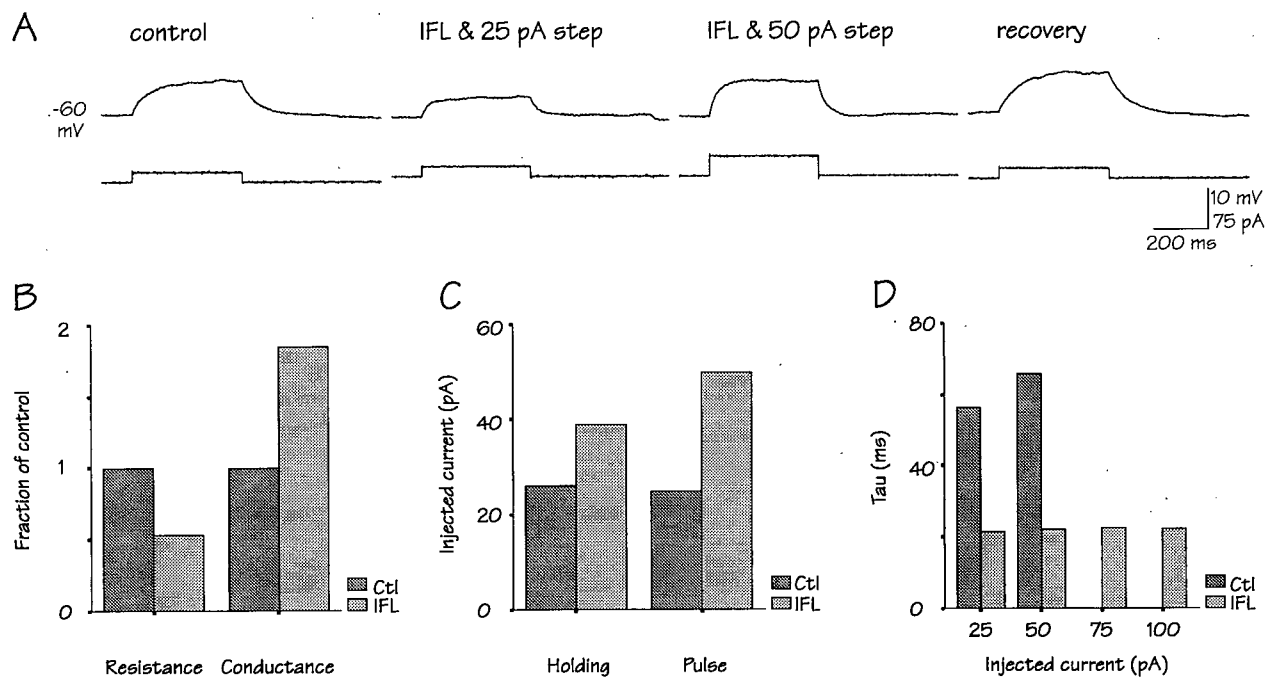


**Fig. 3. Effect of IFL on passive membrane properties.**

**A:** depolarizing current pulses showing subthreshold membrane potential responses before (control), during (IFL) and after (recovery) a IFL 2% application. A manual voltage clamp was used to maintain a constant depolarized holding potential of -60 mV throughout this experiment. Note that IFL reduced the rising and falling trajectory of the membrane potential in both amplitude (shunt) and time. **B:** bar chart showing IFL-induced decrease in input resistance and the reciprocal increase in conductance before and during IFL. **C:** bar chart showing increase in positive DC current required to maintain -60 mV and prevent hyperpolarization, and the increase in pulsed current during IFL to reach the same voltage as control. **D:** bar chart showing change in membrane time constant for a range of subthreshold depolarizing current pulses before and during IFL. Note that the IFL-induced decrease in membrane time constant was similar for a range of current pulses, suggesting that the resistance change was voltage-independent. All panels are from the same neuron.

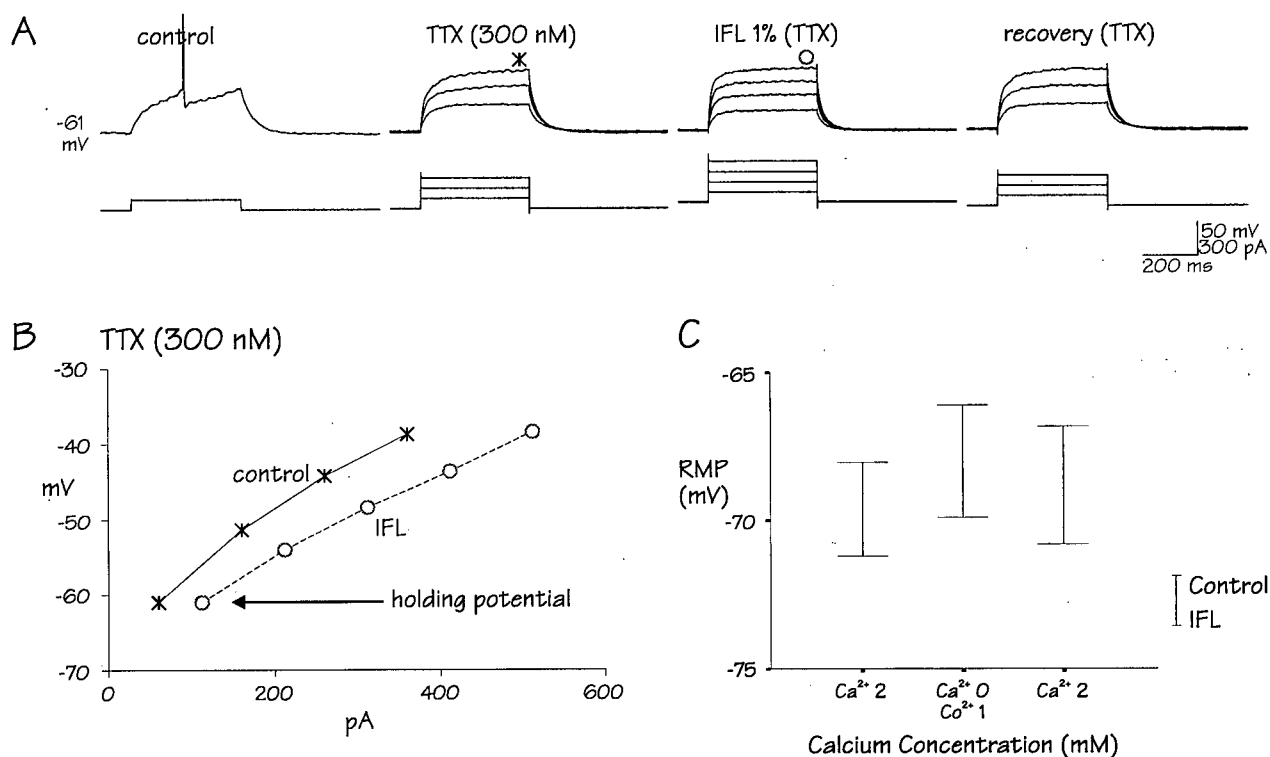


#### Fig. 4. Direct action by IFL.

**A:** current-clamp recordings before and after continuous perfusion with tetrodotoxin 300 nM (TTX), followed by IFL 1% application and IFL recovery. A manual voltage clamp was used to maintain a constant depolarized holding potential and a series of increasing depolarizing current steps were superimposed during each panel. Following TTX, voltage responses decreased, suggesting blockade of a persistent Na<sup>+</sup>-current. Significant outward rectification due to persistent K<sup>+</sup> activity, however, was not seen. Note the IFL-induced decrease in input resistance despite presumed synaptic blockade. **B:** plot of voltage-current (V-I) relationships from the neuron in A. Note the increase in holding current required to prevent hyperpolarization. To compensate for the IFL-induced hyperpolarization and shunt of the maximal control response in TTX, total depolarizing current was increased by 42%. Note also the relatively voltage-independent decrease in resistance during IFL, as reflected by the decreased slope (defined by Ohm's Law:  $R = V/I$ ). **C:** high-low chart showing control resting membrane potential (RMP; top) and IFL-induced hyperpolarization (bottom) in another neuron before, during and after washout of zero Ca<sup>2+</sup> with Co<sup>2+</sup> (1 mM; Mg<sup>2+</sup> 3 mM). Note similar hyperpolarization with IFL despite presumed synaptic blockade.

implied that the IFL-hyperpolarization was not due to action potential-dependent synaptic input. During these tests, the inability to elicit action potentials verified that TTX was effective, and the IFL action in the presence of TTX was noted to be relatively voltage-independent in the voltage range of tonic firing (see Fig. 4B). Second, a solution of zero  $\text{Ca}^{2+}$  ( $\text{CaCl}_2$  0 mM) and high  $\text{Mg}^{2+}$  ( $\text{MgCl}_2$  4 mM) was used to rule out IFL action through  $\text{Ca}^{2+}$ -dependent synaptic transmission. In these experiments, zero  $\text{Ca}^{2+}$  perfusion eliminated the LTS, implying that  $\text{Ca}^{2+}$  was not involved in the IFL increase of membrane conductance ( $n = 6$ ). And third, the rate of IFL-induced increase in membrane conductance as well as the peak increase was found to be preserved during concomitant application of the  $\text{Ca}^{2+}$ -channel blocker,  $\text{Cd}^{2+}$  ( $\text{CdCl}_2$  50  $\mu\text{M}$ ;  $n = 2$ ) and the  $\text{Ca}^{2+}$ -channel blocker,  $\text{Co}^{2+}$  in the absence of external  $\text{Ca}^{2+}$  ( $\text{CoCl}_2$  1 mM,  $\text{CaCl}_2$  0,  $\text{MgCl}_2$  3 mM;  $n = 2$ ; see Fig. 4C). Although experiments combining  $\text{Na}^+$ - and  $\text{Ca}^{2+}$ -channel blockers with zero  $\text{Ca}^{2+}$  perfusion may have provided an additional assurance, one can infer from the above responses that the IFL action on thalamic relay neurons was likely direct (i.e., postsynaptic) and not dependent on synaptic transmission. This does not rule out an action of IFL on the nerve terminal membranes and, indeed, IFL-induced hyperpolarization and shunt in presynaptic membranes would be expected to decrease synaptic activity *in vivo*, producing some additional anaesthetic depression.

#### 3.2.4 The inhibitory effect of IFL was concentration-dependent

The direct IFL action was further quantified by examining the relationship between drug concentration and effect. Three IFL concentrations (0.5, 1 and 2%) were used from the lower end of the vaporizer output range, and input resistance was compared in recordings which mostly were in current-clamp. Small hyperpolarizing pulses elicited subthreshold responses from potentials at or near rest. After 5 to 10 min of continuous IFL application, maximal drug effects were observed. The resistance was statistically decreased by IFL with paired analysis at each concentration.<sup>17</sup> However, a concentration-dependent effect for the decrease in resistance was not apparent when the means of each group was compared (mean control resistance =  $282 \pm 154$  M $\Omega$ ,  $n = 24$ ; IFL 0.5%,  $216 \pm 121$  M $\Omega$ ,  $n = 7$ ; IFL 1%,  $238 \pm 134$  M $\Omega$ ,  $n = 6$ ; IFL 2%,  $161 \pm 80$

---

<sup>17</sup>For example, with the lowest IFL concentration group, 0.5%, the input resistance on IFL application was found to be significantly different than the control resistance by paired *t*-test (2 tail  $P = 0.014$ ,  $n = 7$ ).

$M\Omega$ ,  $n = 11$ ). Examination of the data for each IFL concentration showed a concentration-dependent change in the median resistance, but there was considerable overlap in the data distributions for IFL 1% and 2% (see Fig. 5A).

Although a small sample size may have been responsible for the apparent lack of concentration dependence, neurons that had higher initial resistances had larger IFL-induced decreases. A possible association between the control input resistance and the absolute change was therefore assessed for each IFL concentration. The IFL-elicited change in resistance was plotted against the control value for each concentration and data were fit with three linear relationships (see Fig. 5B). Even an outlier in the upper range of the IFL 2% group was found to fit the 2% correlation quite well. The correlation coefficients indicated strong associations for each IFL concentration (IFL 0.5%:  $r = -0.81$ , 2-tail  $P = 0.027$ ,  $n = 7$ ; IFL 1%:  $r = -0.91$ ,  $P = 0.012$ ,  $n = 6$ ; IFL 2%:  $r = -0.94$ ,  $P < 0.0005$ ,  $n = 11$ ).

Statistical comparison of 95% confidence intervals for the slope of each line forced through the origin ( $x = 0$ ,  $y = 0$ ) revealed significantly distinct relationships (IFL 0.5%:  $-0.074$  to  $-0.16$ ; IFL 1%:  $-0.16$  to  $-0.32$ ; IFL 2%:  $-0.40$  to  $-0.52$ ). In addition, analysis of the mean relative change in input resistance with different IFL concentrations (see Fig. 5C, left) revealed significant concentration-dependent differences (square root transformation; Levene test for homogeneity of variance,  $P = 0.791$ ; analysis of variance,  $P < 0.0005$ ; Bonferroni multiple range test significant for differences between all IFL concentrations at  $P = 0.05$ ). IFL 0.5% induced a  $11 \pm 4\%$  decrease ( $n = 7$ ), IFL 1% induced a  $22 \pm 7\%$  decrease ( $n = 6$ ) and IFL 2% induced a  $43 \pm 9\%$  decrease in resistance ( $n = 11$ ).

Although a wide range of concentrations would be required to adequately establish a relationship of the IFL-concentrations to the effect, these results do provide information about the minimum effective IFL concentration. The concentration-dependent change in input resistance was compared with the change in conductance, since an IFL-induced increase in membrane conductance could be directly related to the shunt compensation by current injections. Resistance was therefore converted to conductance, and a concentration-effect plot was constructed for the relative change for the 3 IFL concentrations (see Fig. 5C, right). The slope of the concentration-effect curve for conductance, however, was steeper than the corresponding

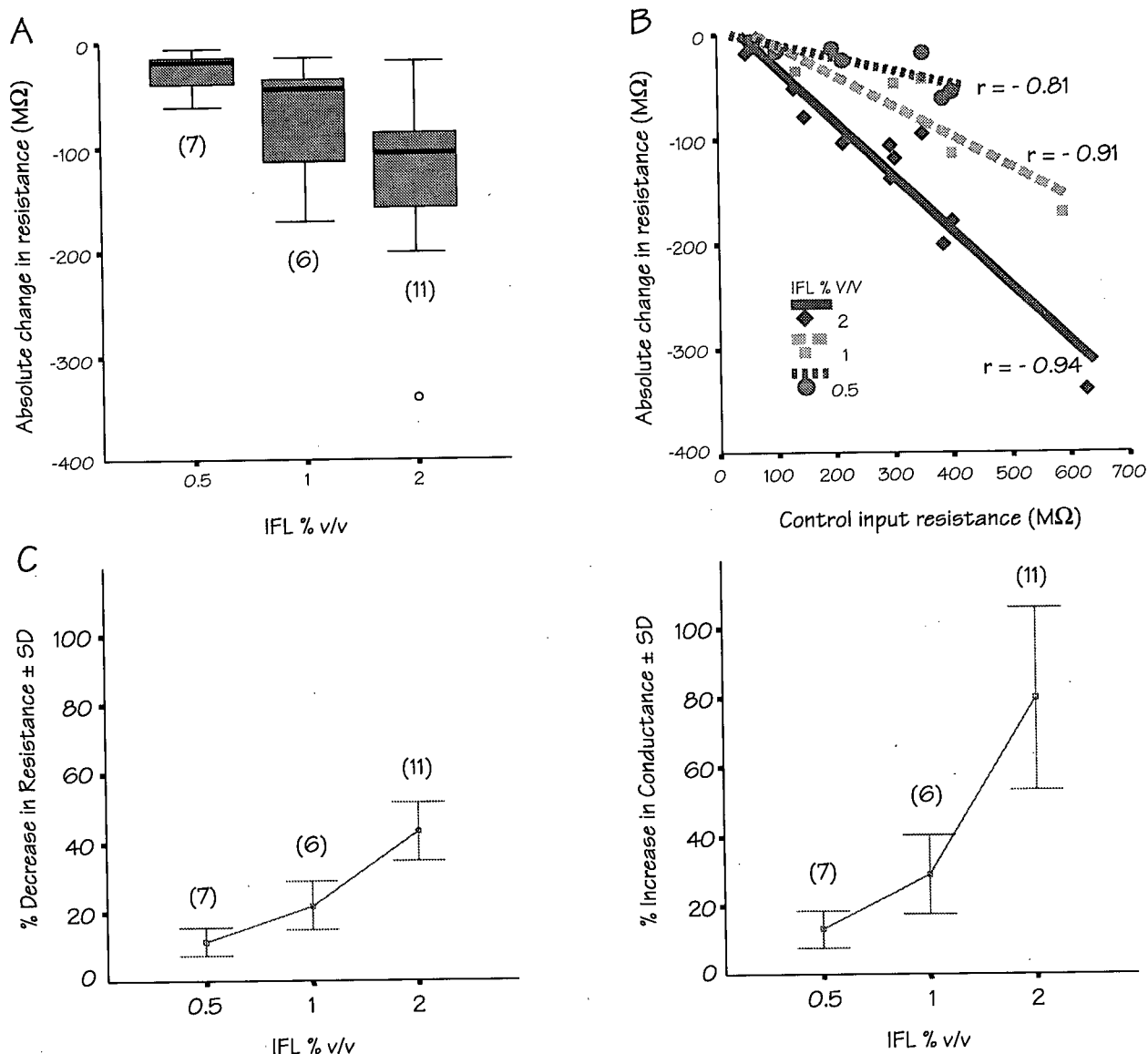


**Fig. 5. Concentration-dependent effect of IFL.**

**A:** boxplot of mean absolute decrease in resistance for 3 IFL concentrations. The thick horizontal line represents the median, the box represents 50% of cases from the 25th percentile to the 75th percentile, the whiskers represent the smallest and largest values that are not outlying values, and the "o" for IFL 2% represents an outlier. Note that the data were similar, especially between IFL 1 and 2%. Numbers in parentheses represent  $n$  at each concentration. **B:** graph of absolute change in resistance from the neurons in **A** (also same scale) versus control input resistance for 3 concentrations of IFL. Linear regression lines show distinct associations between magnitude of IFL effect and control resistance for each concentration ( $r = -0.81$ ,  $-0.91$  and  $-0.94$  for respective 0.5, 1 and 2% IFL concentrations). Note that the outlier in **A** fits the relationship found for the other IFL 2% neurons. **C:** error bar charts of mean relative decrease (%) in input resistance (left) and mean relative increase in conductance (right; bars represent  $\pm 1$  SD) versus IFL concentration (equivalent to a logarithmic scale). Note the different slopes for the two concentration-effect relationships. Numbers in parentheses represent  $n$  at each concentration.

curve for resistance, presumably since the conductance or the reciprocal of resistance, could theoretically increase to infinity. IFL 0.5% induced an increase in conductance of  $13 \pm 5\%$ , IFL 1% induced an increase of  $29 \pm 11\%$  and IFL 2% induced an increase of  $80 \pm 26\%$ . These three values suggest a linear relationship between IFL-concentration and the relative increase in conductance. Interestingly, IFL 4% increased conductance by 177% in one neuron. Although other steady-state applications were not used, the data are at least consistent with a nonreceptor mediated mechanism for IFL.

### 3.2.5 Temperature influence on IFL-induced inhibition

Since the solubility (and hence, the potency) of volatile anaesthetics increases with decreasing temperature, experiments were performed at temperatures greater than  $22^{\circ}\text{C}$ . As mentioned previously, there seemed to be greater difficulty in whole-cell recording at temperatures above room temperature. Although not studied, this difficulty may have related to an increase in evaporative fluid loss and hence slice damage when the pre-warmed slice was transferred to the warm recording chamber.

Initial trials were attempted at  $35^{\circ}\text{C}$  and recordings with IFL applications were completed in only 2 neurons. In one neuron, IFL 1% increased conductance by 39% and hyperpolarized resting membrane potential by 2 mV. In the other neuron, IFL 1.5% hyperpolarized the resting membrane potential by 8 mV. In both neurons, IFL was applied for 10 min but a steady-state effect did not occur.

Because of these difficulties, further experiments were performed at a temperature intermediate between room temperature and  $35^{\circ}\text{C}$ . Experiments with IFL 1% were completed successfully at  $31^{\circ}\text{C}$  in 5 neurons. Temperature-related changes in resting conductance were not evident from this small sample, although paired testing with room temperature controls was not done (cf. Thompson, Masukawa and Prince 1985). A refinement was made to the recording chamber in case the slow onset at  $35^{\circ}\text{C}$  was due to IFL evaporation. IFL vapour was administered over the slice in the bath "interface" heater, along with the warmed and humidified hood gas (95%  $\text{O}_2$  and 5%  $\text{CO}_2$ ). Two observations suggested that the IFL vapour administered over the bath maintained IFL in solution. First, the time to maximal IFL effect at  $31^{\circ}\text{C}$  was similar to the

experiments at room temperature. And second, the drug effect did not reverse in one experiment on discontinuation of the IFL application by perfusion, until the IFL vapour in the hood was also discontinued. Although the additional application of anaesthetic in the gas phase overlying the submerged slice was different from the room temperature experiments, the objective here was to ensure the maintenance of IFL 1% in solution rather than compare effects at different temperatures.

IFL 1% increased resting conductance at 31°C proportionately to the control conductance. Linear regression showed a strong association between the IFL-elicited change in conductance and the initial control value ( $r = -0.99$ , 2 tail  $P = 0.001$ ,  $n = 5$ ; see Fig. 6B). Even an outlying value in the distribution of absolute change in conductance was found to fit the correlation quite well (see Fig. 6A and B). At 31°C, IFL 1% increased conductance by  $15 \pm 3\%$  ( $n = 5$ ), representing about half of the increase induced by IFL at room temperature (see Fig. 6C). When considered with the effect of IFL 0.5% at 22°C, these results suggest that the IFL MAC value of 1.9% for juvenile rats (body temperature, 37°C) would be an effective *in vitro* concentration at 37°C.

### 3.2.6 Analysis of IFL's inhibitory action

In summary, IFL inhibited thalamic relay neurons by increasing resting membrane conductance through direct actions that were concentration-dependent. In addition, IFL was effective at a concentration that was proportionate to *in vivo* anaesthetic concentrations. The increase in conductance produced inhibition in two ways: (1) hyperpolarizing the resting potential; and (2) shunting voltage transfers. IFL also decreased the membrane time constant.

Functionally, a reduction in membrane resistance and time constant in thalamic relay neurons would reduce both the amplitude and time course of incoming postsynaptic potentials. As a result, temporal and spatial summation in the dendrites and soma would be decreased, thereby impairing the characteristic relay of tonic activity to the cortex. In *in vivo* anaesthesia, the relay of sensory transmission as well as the coherent reverberation of oscillating rhythms in thalamocortical-corticothalamic circuits could be disrupted by this action.

The effects of IFL on the firing modes that reflect the relay of tonic firing patterns during

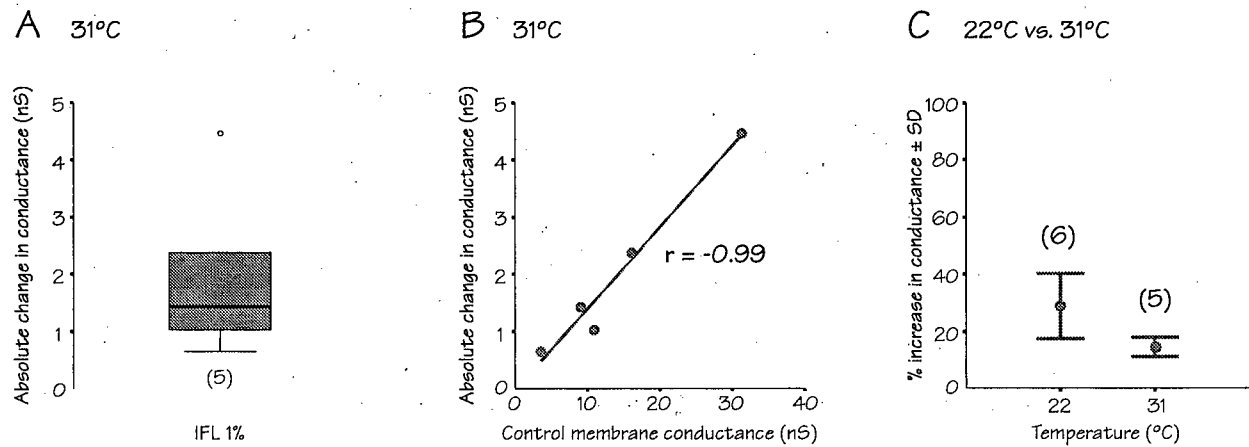


**Fig. 6. Effect of IFL on conductance at 31°C.**

**A:** boxplot for absolute change in input conductance by IFL 1%. The "o" represents an outlying value. The number in parenthesis represents  $n$ . **B:** graph of absolute change in conductance from the neurons in A (also same scale) *versus* control conductance. Linear regression line shows distinct association between magnitude of IFL 1% effect and control conductance ( $r = -0.99$ ). Note that the outlying value in A fits the relationship found for the other IFL 1% neurons at 31°C. **C:** error bar chart of mean relative change in conductance (%; bars represent  $\pm 1$  SD) *versus* 2 temperatures (22 and 31°C).

wakefulness and the phasic patterns of sleep, depolarizing afterpotentials (DAPs), and high-threshold spikes (HTSs), will be presented next.

### 3.3 IFL and firing properties at 22°C and 31°C

#### 3.3.1 IFL prevented the firing modes characteristic of wakefulness and sleep

First, the inhibitory effect of IFL-induced hyperpolarization was tested on firing. Each minute, depolarizing step current was applied to neurons from a depolarized holding potential positive to  $\sim -65$  mV to produce tonic firing. This was followed by a hyperpolarizing step current for detection of changes in resistance and for generating the rebound burst (see Fig. 7). This current protocol can be likened to the awake state with incoming excitatory and inhibitory postsynaptic potentials (EPSPs and IPSPs, respectively). In order to monitor the time course of drug onset and recovery, neither the depolarized holding potential nor the current pulses were adjusted during IFL application. On application of IFL, the potential became more negative, input resistance decreased, and tonic and subsequently burst firing stopped (see Fig. 7). With continued IFL application after the suppression of firing, the hyperpolarization and decreased resistance continued to grow. The depolarizing pulse did not convert from tonic to burst firing during the hyperpolarization as expected (see Fig. 1A), presumably because of a shunted depolarizing response. The hyperpolarizations that simulated IPSPs also were shunted, which led to divergent effects on the "RMP" and the potential achieved by the hyperpolarizing pulses; as the "RMP" became increasingly negative, the hyperpolarizing pulse (paradoxically) produced an increasingly positive membrane potential (see Fig. 7). The reduction in the hyperpolarizing response would have decreased voltage-dependent removal of inactivation, whereas the hyperpolarized holding potential would have restricted voltage-dependent activation of the underlying T-current. During IFL washout, the neuron's ability to fire in either mode was delayed for several minutes until recovery was observed from the induced hyperpolarization and decreased resistance. The tonic firing frequency (TFF) recovered more slowly, compared to the all-or-none-like bursting activity.

Next, the shunting effect of IFL application on firing modes was tested while controlling for the drug-induced hyperpolarization. Despite maintaining the same depolarized holding potential with a manual voltage clamp, tonic and rebound firing were shunted by IFL (see Fig. 8; Ries and

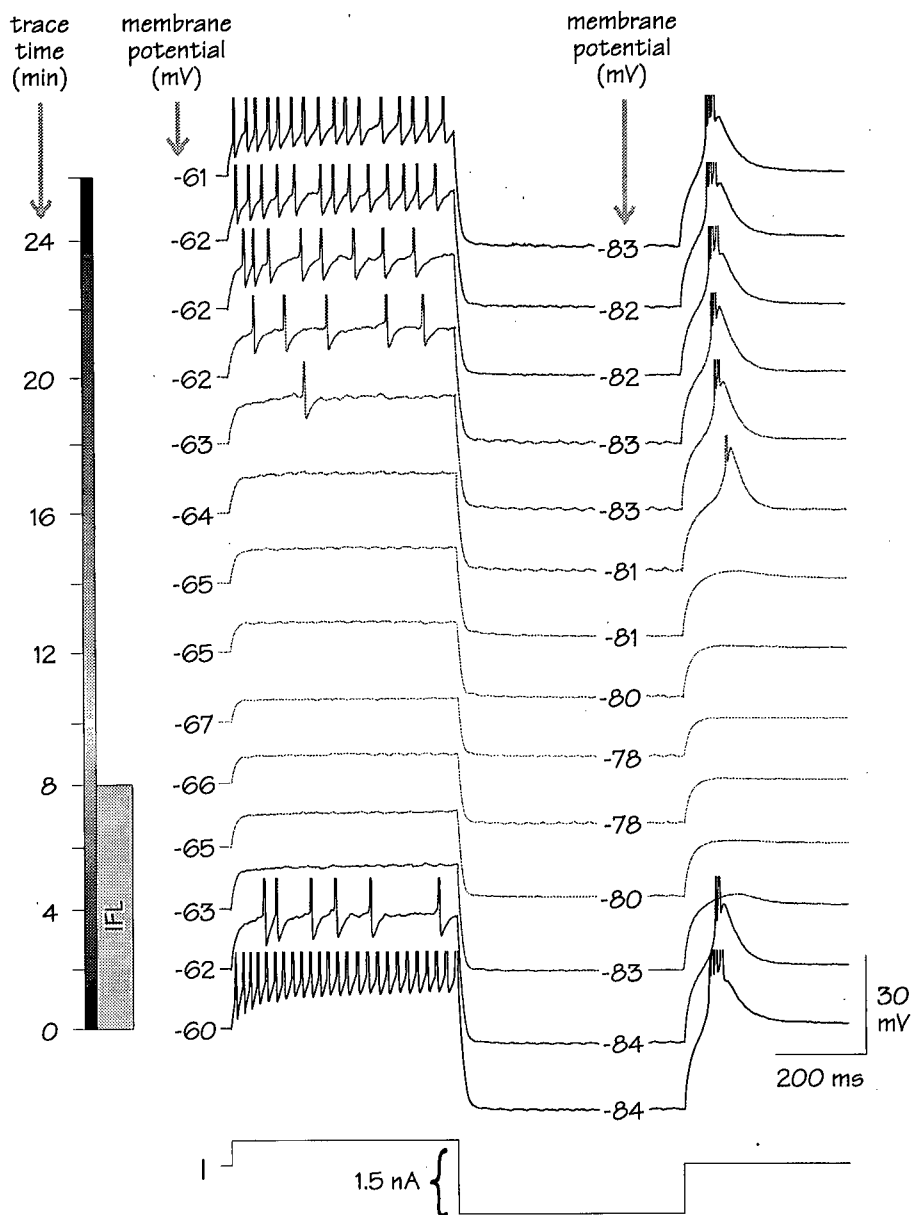


**Fig. 7. Effect of IFL-induced hyperpolarization on firing modes.**

Raster plot of consecutive voltage responses at 2 min intervals (from bottom to top) showing changes (from left to right) in "resting" potential, tonic firing, input resistance (as reflected by a hyperpolarizing voltage response) and rebound burst firing during an 8 min IFL 2% application. Although sufficient depolarizing and hyperpolarizing pulses were applied to initially elicit tonic and burst firing respectively from an imposed depolarized holding ("resting") potential, these injected currents were not changed during the exposure to IFL. IFL then hyperpolarized and shunted inputs to prevent tonic and burst firing. The depolarizing pulse did not convert firing from the tonic to the burst mode. After the firing modes were blocked, the neuron continued to hyperpolarize during the late washin, suggesting that a lesser concentration of IFL would have been sufficient to prevent the firing. As IFL washed out, the membrane potential and the tonic frequency of action potentials recovered slowly in comparison to the all-or-none-like response of the LTS. During onset, resistance decreased as reflected by the voltage change induced by the hyperpolarizing current command. Note the divergent effects on the "resting" potential and the voltage reached by the hyperpolarizing current step. Spikes are truncated.

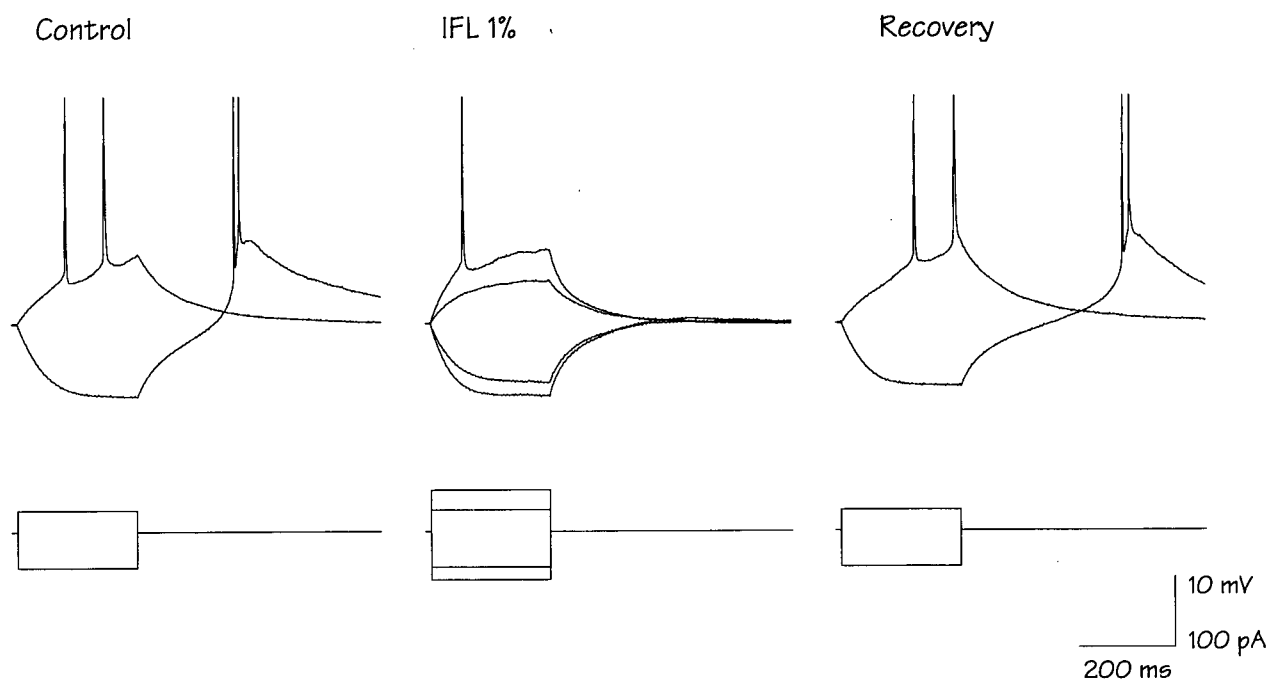


**Fig. 8. Effect of IFL-induced shunt on firing modes.**

Voltage response to depolarizing and hyperpolarizing current pulses from a constant depolarized holding potential, 1 min before, 8 min during, and 10 min after a IFL 1% application. Note that the action potentials in control were completely shunted by IFL, yet an increase in current during IFL elicited a single action potential (superimposed depolarizing voltage response during IFL). To compensate for the IFL-induced hyperpolarization and shunt of the control spike, total depolarizing current was increased by 91%. In control, a hyperpolarizing current pulse produced a rebound LTS with a burst of 2 action potentials. Note that IFL eliminated this rebound spike burst and an increase in hyperpolarizing current did not elicit a slow spike (superimposed response during IFL achieving the control hyperpolarization). However, the shunt of both firing modes was completely reversible. Spikes are truncated.

Puil 1993). An increase in the depolarizing current pulse elicited one or more action potentials at all IFL concentrations tested (IFL 1% and 2%;  $n = 13$ ). However, an increase in the hyperpolarizing current pulse resulted in a greatly reduced rebound LTS (IFL 1% and 2%;  $n = 10$ ). The shunted firing modes characteristic of wakefulness and sleep were investigated further.

### 3.3.2 IFL shunted tonic Na<sup>+</sup>-spike electrogenesis

Prior to the anaesthetic application, the number of repetitively fired action potentials generally increased in proportion to depolarizing current injection. During IFL application, however, this proportionality sometimes disappeared despite DC-compensation for the hyperpolarization and an increase in step current. These varying relationships between injected current and the number of evoked action potentials were analyzed using "electronic" dose-response curves. For example, in neurons in which the TFF continued to increase in a linear manner with increasing current during IFL "antagonism" (i.e., shunt action), the dose-response curve shifted to the right in a parallel manner, consistent with a decrease in "potency" (see Fig. 9A and B). The maximal response, or "efficacy," before or during IFL was not determined, but the parallel shift suggested surmountable antagonism. Instantaneous frequency analysis was then used to assess accommodation during repetitive firing. Although IFL markedly decreased the TFF throughout the duration of constant-amplitude pulses, the degree of accommodation was similar when matched responses were compared in three neurons (see Fig. 9C, D and E). However, most neurons exhibited some nonlinearity in the increase in TFF with increasing current pulses during IFL administration.

Extremely nonlinear responses were occasionally observed when IFL 2% uncoupled repeated Na<sup>+</sup>-spike electrogenesis from DC injections despite compensation for the anaesthetic-induced hyperpolarization and an increase in injected DC ( $n = 3$ ; see Fig. 10A). In these neurons, the membrane potential did not repolarize sufficiently and remained above spike threshold for the duration of the pulse. Instead of eliciting repetitive tonic firing, the depolarizing step generated oscillations in membrane potential. The oscillations presumably represented aborted action potentials due to incomplete removal of sodium channel inactivation. In contrast to the linear IFL responses, this IFL antagonism (i.e., the effect of the shunt) was insurmountable (see Fig. 10B).

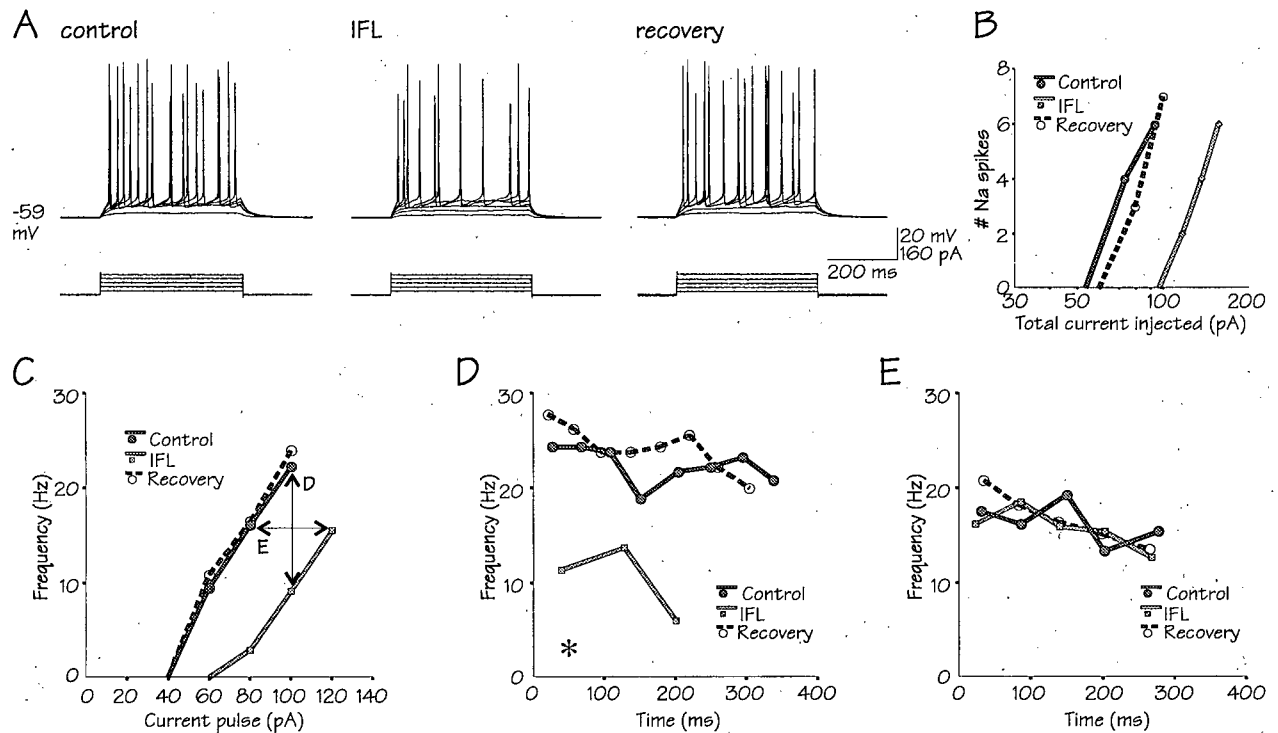


**Fig. 9. Effect of IFL on repetitive tonic firing.**

**A:** tonic firing mode before, during and after IFL 1% from a constant depolarized holding potential using superimposed depolarizing current steps of increasing amplitude. Note that the voltage responses were shunted by IFL, but the injection of more current evoked repetitive firing of action potentials. To compensate for the IFL-induced hyperpolarization and shunt of the threshold response, total depolarizing current was increased by 59%. **B:** graph of the number of Na<sup>+</sup>-spikes *versus* injected current (holding and pulses) to represent an "electronic" dose-response relationship. Note that the IFL-induced increase in membrane conductance "antagonized" (shunted) the tonic firing response by decreasing the "potency" (rightward shift along the dose axis) of the injected current; a change in the "efficacy" (maximal effect) was not determined. **C:** graph of the average tonic firing frequency (TFF) *versus* injected current (pulses only) with reference to the comparisons made in *D* and *E*. **D:** graph of instantaneous firing frequency *versus* time for matched current pulses (100 pA) showing about a 50% decrease in TFF with IFL. Note the even larger decrease in TFF when the total injected current (holding and pulsed) are matched (\*). **E:** graph as in *D*, but during a matched frequency response (80 pA pulse for control and recovery, and 120 pA for IFL). Note similar accommodation for the 3 states. All panels are from the same neuron.

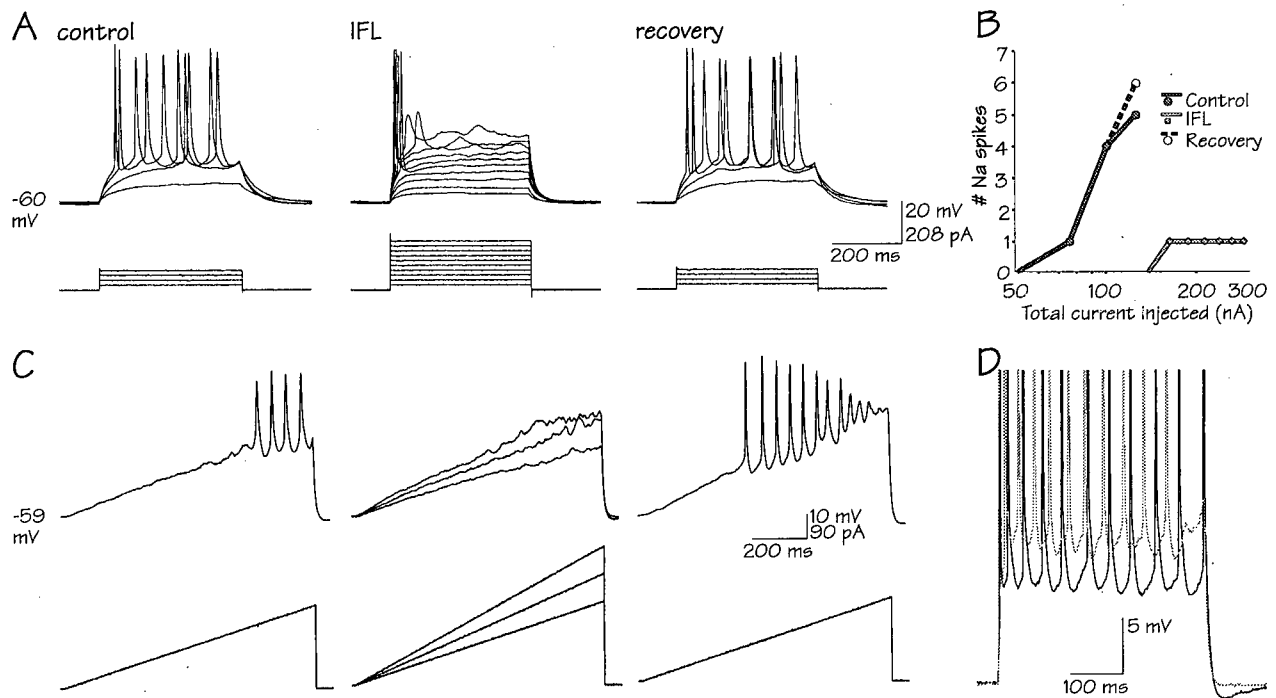


**Fig. 10. Effect of IFL on repolarization during repetitive tonic firing.**

**A:** tonic firing mode before, during and after IFL 2% from a constant depolarized holding potential using superimposed depolarizing current pulses of increasing amplitude. To compensate for the IFL-induced hyperpolarization and shunt of the threshold response, total depolarizing current was increased by 116%. Note that larger depolarizing steps did not elicit repetitive firing presumably since there was a reduction in post-spike repolarization (the membrane potential remained above spike threshold). **B:** electronic dose-response curves for the three conditions in A. Note that IFL antagonized tonic firing in this neuron by decreasing both "potency" and "efficacy" of the injected current. **C:** voltage responses to depolarizing current ramps before, during and after IFL 2% from a depolarized holding potential in the same neuron. In addition to the shunted voltage response during IFL, note that action potentials could not be elicited with larger superimposed current ramps that achieved either the control membrane trajectory or a steeper one. **D:** superimposed spike-train response and post-train AHP from a constant depolarized holding potential in a different neuron before (black) and during IFL 2% (gray). Total depolarizing current was increased 110% to match the number of evoked action potentials to control. Note the restricted repolarization as well as the decrease in amplitude of the post-train afterhyperpolarization (AHP) with IFL. Spikes are truncated in D.

Because of the possibility that the reduction in repolarization could have resulted from suppressed  $\text{Na}^+$ -activation, action potentials were analyzed before and during IFL application. The voltage-threshold for the first spike increased (i.e., the voltage became more positive) with IFL application (1% and 2%) by  $2.4 \pm 1.8$  mV ( $n = 7$ ; increase in 7 of 9 neurons with no change in 2 neurons). Recognizing that the rate of voltage change influences firing threshold, an attempt was made to control the rate of subthreshold depolarization by using injections of slowly rising current ramps. Although the anaesthetic-induced shunt reduced the rate of voltage change making it difficult to match trajectories of membrane potential, an interesting response was observed in a neuron in which IFL 2% uncoupled repetitive  $\text{Na}^+$ -spike firing from DC injection (see Fig. 10C). In addition to shunting the voltage response, IFL prevented the firing of action potentials during current ramps that closely matched or even exceeded the rate of voltage increase during control.

Postspike responses also were compared before and during IFL. For example, the maximal negativity of the postspike afterpotential (AHP) decreased with IFL applications (1% and 2%) by  $4.5 \pm 2.7$  mV ( $n = 7$ ; no change in 2 additional neurons). In addition, IFL reduced the slow posttrain AHP amplitude and duration when the AHP was present ( $n = 4$ ; see Fig. 10D). IFL administration may have directly or indirectly (i.e., the shunt action) reduced the delayed rectifier and  $\text{Ca}^{2+}$ -activated  $\text{K}^+$ -currents. However, the suppressed postspike repolarization would have further reduced repetitive tonic firing by decreasing the removal of  $\text{Na}^+$ -inactivation.

To assess whether or not the shunt alone was responsible for these changes, further experiments were performed with IFL 1% at  $31^\circ\text{C}$ , a more physiologically relevant temperature. During a manual voltage-clamp, IFL consistently shunted depolarizing current pulses to prevent the transition to tonic firing in a reversible manner (5 of 5 neurons; see Fig. 11A). In these neurons, the magnitude of current required to elicit a  $\text{Na}^+$ -spike increased during IFL application (see Fig. 11B). Consistent with the previous results at room temperature, the relative increase in current-threshold ( $43 \pm 25\%$ ) was always greater than the relative increase in conductance ( $15 \pm 3\%$ ; see Fig. 11C), since the latter action produced hyperpolarization as well as shunting effects. For example, IFL 1% at  $31^\circ\text{C}$  increased the voltage-threshold for  $\text{Na}^+$ -spikes during constant amplitude pulses (paired  $t$ -test, 2-tailed  $P = 0.012$ ,  $n = 5$ ; see Fig. 11D). In addition, the maximal negativity of postspike AHPs became more positive (paired  $t$ -test, 2-tailed  $P = 0.034$ ,  $n = 5$ ; see

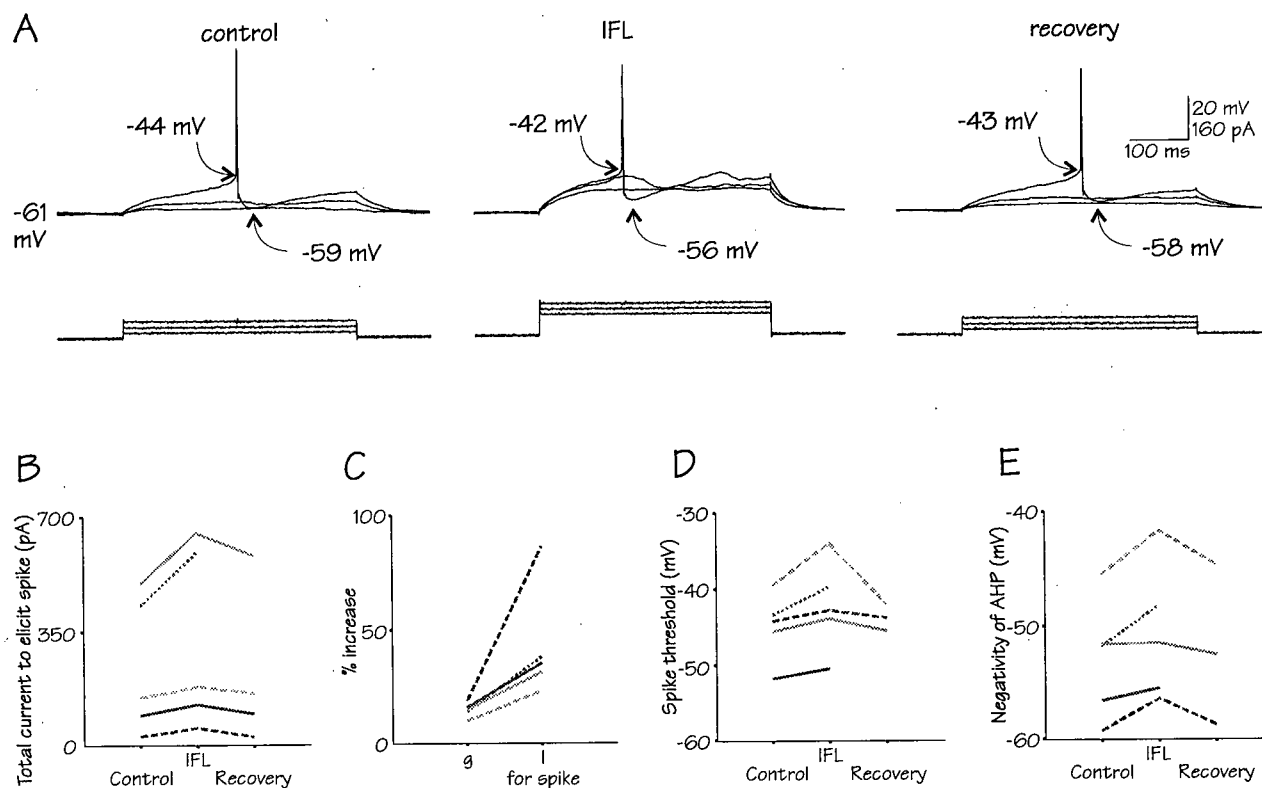


**Fig. 11. Effect of IFL on tonic firing at 31°C.**

**A:** tonic firing response elicited before, during and after IFL 1% application from an imposed depolarized potential. Superimposed depolarizing current pulses of increasing amplitude were administered until a single spike fired. Note that at 31°C, IFL 1% shunted the injected current pulses. Note also the IFL-induced increase in voltage-threshold and the decrease in AHP negativity. **B:** chart of the current-threshold for a single  $\text{Na}^+$ -spike before, during and after IFL 1% at 31°C, plotted for each of 5 neurons. **C:** chart comparing IFL-induced relative increase (%) in membrane conductance ( $g$ ) with relative increase in total current required to reach spike threshold ( $I$ ), plotted for each of the same 5 neurons. Note that the relative increase in required current exceeded the increase in membrane conductance since the current compensated for more than just the shunt, i.e., the hyperpolarization, the shunt and the increase in spike threshold. **D:** chart of voltage-threshold for spikes before, during and after IFL 1% at 31°C, plotted for each of the same 5 neurons. Note that IFL increased the  $\text{Na}^+$ -spike threshold. **E:** chart of the negativity of AHPs before, during and after IFL 1% at 31°C, plotted for each of the same 5 neurons. Note that IFL restricted the AHP. In *B*, *D* and *E*, one neuron became unstable during recovery. As well in *E*, 60-Hz interfered with the recovery analysis of another neuron.

Fig. 11E).

### 3.3.3 IFL suppressed low-threshold $\text{Ca}^{2+}$ -spike electrogenesis

The IFL burst suppression also was investigated further. Since spontaneous bursting behaviour was not observed, IPSPs and their decay again were simulated with pulsed current to evoke the rebound LTS. From an imposed depolarized holding potential within the voltage range for LTS-activation, hyperpolarizing current steps of increasing amplitude were applied to remove voltage-dependent inactivation of the underlying T-current. A manual voltage-clamp was used to compensate for the IFL-induced hyperpolarization and therefore maintain the same potential for activating the LTS. In all neurons, IFL (0.5, 1 and 2%) shunted the hyperpolarizing pulse and suppressed the rebound LTS even when the reduced hyperpolarization was compensated by an increase in injected current (10 of 10 neurons; see Fig. 8). However, the LTS could be evoked during IFL application to some extent by one of two ways: first, by increasing the hyperpolarization beyond the control threshold level for eliciting an LTS; and second, by increasing the duration of the hyperpolarizing stimulus.

By increasing the hyperpolarization beyond the control voltage-threshold during IFL application, the rebound LTS steadily increased in a graded fashion with increasing hyperpolarizing pulse amplitude, in contrast to the all-or-none control LTS (see Fig. 12A). The graded response implied that IFL application had expanded the voltage range for the removal of inactivation for T-current. Maximal rebound LTS amplitudes generally were not attainable with IFL as a fast inward rectifier prevented stable hyperpolarizations beyond -90 mV during current-clamp recordings. However, the rebound LTS also could be returned during IFL application by increasing the duration of the hyperpolarizing current pulse, without any shunt compensation (see Fig. 12B). Besides affecting voltage-dependent removal of T-current inactivation then, IFL appeared to change time-dependent de-inactivation. The recovery of T-current inactivation for the rebound LTS was difficult to assess independent of steady-state inactivation during current-clamp recordings because of the shunted hyperpolarizing pulse.

LTS activation and inactivation also appeared to be affected by IFL since the time-to-peak of the LTS as well as its duration were reduced to varying degrees (see Fig. 13A, upper panels).

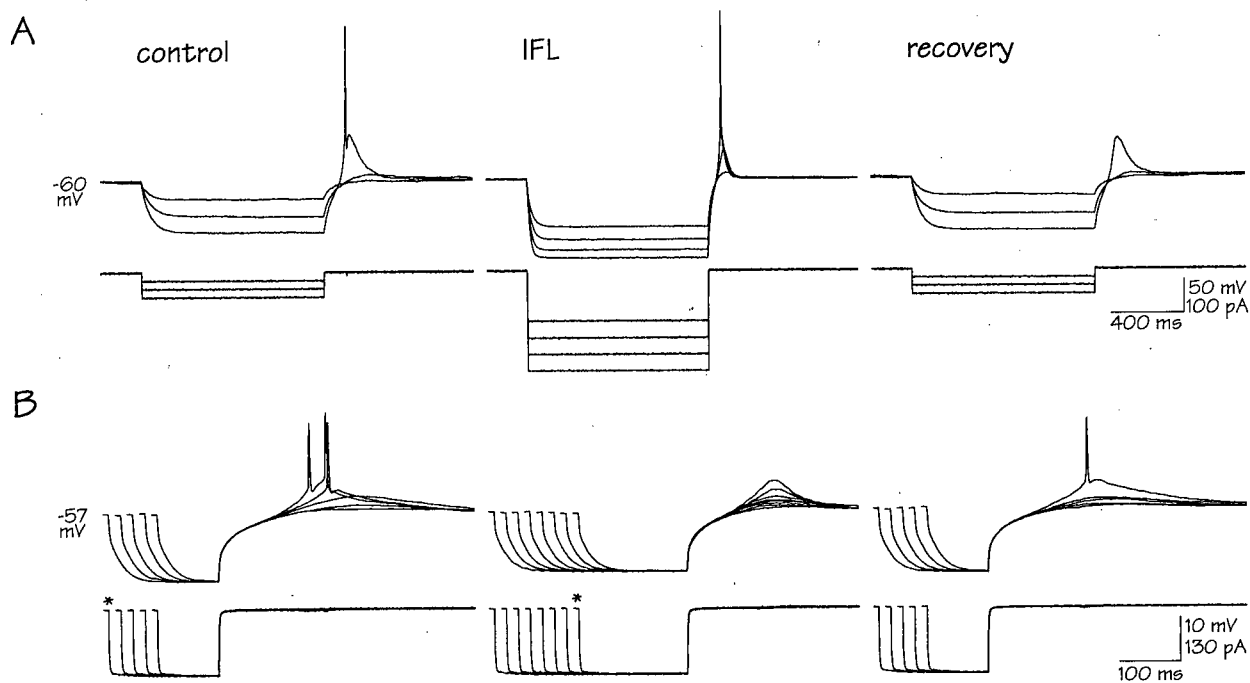


**Fig. 12. Effect of IFL on rebound LTS: de-inactivation of the underlying T-current.**

**A:** superimposed voltage traces of rebound LTS from a constant depolarized holding potential before, during and after IFL 2%. Superimposed hyperpolarizing pulses of increasing magnitude were applied during control and IFL until  $\text{Ca}^{2+}$ - and  $\text{Na}^{2+}$ -spikes were achieved before and during IFL. During IFL, an increase in the maximum control hyperpolarizing current pulse by 100% almost compensated for the IFL-induced shunt, but the LTS was largely suppressed. Note that by hyperpolarizing beyond the voltage associated with a maximum control LTS, the rebound LTS could be regained in a now graded manner. Note also that a 300% increase in pulsed current was required to elicit an LTS-associated  $\text{Na}^{+}$ -spike. **B:** voltage recordings of rebound LTS from a depolarized holding potential before, during and after IFL 0.5% with superimposed increases in the duration of the hyperpolarizing pulses. "\*" indicates the same duration pulse (175 ms) in control (longest control pulse) and IFL (shortest IFL pulse). By shunting the hyperpolarizing pulse, IFL prevented a rebound LTS with the 175 ms pulse. Note, however, that increasing the duration of the shunted hyperpolarizing current step led to a progressive increase in the rebound LTS. Note also during IFL in both A and B the shorter time to peak LTS and the shortened duration of the LTS.

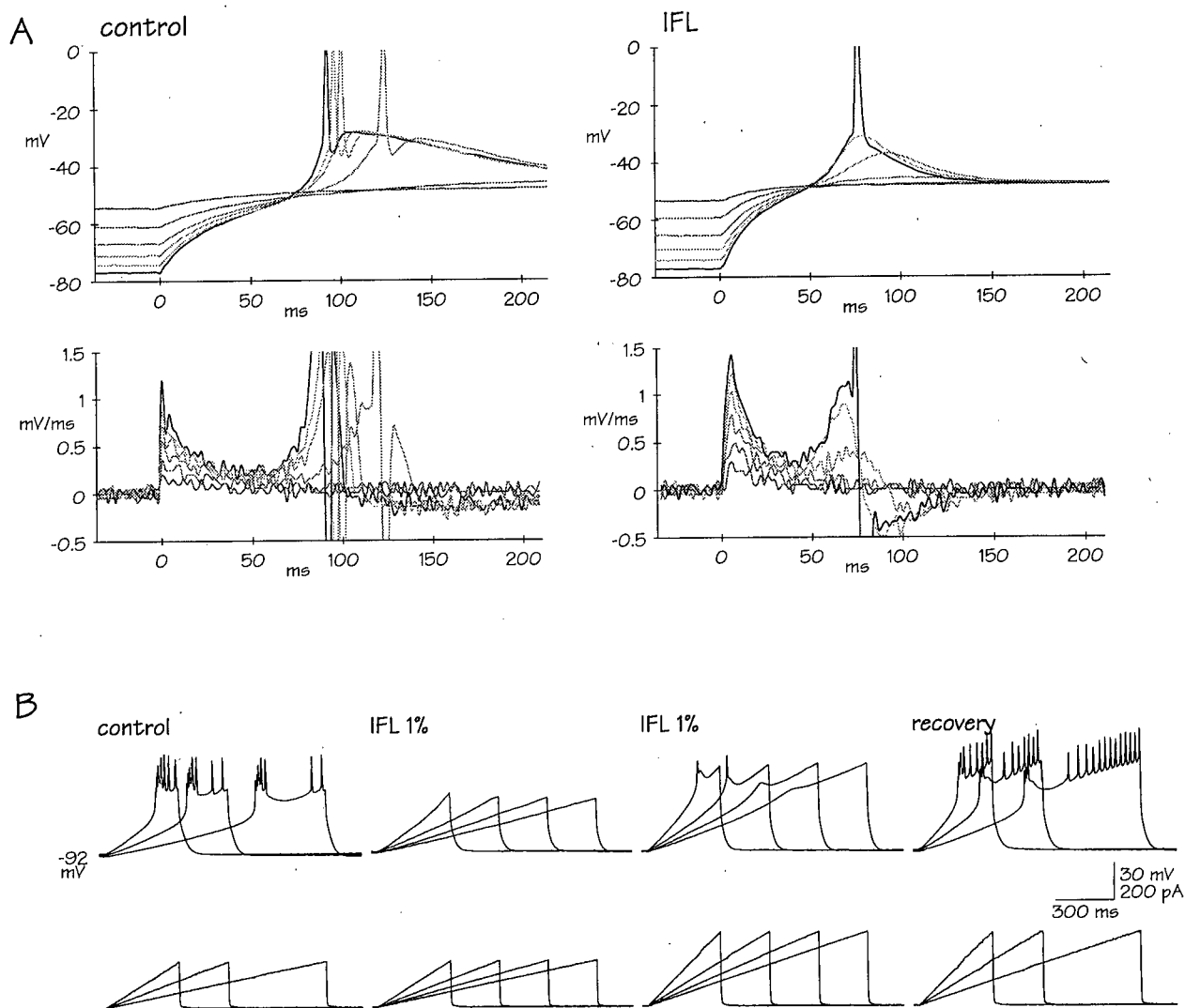


**Fig 13. Effect of IFL on burst firing: time-dependent aspects.**

**A:** control and IFL voltage traces from the neuron in Fig. 12A showing superimposed shunt-compensated hyperpolarizing pulses (above) and rate of change of membrane potential (below) for the rebound LTS before and during IFL 2% application. IFL appeared to activate the LTS earlier and increase the rate of inactivation of the underlying T-current. However, note that IFL shortened the duration of the initial decay of the hyperpolarizing pulse by decreasing the membrane time constant. This alone may have decreased the time to peak LTS and shortened the LTS duration. **B:** superimposed control voltage responses to depolarizing current ramps of increasing amplitude from a constant hyperpolarized holding potential in another neuron before, during and after IFL 1% application. Note voltage-dependent burst firing followed by tonic firing during control, with blockage of firing during IFL due to a shunt of current input (IFL 1%, left). An increased ramp amplitude, that overcompensated for the shunt, elicited a small amplitude LTS, but only with increasing rates of induced voltage change (IFL 1%, right). In addition, the threshold for  $\text{Na}^+$ -bursting appeared to increase during IFL.

However, it was impossible to control for the IFL-shortened membrane time constant. For example, analysis of the rate of voltage change during the offset of a hyperpolarizing pulse revealed that the faster initial, passive decay of the membrane potential contributed to an earlier LTS and a shortened inactivation phase of the underlying T-current (see Fig. 13A, lower panels). This change in membrane time constant made it difficult with current-clamp recording, to determine the changes in voltages due to activation and inactivation of the underlying T-current.

In view of the IFL-induced change in membrane time constant, slowly rising current ramps were used to control the rate of subthreshold depolarization. The depolarizing current ramp elicited burst firing and tonic firing if the voltage displacement continued past the threshold for  $\text{Na}^+$ -spikes. With the steeper current ramps, the burst mode transformed into the tonic mode, as in the so-called "wake-up" pattern (see Fig. 13B, left). Again an interesting response occurred during IFL application in that the LTS was barely visible when the reduced membrane trajectory was compensated by increased current injection, unless the rate of depolarization was increased.

Although further assessment of burst suppression was examined with voltage-clamp studies (see section 3.5), current-clamp recordings were performed with IFL 1% at 31 °C. At this temperature, IFL suppressed the rebound LTS as well as the LTS elicited with depolarized pulses from hyperpolarized holding potentials (see Fig. 14A and C respectively). As at room temperature, the LTS could be largely elicited during IFL application by either increasing hyperpolarizations or depolarizations beyond control thresholds. To quantify the reduction in LTS amplitude and duration, the number of  $\text{Na}^+$ -spikes elicited in burst mode were graphed in a manner reflecting voltage-dependent removal of T-current inactivation and T-current activation (see Fig. 14B and D respectively). At this concentration, however, IFL produced marked reductions in the number of  $\text{Na}^+$ -spikes elicited in the burst mode, despite current compensation for the IFL-induced hyperpolarization.

#### 3.3.4 IFL suppressed depolarizing afterpotentials (DAPs) and high-threshold spikes (HTSs)

Depolarizing afterpotentials accompanied single action potentials elicited by brief (5 ms) supramaximal depolarizing current injections from a range of holding potentials near rest (-55 to -75 mV; see Fig. 15A, left). Although only small AHPs were observed, despite depolarized

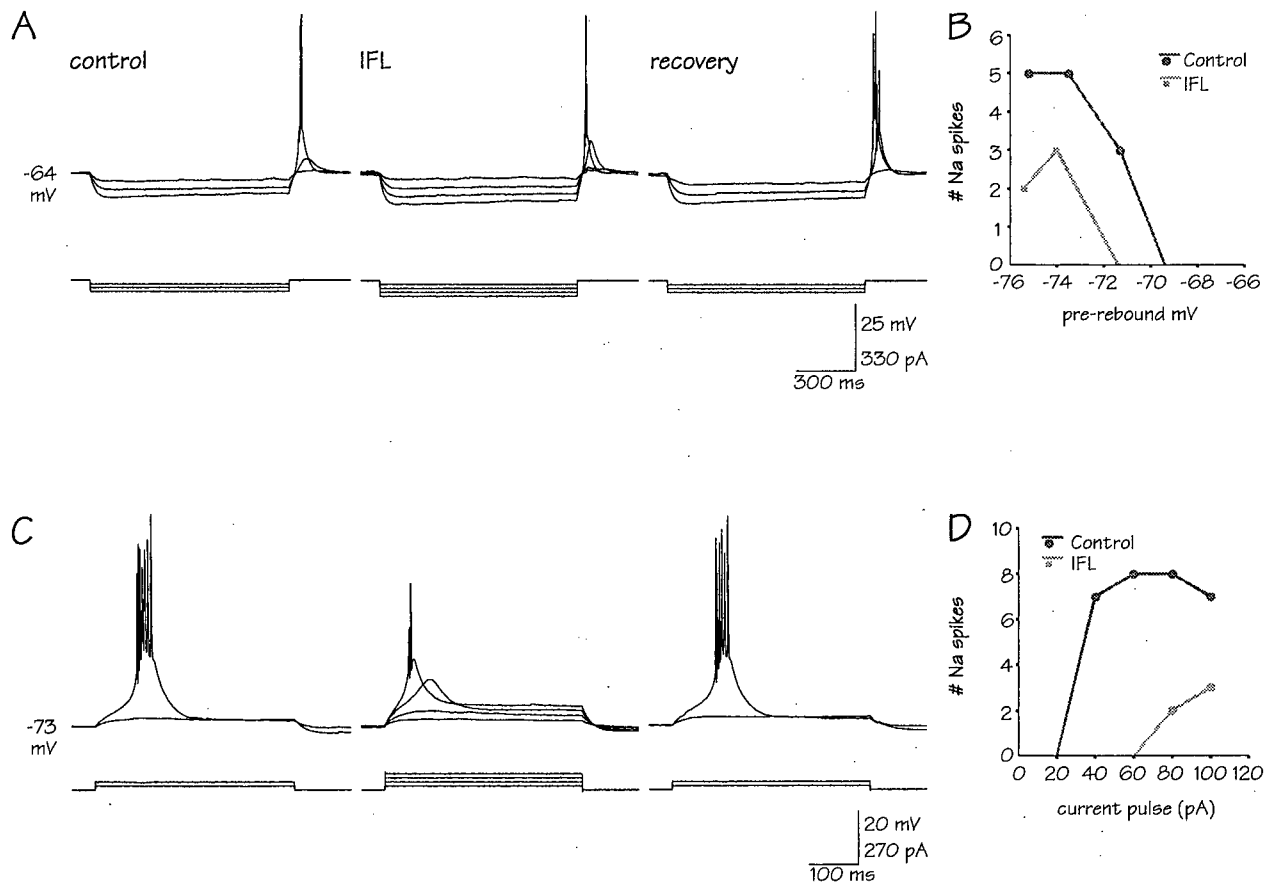


**Fig. 14. Effect of IFL on burst firing at 31°C.**

**A:** rebound LTS elicited following superimposed hyperpolarizing pulses of increasing amplitude from a constant depolarized holding potential before, during and after IFL 1%. Note that IFL shunted the hyperpolarizing pre-rebound potential and reduced the LTS amplitude. **B:** graph of the number of bursting  $\text{Na}^+$ -spikes on the LTS *versus* the pre-rebound potential. **C:** LTS elicited in the same neuron with superimposed depolarizing pulses of increasing amplitude from a hyperpolarized potential before, during and after IFL 1%. In addition to the shunted depolarizing pulses and reduced LTS amplitude, note that IFL may have changed the LTS activation from an all-or-none response to a graded response. **D:** graph of the number of bursting  $\text{Na}^+$ -spikes on the LTS *versus* the injected depolarizing pulses of current. In **B** and **D**, note the minimal decrease in LTS amplitude, yet the large decrease in the number of bursting  $\text{Na}^+$ -spikes.

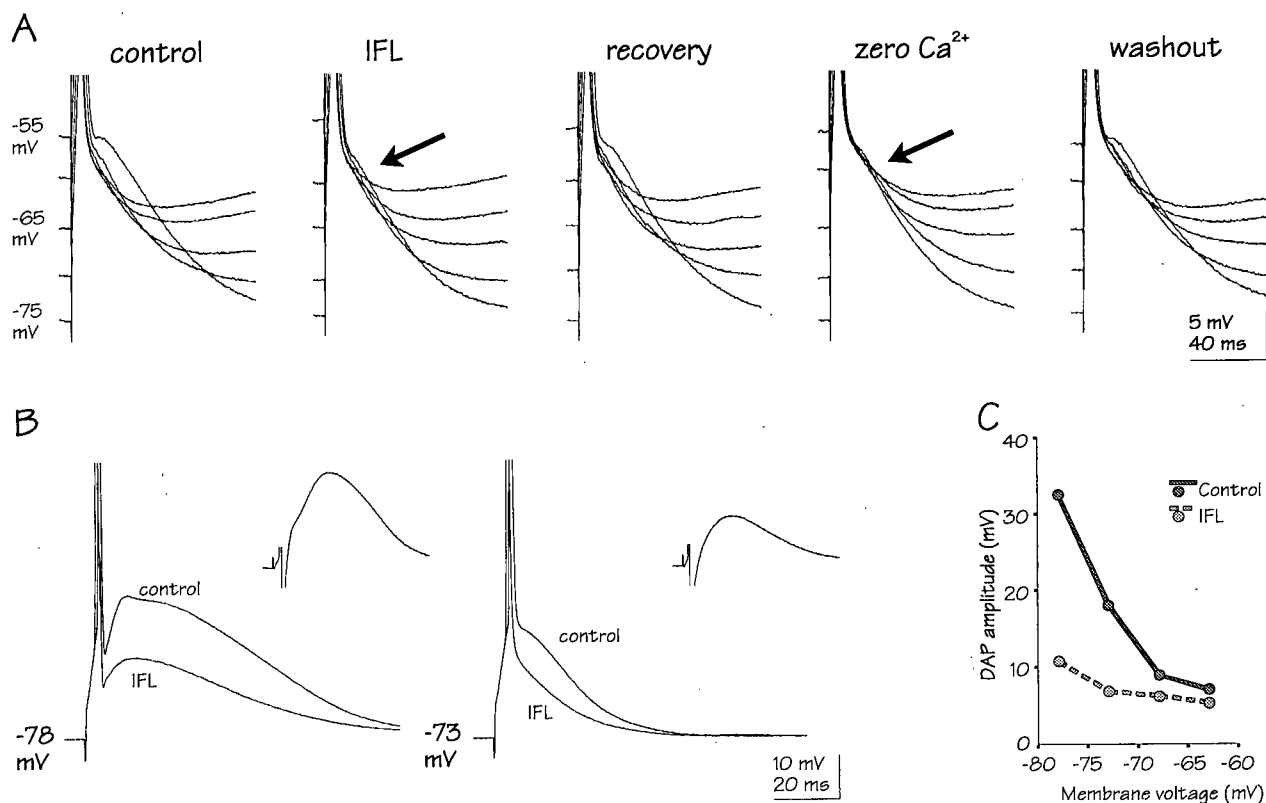


**Fig. 15. Effect of IFL on postspike depolarizing afterpotentials (DAPs).**

**A:** superimposed voltage traces of suprathreshold spike stimulation from 5 manual voltage clamps in the same neuron before, during and after IFL 1% application followed by zero  $\text{Ca}^{2+}$  and washout. Note that the voltage-sensitive DAP was blocked (arrow) by IFL and by zero  $\text{Ca}^{2+}$ . (Note also that the apparent AHP reduction during IFL with the pulse at "-55 mV" is spurious due to an actual manual voltage clamp of 53.9 mV.) **B:** superimposed voltage traces of suprathreshold spike stimulation from 2 manual voltage clamps in another neuron before and during IFL 2% application. In this panel, the control and IFL response are superimposed for -78 mV (left) and -73 mV (right). Inset traces (with 50% time scale) show IFL-induced voltage change after subtracting the IFL response from the control response. Note that IFL reduced the amplitude and the time course of the postspike response. **C:** DAP amplitude plotted against membrane potential from the same neuron as in **B**. Note that IFL markedly reduced the postspike repolarization in a voltage-dependent manner.

membrane potentials, a prominent postspike depolarization occurred in neurons held at hyperpolarized membrane potentials. This DAP response was strongly voltage-dependent, and progressively increased in size with greater hyperpolarized holding voltages below about -70 mV (see Fig. 15B and C). When the IFL-induced hyperpolarization was compensated, IFL application decreased both the amplitude and time course of the DAP (3 of 3 neurons; see Fig. 15A and B). The DAP was reduced in a similar manner when external  $\text{Ca}^{2+}$  was omitted from the media ( $n = 1$ ; see Fig. 15A), implicating a mechanism related to voltage-dependent  $\text{Ca}^{2+}$  entry (Komatsu and Iwakiri 1992; Zhang, Valiante and Carlen 1993; cf. Higashi, Tanaka, Inokuchi and Nishi 1993; cf. Green, Schwindt, and Crill 1994). The predominant voltage-activated  $\text{Ca}^{2+}$  current in thalamocortical neurons is the low-threshold T-current, but experiments with TTX revealed another  $\text{Ca}^{2+}$ -dependent potential.

Regenerative spike-like events could be elicited in neurons during TTX application from a depolarized holding potential of about -62 mV by depolarizing current steps to potentials more positive than -30 mV (cf. thalamic auditory relay neurons, Tennigkeit, Schwarz and Puil 1996). These all-or-none spikes were presumed to be high-threshold  $\text{Ca}^{2+}$ -spikes that arise in dendrites. IFL (1% and 2%) application increased conductance throughout this voltage range and shunted or completely blocked the HTS (4 of 4 neurons; see Fig. 16A and B). Application of a  $\text{Ca}^{2+}$ -channel blocker,  $\text{Ni}^{2+}$  (0.4 mM;  $n = 1$ ) blocked the HTS (see Fig. 16B; cf. neocortical neurons, Kim and Connors 1993).

### 3.3.5 Analysis of IFL actions

The IFL-induced increase in membrane conductance suppressed firing of thalamocortical neurons in both tonic and burst modes. During current-clamp recordings, the hyperpolarization moved the membrane potential away from the  $\text{Na}^{+}$ -spike threshold and the increased conductance reduced the effectiveness of depolarizing and hyperpolarizing DC currents. Application of IFL also shifted the resting potential away from the thresholds for both action potentials and LTSs, and reduced repolarizations of the action potentials. IFL may have affected one or more voltage-gated channel properties, including activation and inactivation properties of transient  $\text{Na}^{+}$ - (Haydon and Urban 1983; Rehberg, Xiao and Duch 1996) and  $\text{Ca}^{2+}$ -channels (Takenoshita and Steinbach 1991; Study 1994), as well as activation of subthreshold non-inactivating  $\text{Na}^{+}$ -channels

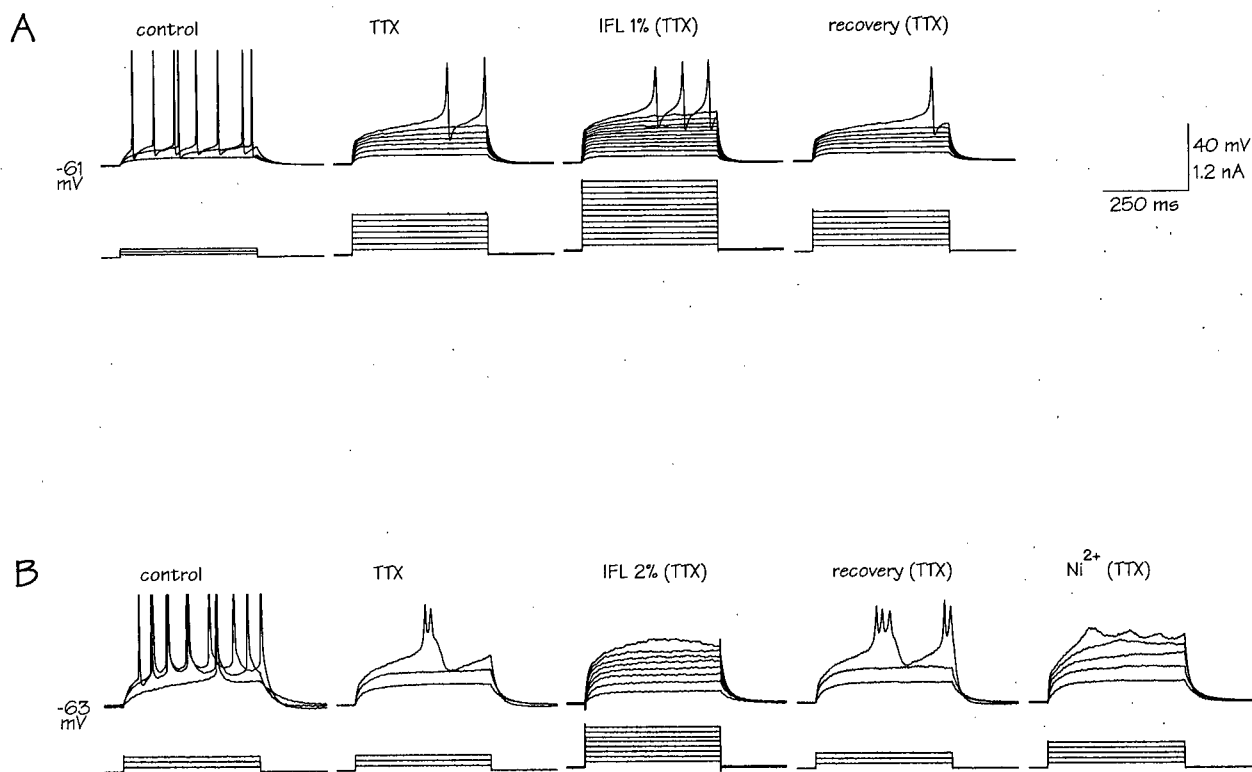


**Fig. 16. Effect of IFL on high-threshold  $\text{Ca}^{2+}$ -spike (HTS) electrogenesis.**

**A:** voltage responses from a constant depolarized holding potential with superimposed depolarizing current pulses of increasing amplitude before and after TTX 300 nM and later IFL 1%. Note the blockade of action potentials and the appearance of two HTSs, which were then shunted by IFL. To compensate for the IFL-induced hyperpolarization and shunt of the control HTS response, total depolarizing current was increased by 81%. **B:** voltage responses from another neuron subjected to similar conditions as in A as well as a  $\text{Ni}^{2+}$  0.4 mM application following IFL recovery. Note that the HTS was shunted and blocked by IFL. Note also the HTS blockade by  $\text{Ni}^{2+}$ , suggesting  $\text{Ca}^{2+}$ -dependence.

(see Fig. 4A). Inhalational anaesthetics reportedly suppress  $\text{Na}^+$ -currents by shifting the voltage-dependence of inactivation in a hyperpolarizing direction. Although the biophysical properties of action potentials were not investigated here due to the presumed confounding influence of the intact neuron and the IFL shunt, voltage-clamp recordings of T-currents are reported in Section 3.5. In addition, the IFL reduction in membrane time constant would suppress electrotonic conduction in these neurons, which have extensive dendritic arborizations. As a result, the magnitude of IFL-induced firing inhibition greatly exceeded the increase in membrane conductance.

### 3.4 Ionic basis of IFL-induced inhibition

#### 3.4.1 IFL elicited an outward current at membrane potentials characteristic of the tonic firing mode

The hyperpolarization (see Section 3.2) that accompanied the increase in membrane conductance, implied that these actions of IFL had a reversal potential which was negative to the membrane potentials characteristic of wakefulness. Further investigations of the IFL-induced hyperpolarization and shunt were done using voltage-clamp recordings in order to elucidate the underlying ionic mechanism(s). When the membrane potential was clamped near  $-62$  mV, IFL application induced a slow and persistent positive deflection in the holding current (62 of 62 neurons), indicating either an increase in outward current or a decrease in inward current (see Fig. 17A). Considering that IFL increased membrane conductance, however, an increased outward current was the stronger possibility. The responsible ion was presumably  $\text{K}^+$ , in view of the negativity of  $E_{\text{K}}$  ( $-85$  mV) in these experiments.

The I-V relationships at various voltages before and during IFL application were constructed in order to determine the reversal potential for IFL-actions. The current responses to slow ( $10$  mV/s) hyperpolarizing voltage ramps were recorded so as to determine "quasi" steady-state relationships. The ramps started from  $\sim -30$  mV during TTX application or from  $\sim -60$  mV in the absence of TTX, to as low as  $\sim -120$  mV. Voltage step commands were not routinely used for this purpose because the holding current took several seconds to return to a stable value following each voltage jump. This delay meant that voltage step protocols were best suited for

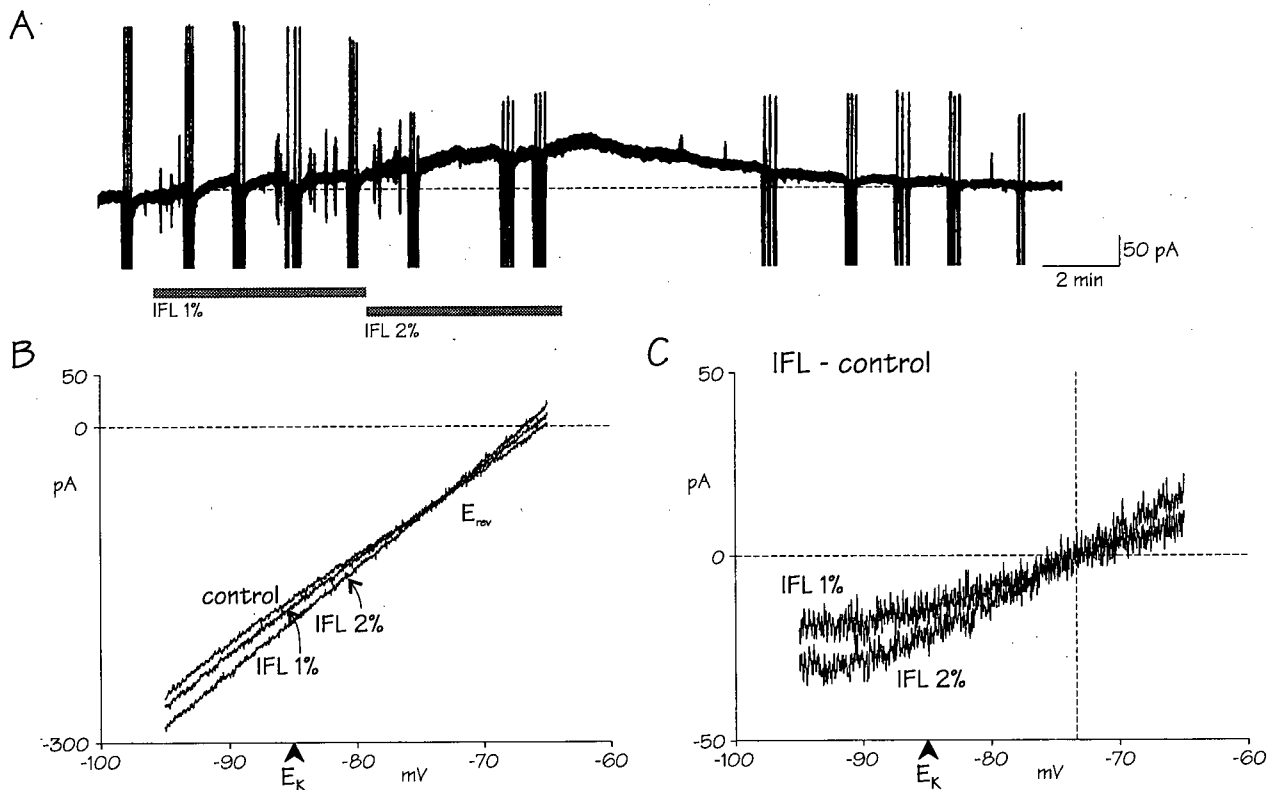


**Fig. 17. Effect of IFL on steady-state currents.**

**A:** voltage-clamp recordings showing chart record of holding current in a cell held at  $-65$  mV, during an cumulative concentration-response experiment consisting of 5 min application of IFL 1% and 5 min application of IFL 2% as indicated by the labelled horizontal thick bars. Each group of vertical deflections (in triplicate) represents hyperpolarizing voltage ramps. Note that the slow upward deflection of baseline indicates an IFL-induced outward current, consistent with the hyperpolarization observed during current-clamp recordings. This steady-state current diminished shortly after IFL was discontinued. **B:** expanded time base of current responses to hyperpolarizing voltage ramps from  $-65$  mV to  $-95$  mV (each ramp 3 s in duration; 3 responses averaged together), before and during application of 2 IFL concentrations from the neuron in A. The current responses were horizontally mirrored and time was converted to voltage in order to reflect a conventional I-V relationship. RMP hyperpolarized with IFL, as indicated by the leftward shift of the voltages along the horizontal dashed line at zero current. The I-V relationships for control and IFL merged as the membrane potential hyperpolarized, indicating that the IFL-induced outward current decreased with hyperpolarization. Note the increased slope with IFL indicating increased conductance, the concentration-dependence, as well as the same intersection point, marked  $E_{rev}$ , for the 3 curves. **C:** IFL-induced current derived from B by subtracting the control current response from each of the IFL current responses. Note the positive and near-linear slope at membrane voltages to the right of  $E_K$  indicating an increase in voltage-independent conductance. Note also that the IFL current became inward in the voltage range reflecting sleep as the reversal potential for IFL ( $E_{IFL}$ ) was approximately 10 mV positive to  $E_K$ . The calculated  $E_K$  is indicated by an arrow along the voltage axis.

steady-state IFL concentrations. In contrast, a voltage ramp could be completed in a few seconds, making it useful in monitoring the change in conductance during an IFL application. A high IFL concentration (4%) for 1 to 2 min was generally used in order to obtain a rapid (not steady-state) effect.

The ramps were applied in a hyperpolarizing direction to avoid activation of the T-current. However, they provided a "ready-made" I-V relationship when they were mirrored horizontally with the corresponding voltage scale. During the control period, an inward rectification always developed at membrane potentials negative to -85 mV, whereas positive to  $E_K$ , the membrane response was generally linear (see Fig. 17B, control). In the latter voltage range the slope of the current responses increased with IFL application, indicating an increase in conductance. Comparing the two I-V relationships, the control and IFL curves began to merge as the membrane potential was hyperpolarized, meaning that there was a decrease in IFL-induced outward current with hyperpolarization. In addition, the curves always intersected at  $\sim 10$  mV positive to  $E_K$  as the mean reversal potential for IFL-actions ( $E_{IFL}$ ) was  $-73 \pm 4$  mV ( $n = 20$ ). Subtraction of current obtained under control conditions from that during IFL revealed a current that had a linear relation to the membrane potential positive to  $E_K$  (see Fig. 17C). The linearity suggested that IFL increased a voltage-independent conductance. The difference between the experimental  $E_{IFL}$  and the calculated  $E_K$  implied experimental error or that  $K^+$  was not the only ion affected by IFL.

#### 3.4.2 The principal ion of the IFL-evoked current was $K^+$

Perfusion solutions containing three different  $K^+$  concentrations (1.25, 2.45 and 9.25 mM) were used with control solutions ( $K^+$ , 5.25 mM) to test a  $K^+$  involvement in the IFL-induced increase in conductance. In these experiments, IFL induced an outward current in both normal and low  $K^+$  (e.g., 1.25 mM) solutions when the membrane potential was held at  $\sim -62$  mV (see Fig. 18A). The IFL-induced outward current was larger in the low  $K^+$  solution. This change in the current magnitude indicated that  $K^+$  was involved in the IFL action to increase conductance because the current became more prominent when the  $K^+$  driving force was increased. The change in  $K^+$  driving force was verified by the increase in holding, outward current when low  $K^+$  was applied and an inward shift in the holding current when normal  $K^+$  was resumed.

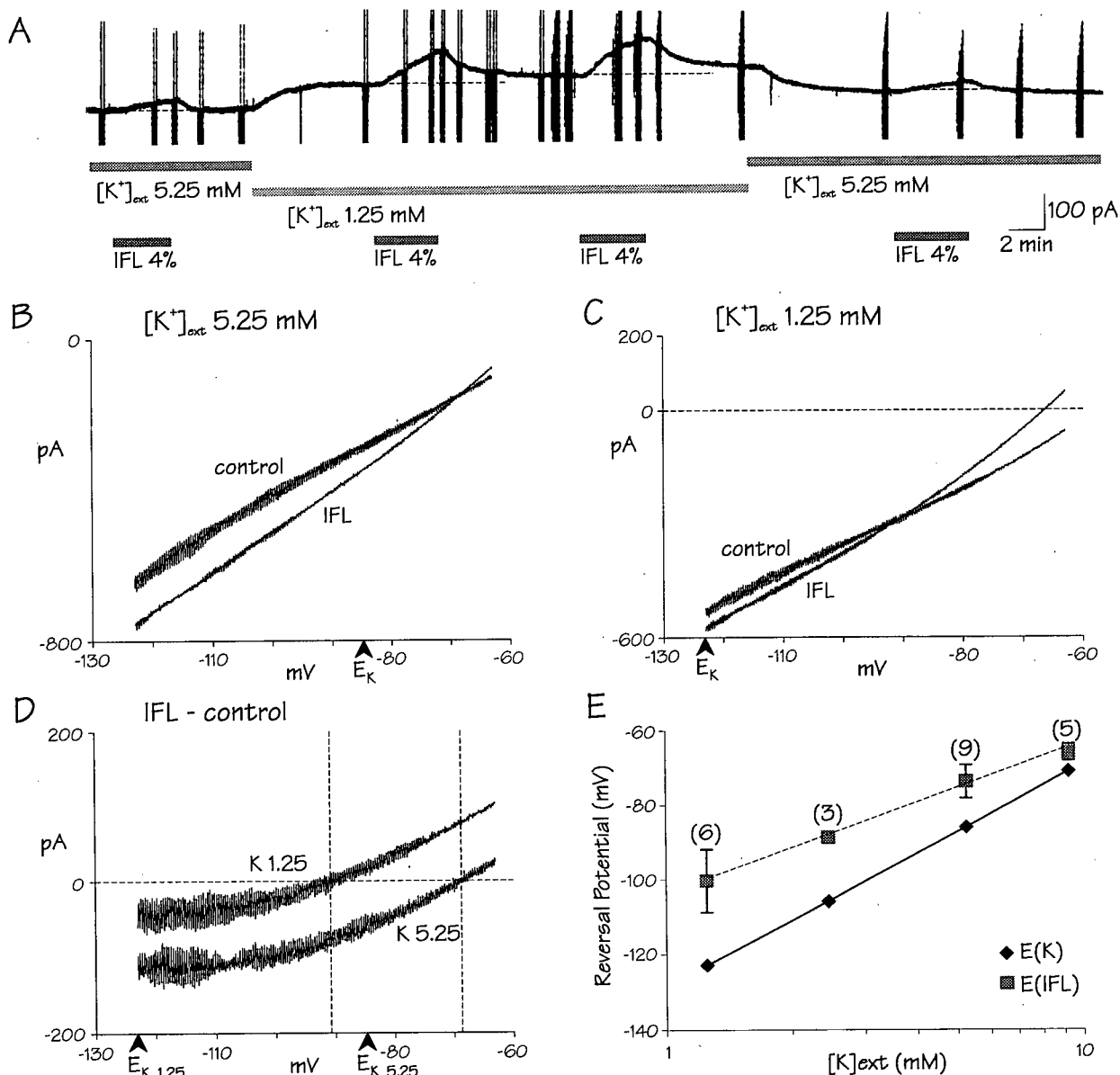


**Fig. 18.** Effect of changes in the extracellular concentration of potassium on  $E_{IFL}$ .

**A:** voltage-clamp recordings showing chart record of current response in a cell held at  $-62$  mV, with multiple applications of IFL during perfusion of normal  $K^+$  ( $5.25$  mM), low  $K^+$  ( $1.25$  mM), and normal  $K^+$ . Note that when a high concentration of IFL was repeatedly applied for the same duration, the amplitude of the IFL-induced outward current was greatest in the low  $K^+$  solution.

**B:** current response to hyperpolarizing voltage ramp ( $-63$  to  $-123$  mV) before and after IFL in  $K^+$   $5.25$  mM. **C:** current response to voltage ramp before and after IFL in  $K^+$   $1.25$  mM. Along with the IFL-induced outward current and the increase in conductance, IFL still hyperpolarized RMP during low  $K^+$ , as indicated by the leftward shift of the voltages along the horizontal dashed line at zero current. **D:** IFL-induced current derived from **B** and **C** by performing the respective current subtractions. Note that for the IFL-induced increase in conductance,  $E_{IFL}$  shifted in a hyperpolarizing direction along with the shift in the calculated  $E_K$ , but  $E_{IFL}$  remained offset from  $E_K$ . **E:** graph of reversal potential versus  $[K^+]_{ext}$  for a series of neurons. Note the increasing disparity between  $E_{IFL}$  and  $E_K$  as  $[K^+]_{ext}$  decreased. The number in parentheses represents  $n$ . The straight line through the experimental data was fitted by eye.

Voltage ramps were used to compare  $E_{\text{IFL}}$  during different  $\text{K}^+$ -containing bathing media. For example, a decrease in extracellular  $\text{K}^+$  to 1.25 mM shifted  $E_{\text{IFL}}$  to a more hyperpolarized value. However, the new  $E_{\text{IFL}}$  remained offset by  $\sim 12$  mV in a positive direction from the new calculated  $E_{\text{K}}$  (6 of 6 neurons; see Fig. 18B, C and D). In fact, at all  $\text{K}^+$  concentrations,  $E_{\text{IFL}}$  was depolarized relative to the calculated  $E_{\text{K}}$ . At external  $\text{K}^+$  concentrations of 1.25, 2.45, 5.25 and 9.25 mM,  $E_{\text{IFL}}$  was  $-101 \pm 9$  ( $n = 6$ ),  $-89 \pm 1$  ( $n = 3$ ),  $-74 \pm 4$  ( $n = 9$ ) and  $-66 \pm 2$  ( $n = 5$ ) mV, whereas the calculated  $E_{\text{K}}$  was  $-123$ ,  $-106$ ,  $-85$  and  $-71$  mV, respectively. A graph of this relationship showed increasing disparity in the association when the external  $\text{K}^+$  concentration decreased, suggesting a possible role for ions other than  $\text{K}^+$  (see Fig. 18E; discussed in detail below).

These results demonstrated that  $\text{K}^+$  was the principal ion involved in the IFL-induced increase in conductance. Further ionic manipulations were performed to investigate the role of other ions. This included changing the external environment by reducing  $\text{Na}^+$  concentrations from 124 to 26 mM by replacement with the impermeant cation, choline ( $n = 4$ ), lowering external  $\text{Cl}^-$  concentrations from 136 to 12 mM by replacement with the impermeant anion, isethionate ( $n = 3$ ), and using a nominally zero external  $\text{Ca}^{2+}$  concentration by replacement with  $\text{Mg}^{2+}$  4 mM ( $n = 7$ ). Additionally, a high internal  $\text{Cl}^-$  concentration was tested (change from 12 to 60 mM, see Section 2;  $n = 3$ ). None of these manipulations changed  $E_{\text{IFL}}$ .

### 3.4.3 The IFL-induced outward current became inward at potentials consistently positive to $E_{\text{K}}$

The use of voltage ramp technique may have underestimated  $E_{\text{IFL}}$ , so steady-state I-V relationships were constructed using hyperpolarizing voltage commands of long duration (2 s) to  $\sim -100$  mV from a holding potential of  $\sim -60$  mV. These protocols from cumulative concentration-response relationships for the T-current were performed during perfusion with TEA (10 mM), which blocked fast inward rectification. Despite this  $\text{K}^+$ -channel blockade with TEA as well as with 4-AP (3 mM) and  $\text{Na}^+$ -channel blockade with TTX (300 nM; also  $\text{Ca}_2\text{Cl}$  1 mM and  $\text{Mg}_2\text{Cl}$  3 mM), IFL application increased a voltage-independent, non-inactivating current in a concentration-dependent manner (8 of 8 neurons; see Fig. 19A). Although IFL testing was not done before TEA and 4-AP were applied, the magnitude of the IFL concentration-dependent increase in conductance was similar to previous measurements with current-clamp techniques. The I-V relationships for these current responses consistently

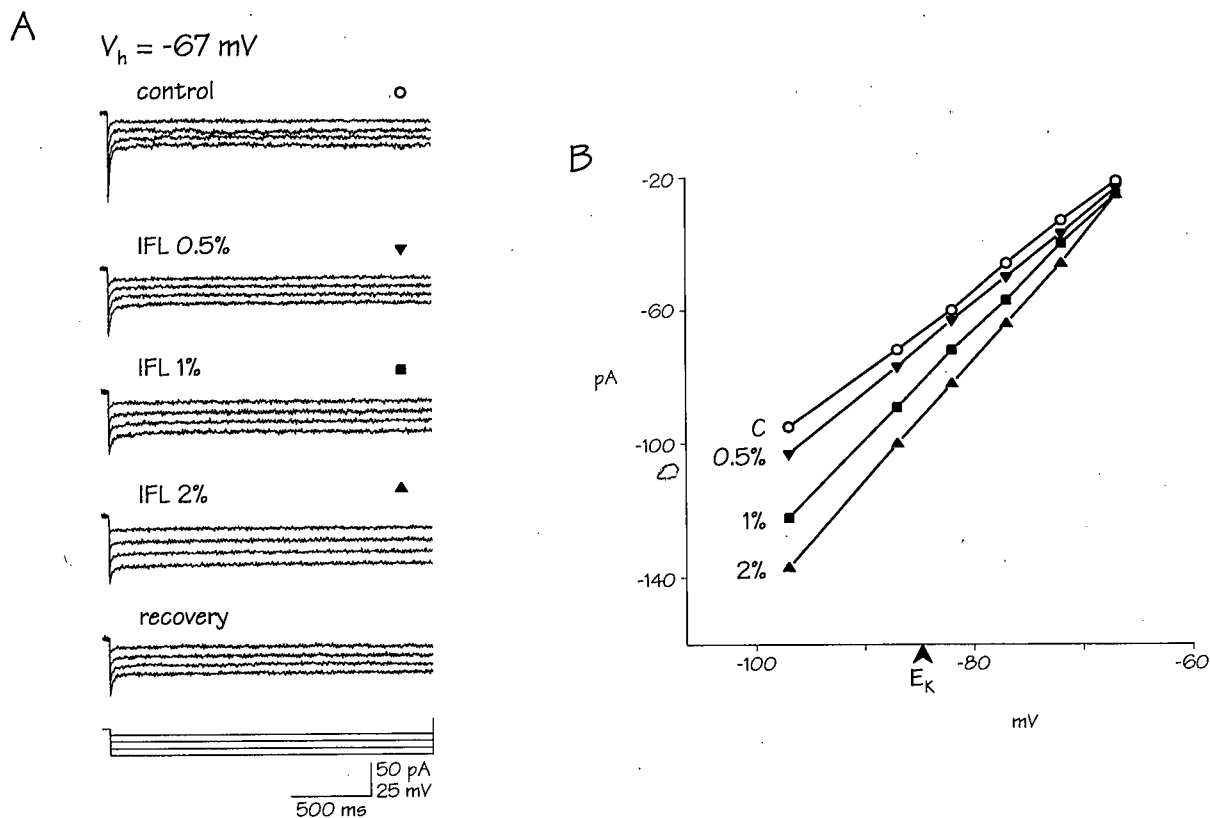


**Fig. 19. Concentration-dependent effect of IFL.**

**A:** voltage-clamp recordings in a cell held at  $-67 \text{ mV}$  showing current responses (upper traces) to superimposed long, hyperpolarizing voltage commands (lower traces) during cumulative IFL concentrations. These responses were obtained in a solution containing TTX  $300 \text{ nM}$  and the  $\text{K}^+$  antagonists tetraethylammonium (TEA)  $10 \text{ mM}$  and 4-aminopyridine (4-AP)  $3 \text{ mM}$ . The current responses activated rapidly and did not inactivate with time. Note the IFL-induced increase in the spacing of the steady-state current at all voltages. **B:** steady-state I-V relationships for the neuron in **A** before and during multiple cumulative IFL concentrations (C = control; 0.5% = IFL 0.5%; 1 = IFL 1%; 2 = IFL 2%). The IFL-induced current was voltage-independent and increased in a concentration-dependent manner. Note that the current response to voltage jumps reversed polarity at a potential positive to  $E_K$  in a similar manner as the current response to voltage ramps.

intersected 10 to 20 mV positive to  $E_K$  (see Fig. 19B for one case). However, the variability in  $E_{IFL}$  was greater with voltage step protocols than voltage ramps.

Could other experimental limitations have contributed to a possible underestimation of  $E_{IFL}$ ? For example, as IFL would presumably act unspecifically on both somatic and dendritic membranes, one might expect spatial control to deteriorate during voltage-clamp recording and IFL-application. However, an electrotonically distant  $K^+$  conductance would have shifted the apparent  $E_{IFL}$  to values more negative than  $E_K$  and resulted in an overestimation of the negativity, not an underestimation. It seemed that one should first rule out errors in the preparation of  $K^+$  solutions, as well as a junction potential problem due to equilibration restrictions between pipette and neuron. An attempt then was made to verify the calculated  $E_K$ . This was done in three ways.

Because  $GABA_B$  receptors mediate an increase in  $K^+$  conductance (Crunelli *et al.* 1988), the  $GABA_B$  agonist, baclofen, was used to confirm the predicted  $E_K$ . Like IFL, baclofen application (10  $\mu$ M) was found to rapidly induce a persistent outward current when the membrane potential was clamped  $\sim$ -60 mV (see Fig. 20A). However, baclofen's outward current reversed polarity at  $-84 \pm 1$  mV ( $n = 3$ ) in experiments using separately prepared external and internal solutions. Baclofen's reversal potential was essentially the same value as the calculated  $E_K$  (-85 mV; see Fig. 20B to E).

Second, the anticholinesterase agent, tacrine, was used as a biological assay for  $E_K$ . Used in treating Alzheimer's disease, tacrine also has a direct blocking effect on a resting  $K^+$  conductance (Stevens and Cotman 1987). In contrast to IFL, tacrine application (100  $\mu$ M) induced non-inactivating inward current when the membrane potential was clamped around -60 mV (see Fig. 21A). Voltage ramps showed that tacrine's "inward" current was actually a decrease in outward current, as membrane conductance decreased (see Fig. 21B). As expected, tacrine's reversal potential was -85 mV in two neurons from different experimental preparations (see Fig. 21B to E). Interestingly, an antagonism of IFL action was not observed during tacrine application at 100  $\mu$ M in 1 neuron (see Fig. 21A).

And third, the fast inward rectifier ( $I_{Kir}$ ) was used to verify the calculated  $E_K$  in both current-clamp and voltage-clamp recordings. In current-clamp, voltage responses to hyperpolarizing

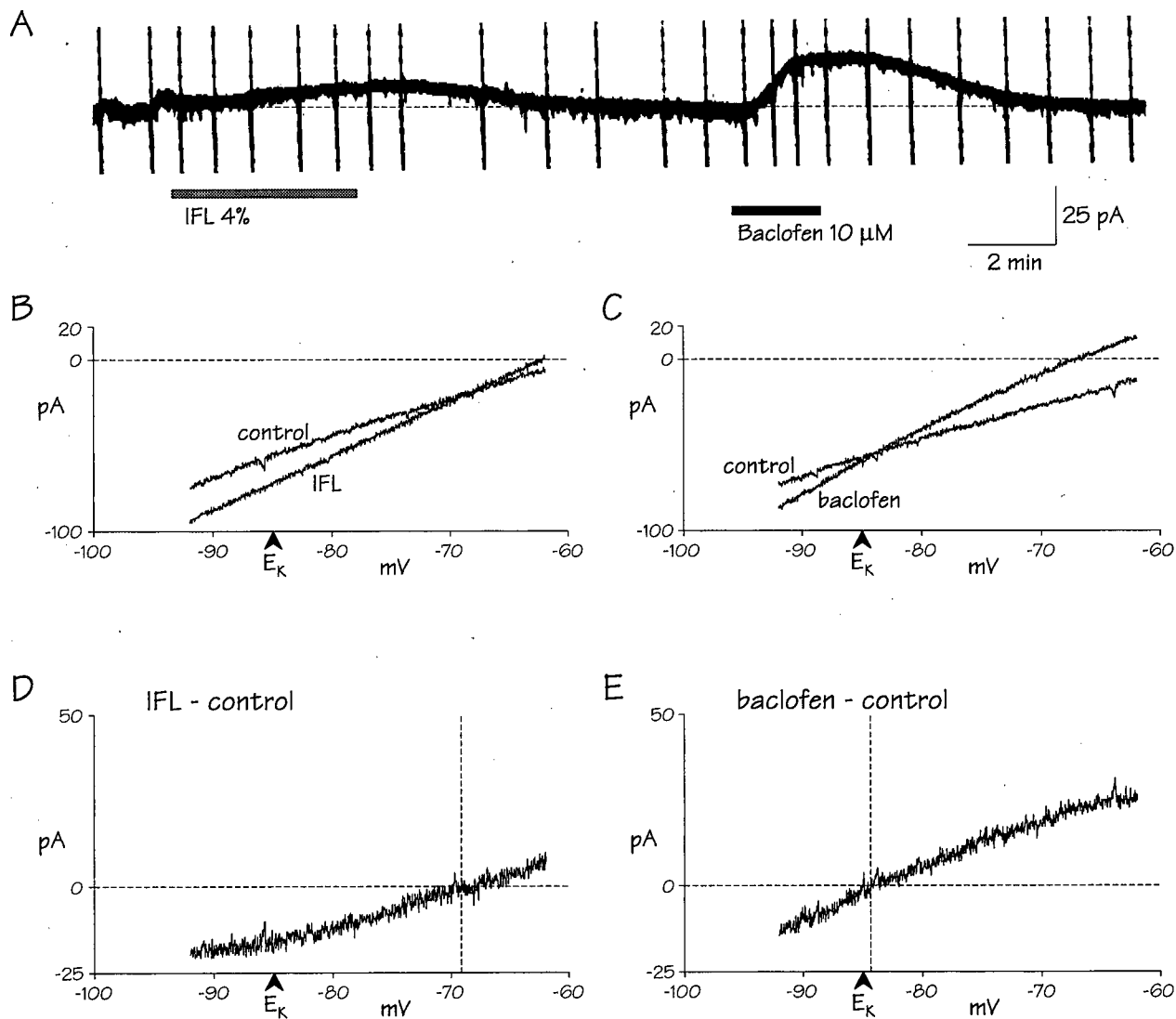


**Fig. 20.**  $E_{\text{baclofen}}$  as a biological assay for  $E_K$ .

**A:** voltage-clamp recordings showing chart record of current response from a neuron held at  $-62$  mV during IFL and later baclofen applications. Note that the GABA<sub>A</sub> agonist, baclofen, like IFL, induced an outward current. **B:** current response to hyperpolarizing voltage ramp ( $-62$  to  $-92$  mV) before and after IFL. **C:** current response to voltage ramp before and after baclofen. Note that baclofen, like IFL, increased membrane conductance and hyperpolarized RMP, as indicated by the leftward shift of the voltages along the horizontal dashed line at zero current. **D:** IFL-induced current derived from **B** by performing a current subtraction. **E:** baclofen-induced current derived from **C** by performing a current subtraction. Note that unlike IFL, the baclofen-induced increase in voltage-independent conductance reversed as expected at the calculated  $E_K$ , in contrast to  $E_{\text{IFL}}$ . All panels were from the same neuron.

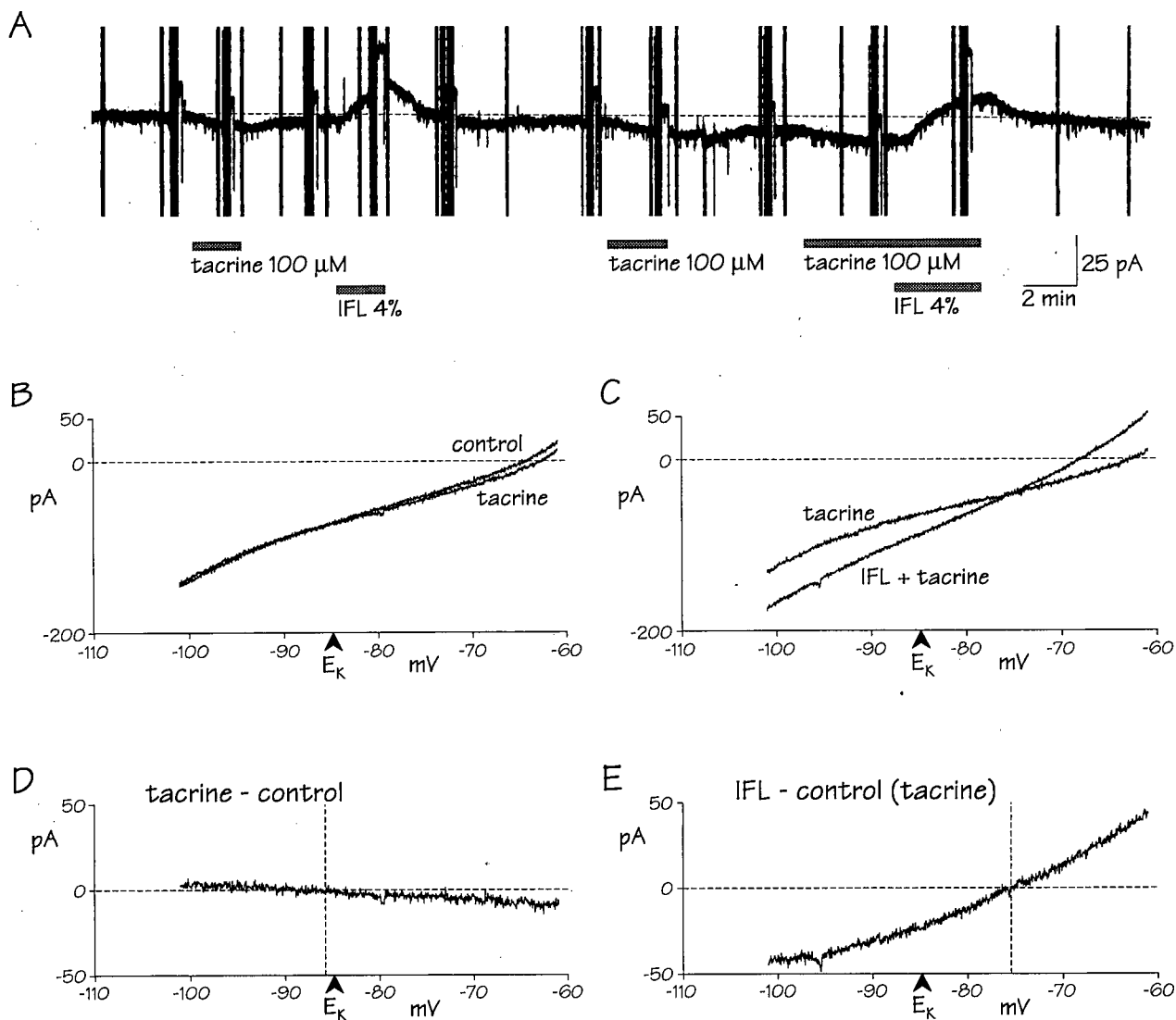


**Fig. 21.**  $E_{\text{tacrine}}$  as a biological assay for  $E_K$ .

**A:** voltage-clamp recordings showing chart record of current response from a neuron held at -61 mV during IFL and later tacrine applications. Note that the anticholinesterase, tacrine, unlike IFL, induced an apparent inward current, as indicated by the downward deflection of the holding current. **B:** current response to hyperpolarizing voltage ramp (-61 to -101 mV) before and after tacrine. Note that tacrine, unlike IFL, decreased membrane conductance, and therefore the "inward" current was really a decrease in outward current. Note also that tacrine depolarized RMP, as indicated by the rightward shift of the voltages along the horizontal dashed line at zero current. **C:** current response to voltage ramp before and after IFL. **D:** tacrine-induced current derived from B by performing a current subtraction. **E:** IFL-induced current derived from C by performing a current subtraction. Note that tacrine decreased a voltage-independent membrane conductance that reversed as expected near the calculated  $E_K$ . All panels were from the same neuron.

current pulses revealed a fast and persistent inward rectifier (see Fig. 22A). The "instantaneous" V-I relationships demonstrated that this current activated with hyperpolarizations just beyond the calculated equilibrium potential for  $K^+$  (see Fig. 22B). In addition, voltage ramps during voltage-clamp experiments with different external  $K^+$  solutions showed that the activation of the inward rectification shifted according to the change in the calculated  $E_K$ . For example, an increase in extracellular  $K^+$  produced a depolarizing shift in the activation potential according to the Nernstian increase in the calculated  $E_K$  (see Fig. 22C and D). This  $K^+$  sensitivity helped to identify the current as  $I_{Kir}$ . In addition, application of low concentrations of  $Ba^{2+}$  (100  $\mu M$ ; Sutor and Hablitz 1993) blocked most of the inward rectification expected from  $I_{Kir}$  during voltage ramps (see Fig. 22E). Again, the reversal potential for the decrease in inward rectification with low  $Ba^{2+}$  concentration was -85 mV in two neurons (see Fig. 22F).

Although these studies suggested that  $[K^+]$  and junction potential errors were not responsible for the difference between  $E_{IFL}$  and  $E_K$ , a systematic error could have resulted. To further investigate the involvement of a  $K^+$  conductance, the effects of external  $Ba^{2+}$  and internal  $Cs^+$  were examined on the IFL-induced increase in conductance.

#### 3.4.4 IFL increased steady-state conductance through nongated "leak" channels

As the IFL-induced current was resistant to blockade by 4-AP and TEA, other  $K^+$  channel blockers were used to identify the channels mediating the increase in conductance. External  $Ba^{2+}$  (2 mM with zero  $Ca^{2+}$ ) depolarized neurons held near rest by decreasing membrane conductance as well as inward rectification (see Fig. 23A).  $Ba^{2+}$ , however, prevented IFL (1%) action, but the blockade could be overcome in all neurons by application of a higher concentration of IFL (4%;  $n = 4$ ). In addition, the  $Ba^{2+}$  reversal potential ( $E_{Ba}$ ) was similar to  $E_{IFL}$  (paired  $t$ -test, 2-tailed  $P = 0.297$ ,  $n = 4$ ; see Fig. 23B to D), meaning that  $E_{Ba}$  was also positive ( $\sim 8$  mV) to the calculated  $E_K$ . In another set of experiments, internal  $Cs^+$  (see Methods) prevented the actions of IFL applied in concentrations of 1 or 2%, but the blockade could again be overcome with long applications of IFL at higher concentrations (4%; 3 of 4 neurons). In the  $Cs^+$ -loaded neurons where IFL (4%) increased membrane conductance, an inward current developed from a holding potential near rest (see Fig. 24A). The I-V relationships for the control and IFL conditions intersected at a membrane voltage positive to  $\sim -55$  mV in both voltage step and voltage ramp

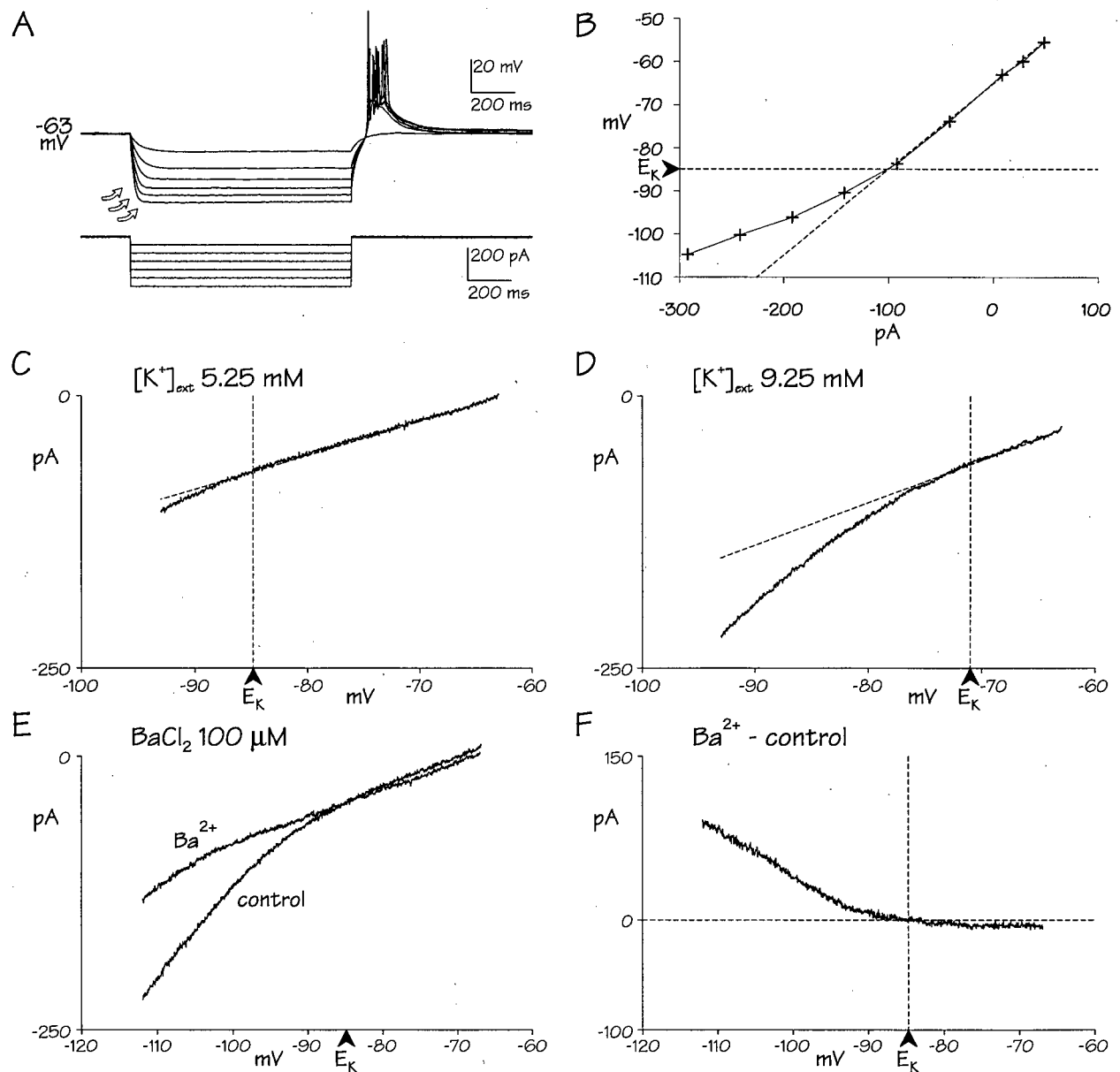


**Fig. 22. Voltage-dependent gating of K<sup>+</sup>-mediated inward rectification and E<sub>K</sub>.**

**A:** current-clamp recordings from a manual voltage-clamp of -63 mV showing hyperpolarization-activated inward rectification. Arrows indicate saturation of voltage responses to superimposed hyperpolarized current steps of increasing amplitude. Note, however, the absence of hyperpolarization-activated depolarizing sag. **B:** instantaneous V-I relationship showing inward rectification (upward deflection) at a potential negative to E<sub>K</sub>. **C:** voltage-clamp recording in the same neuron of current response to a hyperpolarizing voltage ramp (-63 to -93 mV) showing I-V relationship and inward rectification (downward deflection) at a potential negative to E<sub>K</sub> in [K<sup>+</sup>]<sub>ext</sub> 5.25 mM. **D:** current response to voltage ramp showing inward rectification at a potential negative to E<sub>K</sub> in [K<sup>+</sup>]<sub>ext</sub> 9.25 mM. Note that due to K<sup>+</sup>-mediation, the inward rectification followed the depolarizing shift in E<sub>K</sub>. **E:** current response to voltage ramp in another neuron before and during BaCl<sub>2</sub> 100 μM showing blockade of inward rectification. **F:** Ba<sup>2+</sup>-blocked current derived from E by performing a current subtraction. Note that Ba<sup>2+</sup> decreased conductance negative as expected to E<sub>K</sub>.

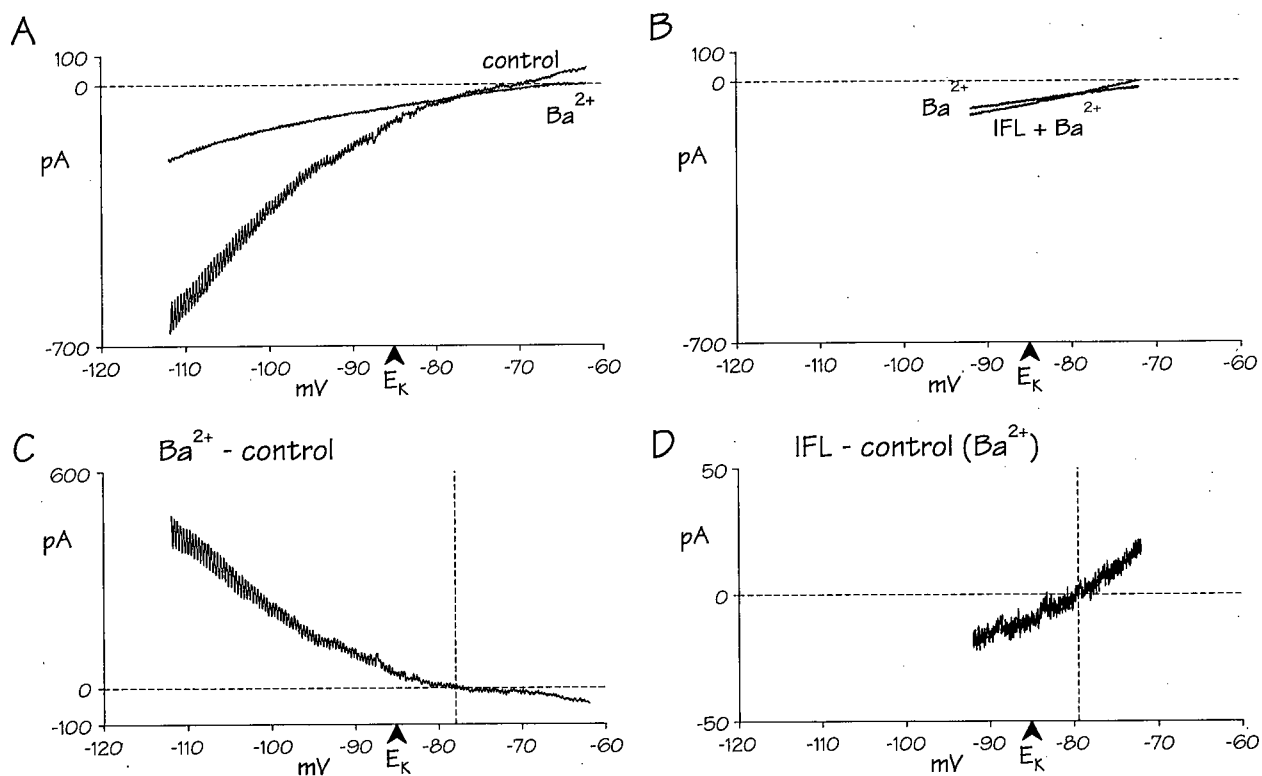


**Fig. 23. Effect of barium on IFL-induced current.**

**A:** voltage-clamp recordings showing current response to hyperpolarizing voltage ramp (-62 to -112 mV) before and during Ba<sup>2+</sup> (2 mM) substitution for Ca<sup>2+</sup>. Note that Ba<sup>2+</sup> blocked inward rectification and depolarized RMP, as indicated by the rightward shift of the voltages along the horizontal dashed line at zero current. **B:** current response to voltage ramp (-72 to -92 mV) following Ba<sup>2+</sup> application in the neuron in A, before and during a 5 min application of IFL 4%. Note that IFL increased conductance slightly and hyperpolarized RMP, as indicated by the leftward shift of the voltages along the horizontal dashed line at zero current. **C:** Ba<sup>2+</sup>-induced current derived from A by performing a current subtraction. **D:** IFL-induced current during Ba<sup>2+</sup>, derived from B by performing a current subtraction. Note that the reversal potential for high-dose Ba<sup>2+</sup> was similar to E<sub>IFL</sub> in that both were shifted in a depolarized direction from E<sub>K</sub>. All panels were from the same neuron.

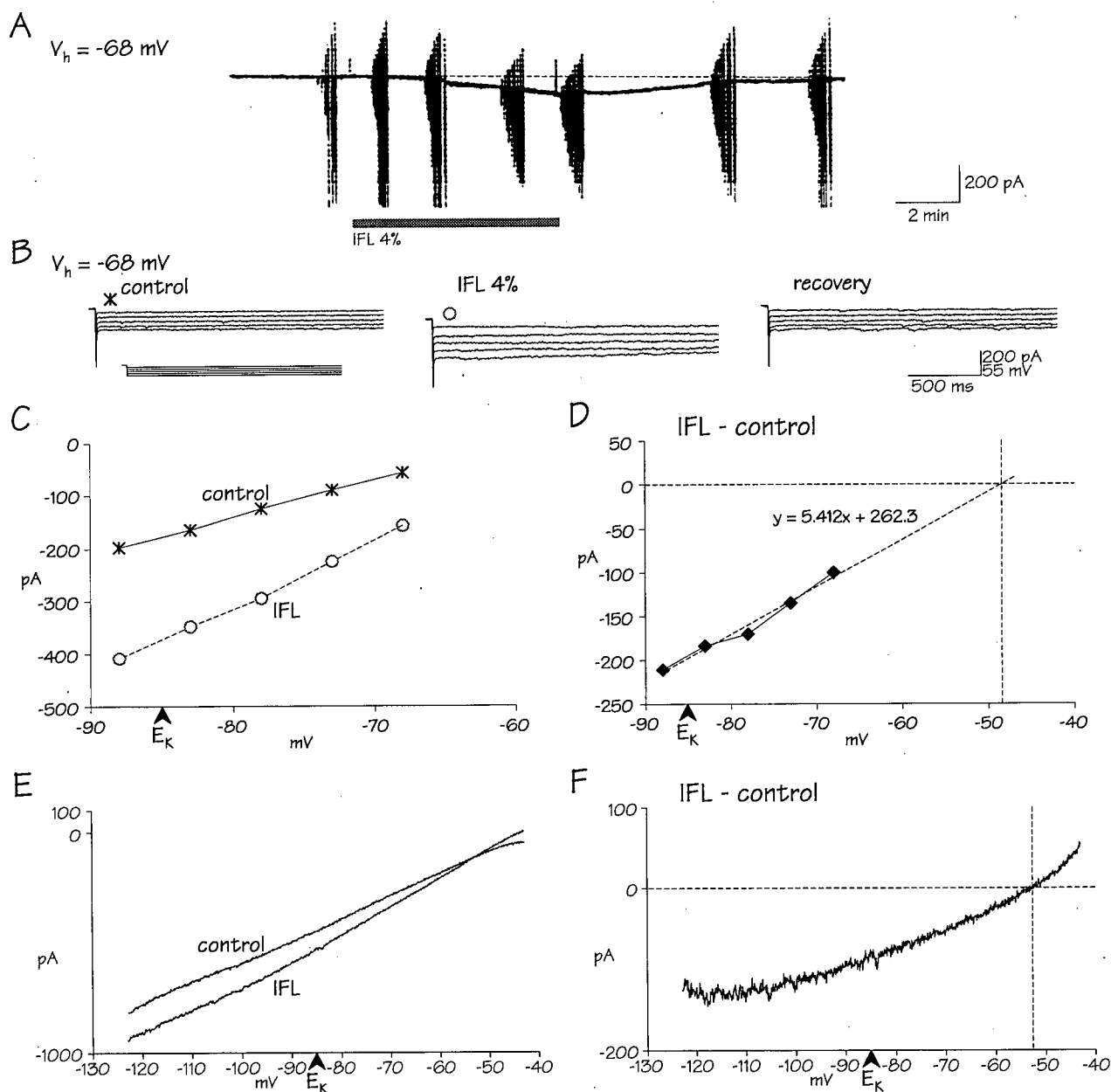


**Fig. 24. Effect of internal  $\text{Cs}^+$  on  $E_{\text{IFL}}$ .**

**A:** voltage-clamp recordings showing chart record of current response from a neuron with intracellular  $\text{Cs}^+$  held at  $-68$  mV. Note that a 6.5 min application of IFL 4% induced an "inward" current (downward deflection) when voltage-clamped near "normal" RMP. **B:** current response to superimposed long, hyperpolarizing voltage steps of increasing amplitude before and during IFL from the same neuron. Note that IFL induced an increase in the steady-state current amplitudes. **C:** I-V relationship from the currents in **B**. **D:** IFL-induced current derived from **C** by performing a current subtraction. Note that IFL induced a linear voltage-independent increase in conductance that reversed at a potential positive to normal RMP when extrapolated ( $-48$  mV) by linear regression. **E:** current response to a hyperpolarizing voltage ramp from  $-43$  to  $-123$  mV in another neuron with intracellular  $\text{Cs}^+$  before and during a 5 min application of IFL 4%. **F:** IFL-induced current derived from **E** by performing a current subtraction. Note that the positive shift of  $E_{\text{IFL}}$  with internal  $\text{Cs}^+$  was similar during voltage steps or voltage ramp experiments.

experiments (see Fig. 24C to E). Note that if  $K^+$  was the only ion influenced by IFL,  $Cs^+$  dialysis could conceivably have left electronically distant sites unblocked. However, this would have led again to an overestimation of the negativity of  $E_{IFL}$ .

Notwithstanding the lack of change in  $E_{IFL}$  with zero external  $Ca^{2+}$ , IFL action during blockade of  $Ca^{2+}$ -dependent processes was examined in greater detail. The activation of  $Ca^{2+}$ -dependent  $K^+$  currents ( $I_{K(Ca)}$ ) by increases in free internal  $Ca^{2+}$  would be expected to have voltage-dependence from voltage-dependent  $Ca^{2+}$  entry (Heyer and Lux, 1976). Consistent with the results obtained under conditions of TEA blockade of fast  $I_{K(Ca)}$ , blockade of  $Ca^{2+}$ -channels with  $Co^{2+}$  (1 mM) or  $Cd^{2+}$  (50  $\mu M$ ) did not influence either the increase in conductance induced by IFL application or  $E_{IFL}$  ( $n = 4$ ). The influence of internal  $Ca^{2+}$  buffering also was tested by using internal BAPTA (10 mM; same internal  $[Ca^{2+}]$ ), a faster  $Ca^{2+}$  chelator than EGTA. In a small sample of neurons in which internal BAPTA was substituted for EGTA, the IFL-induced increase in conductance was unchanged, and  $E_{IFL}$  was  $-80.3 \pm 0.6$  mV ( $n = 3$ ). This value of  $E_{IFL}$  with BAPTA was the same as the minimum value for  $E_{IFL}$  of -80 mV obtained with EGTA.

Despite the BAPTA result, the antagonism of the IFL-induced increase in  $K^+$  conductance by external  $Ba^{2+}$  as well as the current's voltage- and time-independence suggested that IFL was influencing the channel responsible for RMP. For neurons, RMP is positive to  $E_K$  since nongated "leakage" channels, which are always open, are permeable not only to  $K^+$  ions but to  $Cl^-$  and  $Na^+$  ions. Although RMP was between  $E_K$  and  $E_{Na}$ , RMP is closest of course to  $E_K$  because of a predominance of active  $K^+$  channels over  $Cl^-$  or  $Na^+$  channels. Presumably, the RMP varies from neuron to neuron because of differences in the electrochemical forces for the three ions. In view of the difference between  $E_{IFL}$  and  $E_K$ , however, it seemed reasonable to consider that the IFL action may relate to the mechanism separating the RMP from  $E_K$ .

A possible relationship between  $E_{IFL}$  and RMP was explored to test the hypothesis that since leakage channel conductance determines RMP and if IFL increased the conductance of leakage channels,  $E_{IFL}$  should be influenced by RMP. Again, notwithstanding the lack of change in  $E_{IFL}$  with manipulations of  $Na^+$  and  $Cl^-$  in the external media, two observations suggested that IFL may have increased the leakage of ions other than  $K^+$ . First, in the graph of  $E_{IFL}$  and  $E_K$  versus external  $[K^+]$ , the poorer correlation at lower  $K^+$  concentrations (see Fig. 18E) suggests the minor

involvement of an additional ion. And second, in a graph of  $E_{\text{IFL}}$  versus RMP prior to IFL application, an association was found to exist as the variation in  $E_{\text{IFL}}$  was correlated to the variation in RMP ( $r = 0.74$ , 2-tail  $P < 0.0005$ ,  $n = 20$ ; see Fig. 25, EGTA data). Of course, a systematic error in junction potential from neuron to neuron would have resulted in a correlation between RMP and  $E_{\text{IFL}}$ .

As the initial RMPs in the BAPTA sample were noted to be relatively hyperpolarized (cf. Schwindt, Spain and Crill 1992), the relevant BAPTA data were plotted on the graph of  $E_{\text{IFL}}$  versus RMP (see Fig. 25, BAPTA data). The  $E_{\text{IFL}}$  measured in the presence of internal BAPTA approximated the above correlation to RMP reasonably well at the hyperpolarized end of the relationship. One therefore could infer that  $\text{Ca}^{2+}$  did not have a unique role in the IFL-action.

#### 3.4.5 IFL decreased inward rectification

Although IFL application increased membrane conductance for potentials positive to  $E_{\text{K}}$ , IFL decreased inward rectification for potentials negative to  $E_{\text{K}}$  during voltage-ramp experiments (see Fig. 26A and B). As a result, total membrane conductance for potentials negative to  $E_{\text{K}}$  was either unchanged by IFL or reduced (see Fig. 26B). Presumably, the decrease in inward rectification was occasionally greater than the increase in leakage conductance. Although the voltage-step experiments had shown that the increase in conductance was linear both above and below  $E_{\text{K}}$  when fast inward rectification was blocked by TEA (see Fig. 19B), voltage ramps were compared to voltage steps in the absence of  $\text{K}^{+}$ -channel blockers. In voltage step experiments, the current traces and their I-V relationships before and during IFL provided confirmation that the decrease in inward rectification was due to a decrease in  $I_{\text{Kir}}$  (see Fig. 26C, D and E).

In the case that an IFL-induced decrease in inward rectification shifted the  $E_{\text{IFL}}$  towards  $E_{\text{K}}$ , an attempt was made to block inward rectification during voltage ramps. There were two reasons why this was done. First, when fast inward rectification had been blocked with TEA during voltage steps, the  $E_{\text{IFL}}$  values represented some of the more positive ones ever recorded. However, it was difficult to get consistent  $E_{\text{IFL}}$  data from voltage step protocols due to the need for steady-state IFL action at a given concentration. And second, during the internal  $\text{Cs}^{+}$  experiments when inward rectification was blocked,  $E_{\text{IFL}}$  was positive relative to  $E_{\text{IFL}}$  without

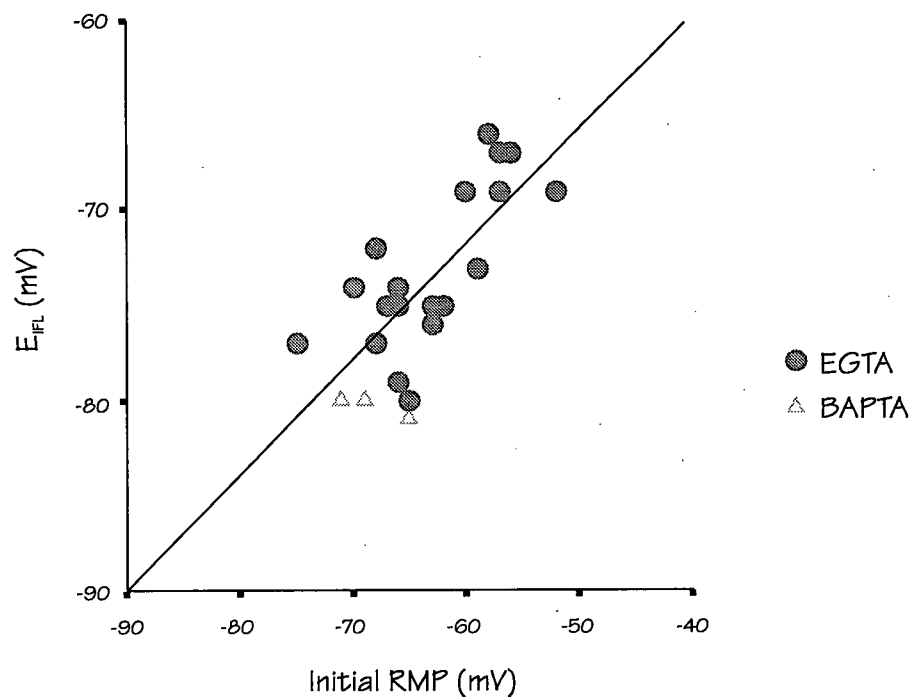


**Fig. 25. Effect of resting membrane potential on  $E_{IFL}$ .**

Graph of  $E_{IFL}$  versus initial RMP for individual neurons ( $n = 23$  with one result in duplicate). Results were plotted for 2 groups of neurons based on the type of internal  $Ca^{2+}$  chelation: intracellular ethylene glycol-bis( $\beta$ -aminoethylether) N,N,N',N'-tetraacetic acid (EGTA,  $n = 20$ ) 10 mM; and intracellular 1,2-bis(2-aminophenoxy)ethane N,N,N',N'-tetraacetic acid (BAPTA,  $n = 3$ ) 10 mM. Note the apparent association between  $E_{IFL}$  and RMP ( $r = 0.74$  for EGTA data) that does not depend on the type of  $Ca^{2+}$  chelation.

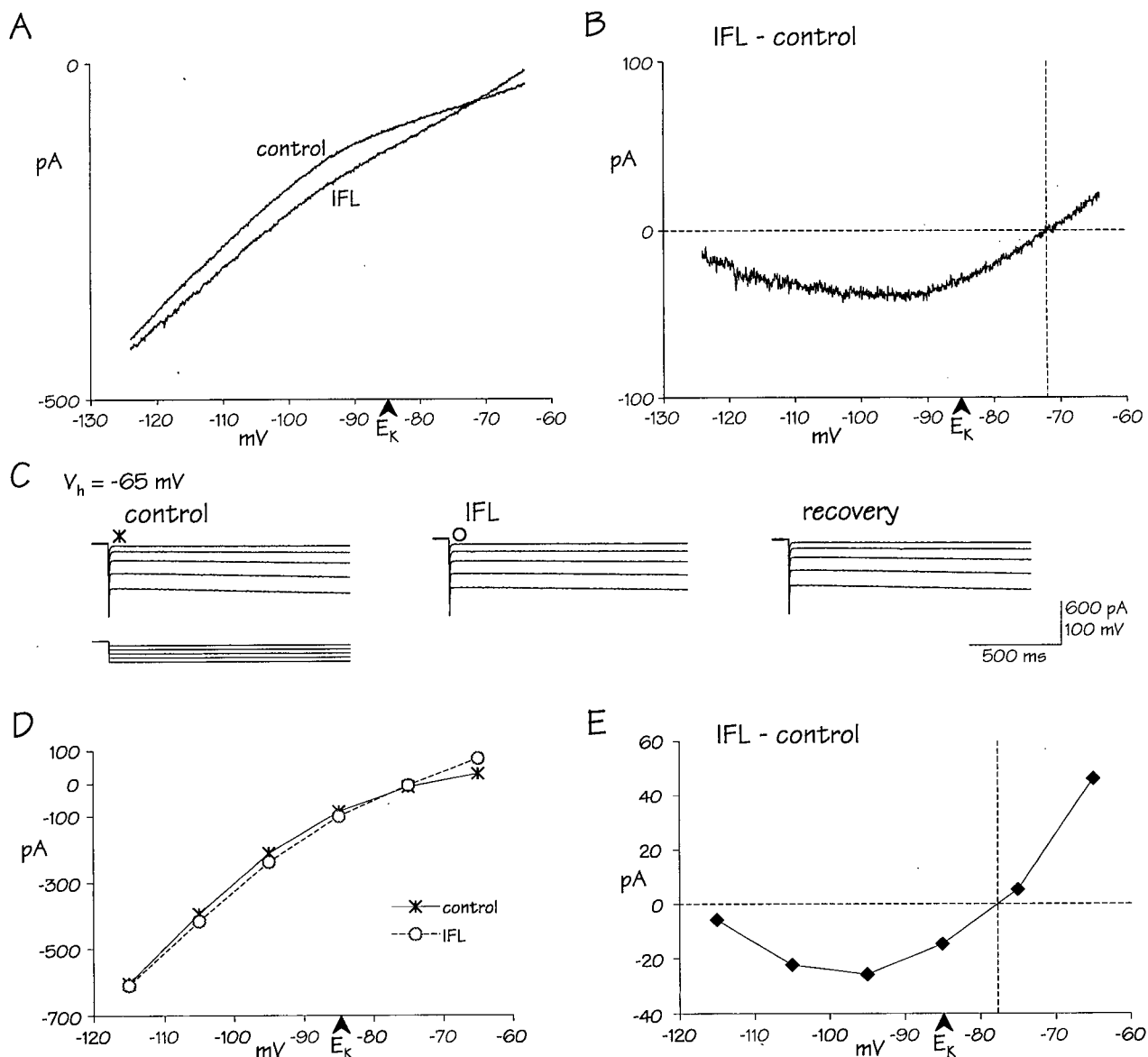


**Fig. 26. Effect of IFL on inward rectification.**

**A:** voltage-clamp recordings showing current response to hyperpolarizing voltage ramp (-64 to -124 mV) before and after IFL. Note the decrease in inward rectification by IFL. **B:** IFL-induced current derived from **A** by performing a current subtraction. Note the IFL-induced increase in conductance positive to  $E_K$  (increase in slope) and the decrease in conductance negative to  $E_K$  (decrease in slope). **C:** current response from a voltage-clamp of -65 mV to superimposed long, hyperpolarizing voltage steps of increasing amplitude before and after IFL in another neuron. Note that the inward rectification seen in voltage ramps was due to  $K_{ir}$ -current. Note also that IFL did not increase current amplitudes in the voltage range for  $K_{ir}$ -current. **D:** instantaneous I-V relationship for the currents in **C**. **E:** IFL-induced current derived from **D** by performing a current subtraction. Note the similar response to voltage steps in **D** and **E** as to voltage ramps shown in **A** and **B**. Panel **C**, **D** and **E** are from the same neuron.

internal  $\text{Cs}^+$ . Of course, the  $\text{Cs}^+$  result was presumably related mainly to a decrease in  $\text{K}^+$  leakage conductance with preservation of non- $\text{K}^+$  leakage. In any case, a low concentration of  $\text{Ba}^{2+}$  (100  $\mu\text{M}$ ) was applied to block fast inward rectification due to  $I_{\text{Kir}}$ . During a current-clamp recording,  $\text{Ba}^{2+}$  blocked the fast inward rectification with a time-dependent lag, but exposed a sag-like response in the membrane potential when hyperpolarizing current steps were injected ( $n = 1$ ; see Fig. 27A; cf. Nisenbaum and Wilson 1995). The exposed sag was likely responsible for the residual inward rectification seen during voltage ramps ( $n = 2$ ; see Fig. 27B). Similar to the experiments with a high concentration of  $\text{Ba}^{2+}$ , however, the application of IFL resulted in the same  $E_{\text{IFL}}$  with or without a low  $\text{Ba}^{2+}$  concentration ( $n = 1$ ).

In this low  $\text{Ba}^{2+}$  concentration experiment, IFL also decreased the residual inward rectification (see Fig. 27C). Presumably IFL decreased the sag current, a finding which had been occasionally seen during voltage-step experiments ( $n = 3$ ) when  $I_{\text{Kir}}$  was blocked by TEA (3 of 3 neurons). An effort was made to completely remove inward rectification during voltage ramps before applying IFL. External  $\text{Cs}^+$  (5 mM) was used to block  $I_{\text{Kir}}$  and the presumed  $I_{\text{H}}$  (see Fig. 27D). Voltage ramps then showed no inward rectification with hyperpolarization, and IFL increased membrane conductance both above and below  $E_{\text{K}}$  ( $n = 1$ ; see Fig. 27E). In addition,  $E_{\text{IFL}}$  was unchanged with external  $\text{Cs}^+$  (see Fig. 27F).

#### 3.4.6 IFL did not increase steady-state conductance through the ATP-sensitive $\text{K}^+$ channel that is suppressed by glibenclamide

Anoxic insults to central neurons reportedly induce an early hyperpolarization with an increase in membrane conductance due to increased  $\text{K}^+$  efflux (Fujiwara et al. 1987; Leblond and Krnjević 1989). ATP-sensitive  $\text{K}^+$  channels are partly responsible for this hyperpolarization during energy depletion (Zhang and Krnjević 1993) because the specific ATP-sensitive  $\text{K}^+$  channel blocker, glibenclamide, prevents much of the conductance change (Jiang and Haddad 1991; Politi and Rogawski 1991). Since rapid unconsciousness, similar to the anaesthetic state, develops during *in vivo* anoxia, glibenclamide was used to determine if the ATP-sensitive  $\text{K}^+$  channel was involved in the IFL-induced increase in membrane conductance.

During current-clamp recordings from a manual voltage clamp at an imposed depolarized

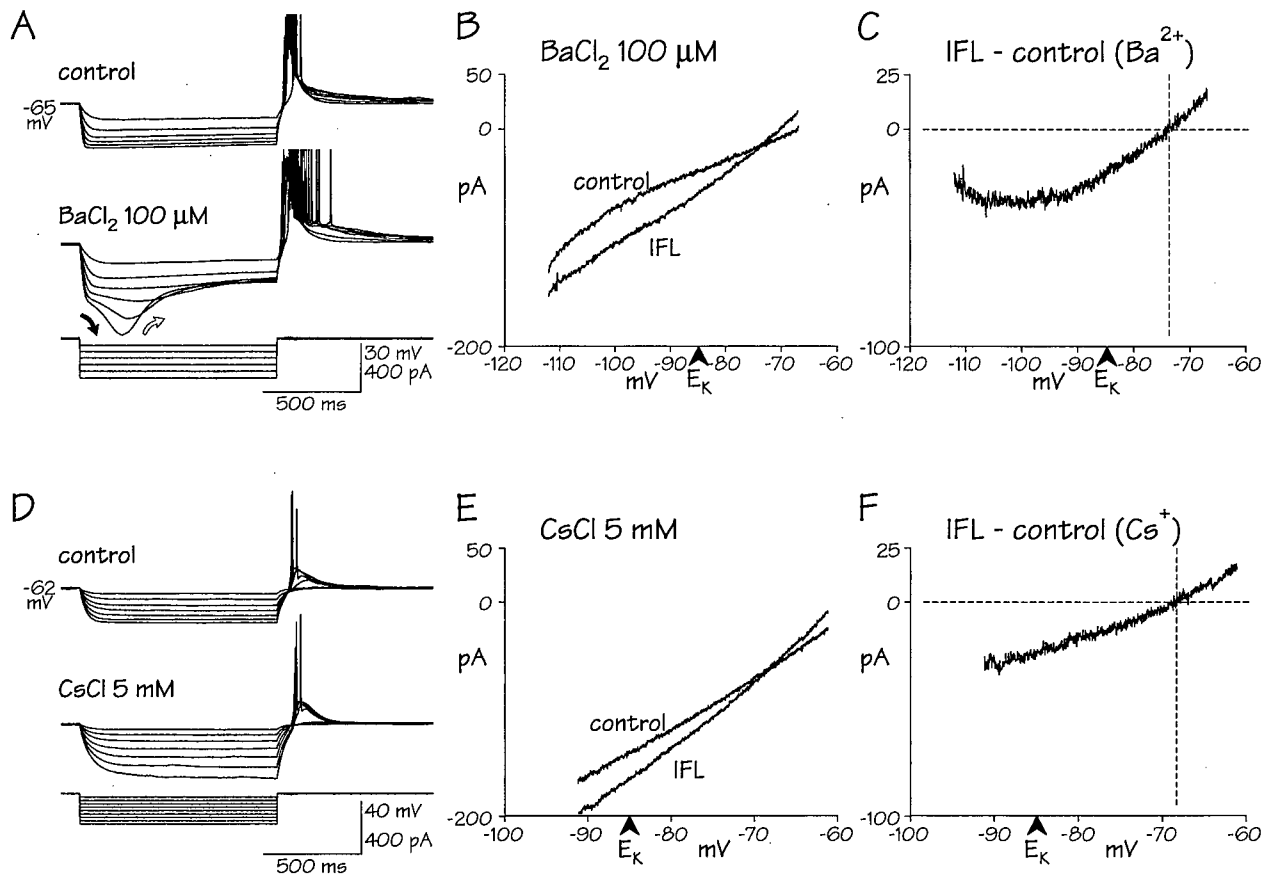


**Fig. 27. Effect of IFL on steady-state conductance during blockade of inward rectification.** **A:** current-clamp recordings showing voltage response from a depolarized potential to superimposed hyperpolarizing current steps of increasing amplitude with the hyperpolarization-activated fast inward rectification in control. During application of BaCl<sub>2</sub> 100 μM, note the blockade of the underlying Kir-current with a time-dependent lag (filled arrow), and the exposure of a depolarizing sag in the hyperpolarized membrane potential (outlined arrow). **B:** voltage-clamp recordings during perfusion with low-dose Ba<sup>2+</sup> showing current response to hyperpolarizing voltage ramp (-67 to -113 mV) before and after IFL in another neuron. Note the persistent inward rectification in control presumably due to either the partial time-dependent block of I<sub>Kir</sub> or the exposed sag current. **C:** IFL-induced current derived from B by performing a current subtraction. Note that IFL decreased the inward rectification at very negative potentials presumably to a greater extent than the increase in leakage conductance. **D:** current-clamp recordings in another neuron showing voltage response from a depolarized potential to superimposed hyperpolarizing current steps of increasing amplitude with hyperpolarization-activated fast inward rectification in control. During application of CsCl 5 mM, note the blockade of all inward rectification. **E:** voltage-clamp recordings during perfusion with Cs<sup>+</sup> showing current response to hyperpolarizing voltage ramp (-62 to -92 mV) without inward rectification before and after IFL in the neuron in D. **F:** IFL-induced current derived from E by performing a current subtraction. Note the increase in conductance at potentials positive and negative to E<sub>K</sub>.

membrane potential of  $\sim -60$  mV, input conductance was monitored with small, intermittent hyperpolarizing current pulses. A standardized 1 to 1.5 min application of IFL at 4% was applied before, during and after an application of glibenclamide (1 - 80  $\mu$ M;  $n = 7$ ). Glibenclamide application at 40 and 80  $\mu$ M ( $n = 4$ ) decreased input conductance and slightly decreased a positive holding current (implying depolarization), but there was no change in the IFL-induced increase in conductance by any of the glibenclamide applications. Even though the  $K^+$  anoxic response of some neurons is insensitive to glibenclamide (Godfraind and Krnjević 1993), the results presented here are consistent with a TEA suppression of the anoxic response (Krnjević and Leblond 1989).

#### 3.4.7 IFL's effect on non-spiking cells was consistent with leakage of $K^+$ from spiking cells

Intracellular recordings were made from unresponsive cells presumed to be glia according to the following criteria: (1) a relatively negative initial RMP ( $-79 \pm 1$  mV;  $n = 5$ ); (2) an extremely low input resistance ( $4 \pm 3$  M $\Omega$ ); (3) an extremely small membrane time constant ( $1.5 \pm 1.1$  ms); and (4) the absence of action potentials, even with very large depolarizing pulses. During voltage-clamp recordings in these cells at RMP, applications of a high concentration of IFL (4%) produced an inward current that was both reversible and reproducible (5 of 5 cells; see Fig. 28A). Similarly, an inward current developed during the application of high concentrations of  $K^+$  (see Fig. 28A). Since glial cells have an almost exclusive permeability to  $K^+$  ions, the inward current must have been due to a decrease in outward current. Consistent with a decrease in  $K^+$  efflux, both the IFL- and the  $K^+$ -induced decreases in outward current were associated with depolarization (see Fig. 28B). For example, application of a high  $[K^+]$  solution (9.25 mM) resulted in a depolarization (23 mV; see Fig. 28B) nearly equivalent to the Nernstian depolarizing shift of  $E_K$  from  $-85$  to  $-71$  mV.

In presumed glial cells, the amplitude of the IFL-induced "inward" current at RMP was proportional to the duration of application of a high concentration of IFL (4%; see Fig. 29A). However, the time for recovery was not dependent on the duration of the IFL application (cf. Croning et al. 1995). Similar to the paradoxical effects of anoxia on hippocampal neuronal RMP and glial RMP (cf. Leblond and Krnjević 1989), the IFL-induced depolarization of non-spiking cells suggested an indirect effect due to  $K^+$  leakage from spiking cells.

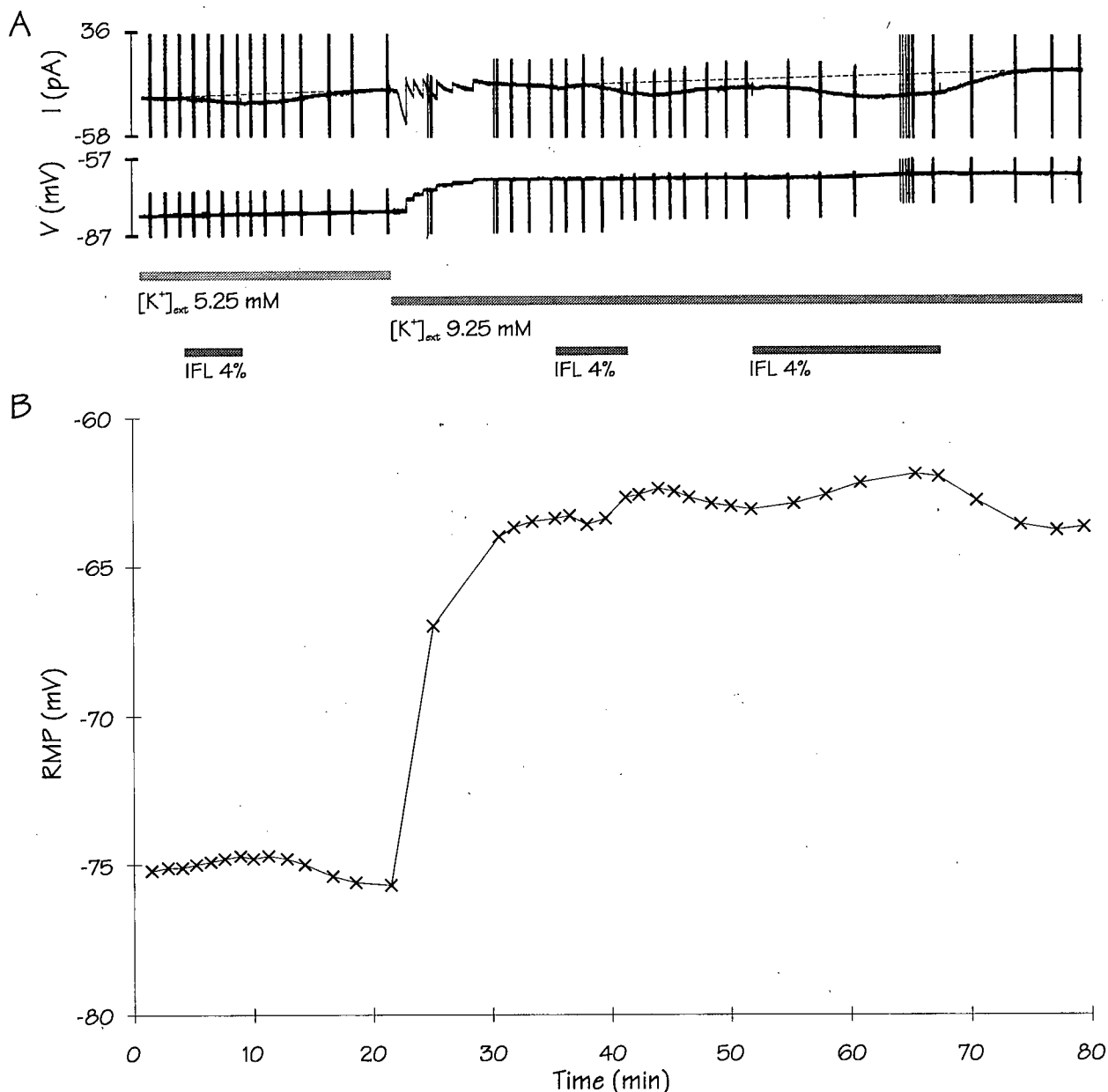


**Fig. 28. Effect of IFL on non-spiking cells.**

**A:** voltage-clamp recordings showing chart record of current response from a non-spiking cell held at  $-75$  mV during multiple IFL applications of increasing duration before and after a change to high  $[K^+]_{ext}$  (9.25 mM). Note that in contrast to neurons held near rest, IFL induced an apparent "inward" current. This current was both reversible and reproducible. The chart record of the clamped holding potential is also shown since the voltage was gradually changed to increasingly depolarized levels during equilibration of high  $[K^+]_{ext}$ . **B:** time-series plot of membrane potential at zero current derived from hyperpolarizing voltage ramps in A. The resting potential in this cell had initially been  $-79$  mV. Note the depolarization with IFL and with an increase in  $[K^+]_{ext}$ . Note also that the change in  $[K^+]_{ext}$  from 5.25 mM to 9.25 mM resulted in a depolarizing shift of RMP by 23 mV. As the calculated  $E_K$  would have shifted 24 mV, the depolarization was consistent with an exclusive permeability to  $K^+$ . Presumably then, the IFL-induced "inward" current was due to a decrease in outward current, similar to the high  $K^+$ -induced depolarization.

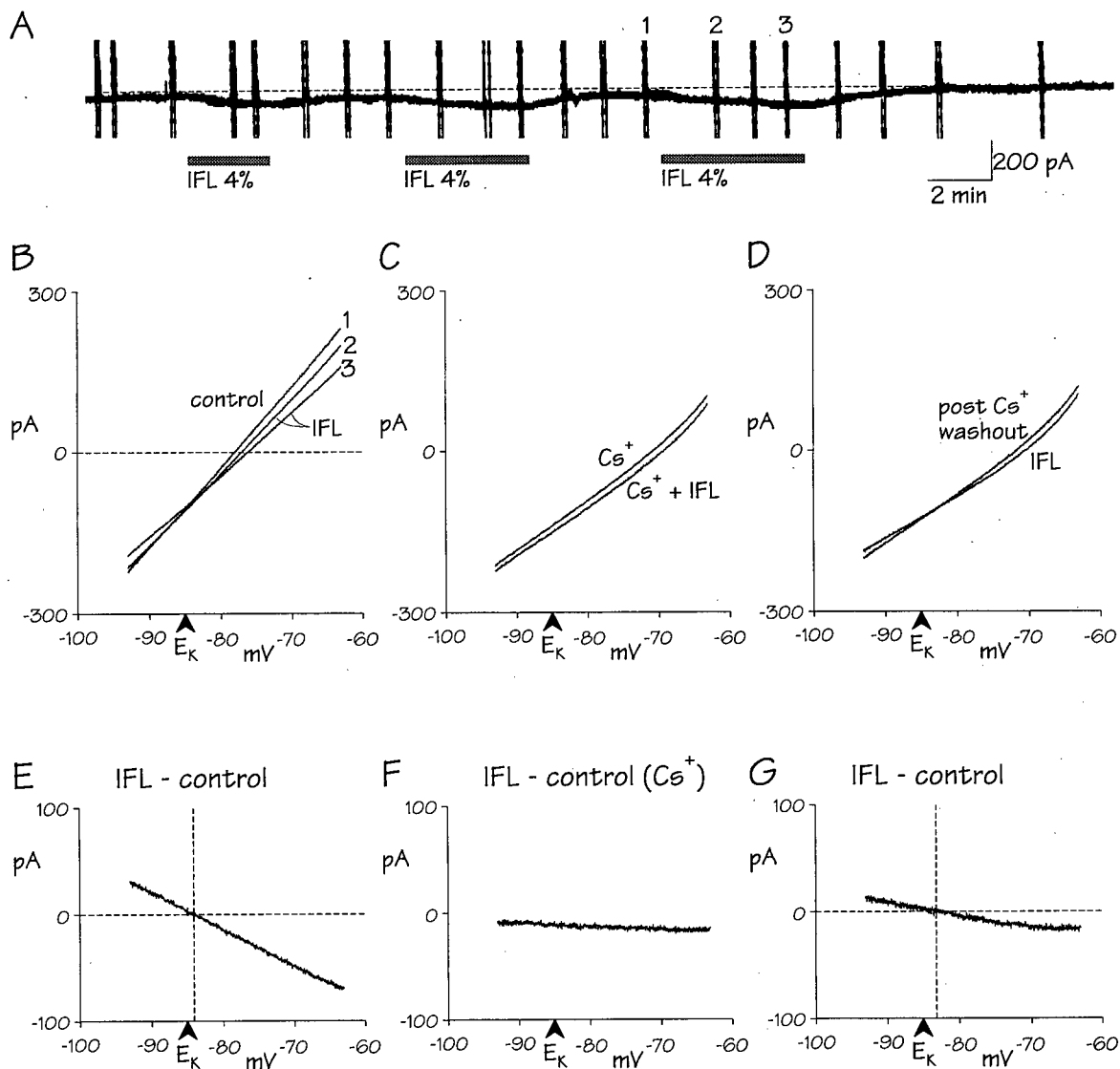


**Fig. 29. Effect of Cs<sup>+</sup> on IFL-induced current in non-spiking cells.**

**A:** voltage-clamp recordings showing chart record of current response from another presumed glial cell held at  $-78$  mV during multiple IFL applications. Note that the amplitude of IFL-induced decrease in outward current was proportional to the duration of IFL application, yet the recovery time was brief, suggesting that glial depolarization was due to IFL-induced increase in K<sup>+</sup> leakage from spiking cells. **B:** current response to hyperpolarizing voltage ramp ( $-64$  to  $-94$  mV) before and during IFL application in the same non-spiking cell. Note that IFL decreased conductance and depolarized RMP, as indicated by the rightward shift of the voltages along the horizontal dashed line at zero current. **C** and **D:** current response to voltage ramp with external Cs<sup>+</sup> 5 mM and after Cs<sup>+</sup> washout respectively, before and during IFL. **E, F** and **G:** IFL-induced current derived from **B, C** and **D** respectively by performing current subtractions. Note that Cs<sup>+</sup> blunted the IFL-induced conductance decrease, consistent with a postulated Cs<sup>+</sup>-related blockade of K<sup>+</sup>-induced depolarization in glial cells. All panels were from the same non-spiking cell.

Voltage ramps were also used during IFL applications to investigate conductance changes in non-spiking cells. Along with the depolarization, IFL induced a decrease in membrane conductance in a voltage-independent manner throughout a hyperpolarized voltage range ( $\sim -65$  to  $\sim -95$  mV; 5 of 5 cells; see Fig. 29B and E). The decreased conductance had a reversal potential of  $-83 \pm 1$  mV that was close to  $E_K$  ( $-85$  mV). A positive separation in these values was consistent with a postulated increase in external  $[K^+]$  and a corresponding depolarizing shift in the equilibrium potential. In addition, the IFL-induced depolarization of RMP ( $1.0 \pm 0.5$  mV) was of a similar magnitude as the presumed Nernstian shift in  $E_K$ .

Finally, an attempt was made in one non-spiking cell to block the IFL-induced changes with  $K^+$  antagonists. Following recovery from IFL,  $Cs^+$  5 mM application decreased the outward current at RMP, depolarizing the RMP and decreasing input conductance throughout a hyperpolarized voltage range. Recovery of this effect occurred during washout. During a second application of  $Cs^+$ , the IFL-induced decrease in conductance was largely prevented (see Fig. 29C and F). Following IFL washout, the cell recovered from  $Cs^+$ . A third application of IFL without  $Cs^+$  was then found to again induce a decrease in conductance (see Fig. 29D and G). Although inward rectification was not apparent during voltage ramps, application of  $Ba^{2+}$  100  $\mu$ M produced changes similar to  $Cs^+$ , but of smaller magnitude.  $Cs^{2+}$  or  $Ba^{2+}$  reportedly block glial  $I_{Kir}$  (Ransom and Sontheimer 1995) and  $Ba^{2+}$  blocks  $K^+$ -induced depolarization (Pappas and Ransom 1994) as well as glial  $K^+$  leakage (Reichelt and Pannicke 1993). It seemed possible that  $Cs^+$  may have reduced the response to a slight increase in external  $K^+$  concentration.

#### 3.4.8 Analysis of IFL-induced increase in $K^+$ conductance

The IFL-induced hyperpolarization and shunt, therefore, were due to an increase in a voltage-independent  $K^+$  conductance. Reversal potential experiments suggested a minor role for another ion, but this was not supported by ion substitution experiments. In any case, the action on thalamocortical neurons appeared to be associated with generalized  $K^+$  efflux as unresponsive non-spiking cells depolarized during high concentrations of IFL. The changes in leak conductance during IFL application in neurons were insensitive to external TEA, 4-AP and  $Cs^+$ , yet sensitive to external  $Ba^{2+}$  and internal  $Cs^{2+}$ . In addition,  $Ca^{2+}$  chelation and  $I_{K(Ca)}$ -blockers did not suppress the IFL action. Furthermore, long-acting voltage-dependent  $K^+$ -currents such as  $I_{Kir}$

and  $I_H$  which involves  $K^+$  and  $Na^+$  (McCormick and Pape 1990) did not contribute to the increase in steady-state permeability. In fact, IFL decreased inward rectification due to these two currents. Although inhalational anaesthetics reportedly reduce the H-conductance in sympathetic ganglia neurons (Tokimasa *et al.* 1990), it is possible that the IFL-conductance increase shunted these two currents.

Assuming that  $K^+$ -leak channels are distributed in both somatic and dendritic membranes, voltage-gated conductances in the dendrites would be particularly vulnerable to an IFL-induced shunt. For example, when current is injected into a dendrite, the imposed change in membrane potential decays with distance along the dendrite due to membrane current leakage. However, if IFL increased dendritic membrane conductance and thereby reduced the electrotonic spread of potentials, the current would in effect leak across the membrane to a greater extent and the distance along the dendrite of passive voltage spread would be shortened. A voltage-gated conductance located in the dendrites then could be isolated from changes in somatic potential. A shunt of dendritic T-current, therefore, was considered in the mechanism of the IFL-induced burst suppression.

### 3.5 Mechanism of IFL-induced burst suppression

#### 3.5.1 IFL-induced burst suppression appeared related to a dendritic shunt

In shunting the LTS, IFL appeared to affect the voltage- and time-dependent gating properties of the underlying T-current. In many neurons, however, much of the LTS amplitude could be regained by increasing either the hyperpolarizing current pulse before the rebound LTS or the depolarizing current pulse when eliciting the LTS from a steady hyperpolarized potential. In addition, much of the rebound LTS suppression could be overcome by increasing the duration of the hyperpolarizing pulse. In view of the IFL-induced increase in  $K^+$  leakage, the extensive dendritic arborization of thalamic relay neurons, and the predominance of T-channels in dendrites (thalamic reticular neurons: Destexhe *et al.* 1996; hippocampal: Karst, Joëls and Wadman 1993, Magee and Johnston 1995, Christie *et al.* 1995; cerebellum: Bossu, Dupont and Feltz 1989), the IFL-induced burst suppression may have partly resulted from a dendritic shunt.

One way of investigating a dendritic shunt mechanism by IFL is with dissociated neurons. However, presumed neuronal excision occurred during electrode withdrawal from the slice on at least three occasions following successful whole-cell recording. In these cases, the electrode potential remained near RMP in the perfusing solution after exiting the slice. From one electrode only a passive electrotonic response could be elicited, but in the other two situations an LTS could be evoked. These two neurons were initially located at depths of 50 and 65  $\mu\text{m}$  from the slice surface, which probably accounted for their excision. Electrical measurements demonstrated a decrease in membrane time constant and an increase in input resistance compared to control values, consistent with a marked decrease in cell surface area (see Fig. 30A, B and C). In fact, the capacitance derived from  $\tau = RC$ , which is proportional to surface area (Brown, Schwandt and Crill 1993), decreased by 95% and 92% in the two neurons with intact LTS. Presumably the distal dendritic arborization was left behind in the slice, thereby accounting for the significant reduction in cell surface area. Fortunately, one of the two neurons survived long enough to test with IFL. In this cell, the depth of the perfusing solution above the slice had been noted to be 850  $\mu\text{M}$  during the original electrode placement, so the electrode was withdrawn close to the fluid surface to ensure complete excision from the slice. After the neuron "died" (RMP 0 mV), the depth of fluid was measured and found to be unchanged from the original value, supporting the assumption that the neuron had been completely excised from the slice during the application of IFL.

Although  $\text{Na}^+$  spikes could not be elicited in this excised neuron, an obvious LTS was evoked from a hyperpolarized holding potential with depolarizing current pulses (see Fig. 30A and B). Consistent with a reduction in dendritic LTS, the amplitude of the excised LTS was less than the control LTS using similar hyperpolarized and depolarized potentials (see Fig. 30B). As the required holding potential was stable, it seemed reasonable to test the LTS response to IFL.

Application of IFL 4% for 2 min was associated with a reversible 6% decrease in negative (hyperpolarizing) holding current, consistent with an implied IFL-induced hyperpolarization. In addition, IFL produced a reversible 9% increase in input conductance and a reversible decrease, but largely preserved LTS amplitude (see Fig. 30D). This result with a high IFL concentration completely bathing the neuron supported the hypothesis that a large part of IFL's effect on the LTS in intact cells was due to a dendritic shunt. Interestingly, only a one minute application of

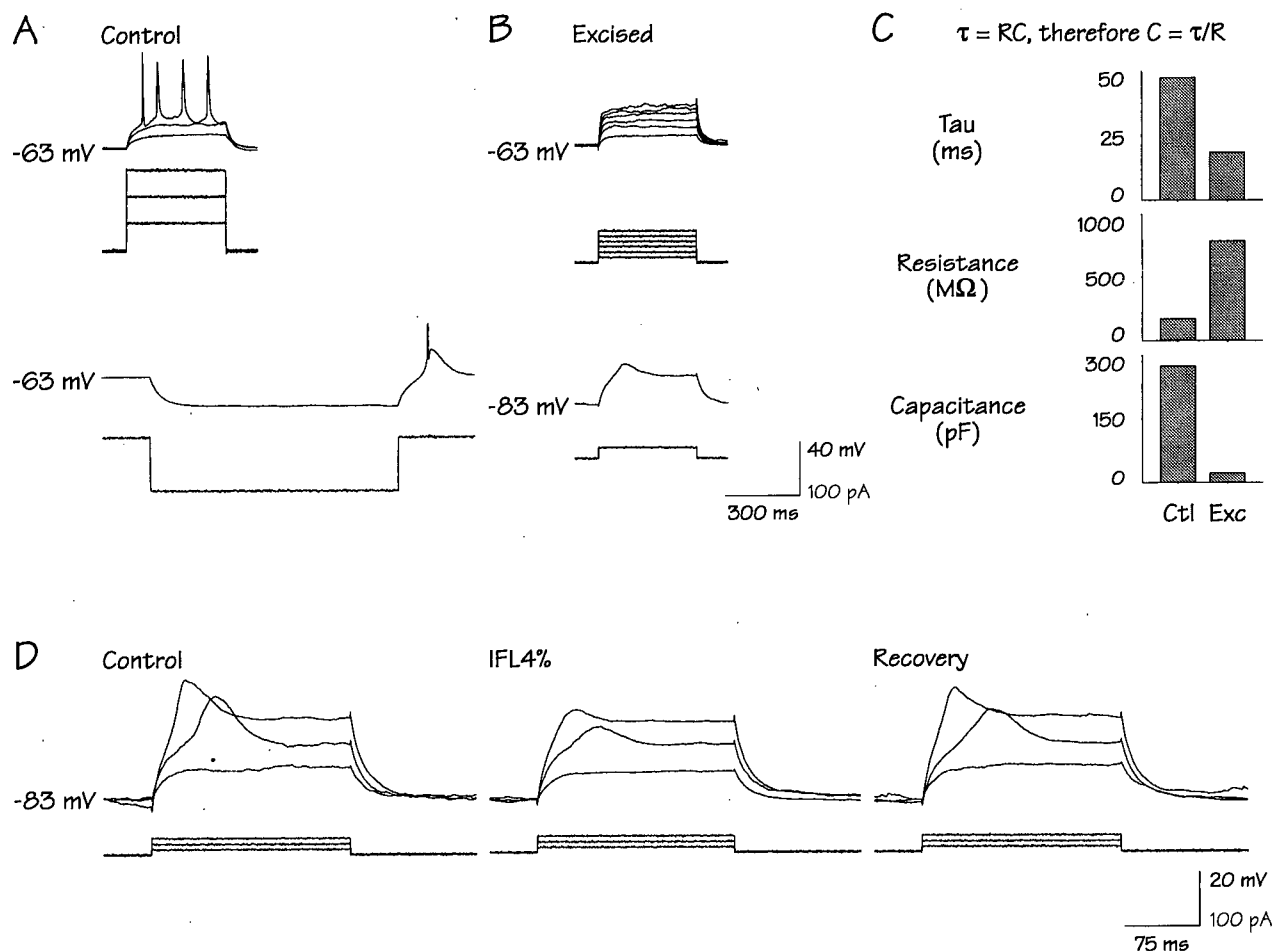


**Fig. 30. Effect of IFL on LTS in an acutely "dissociated" neuron.**

**A:** current-clamp recordings showing voltage response to superimposed depolarizing current pulses (top) and a longer hyperpolarizing pulse (bottom) from a depolarized holding potential before neuronal "excision." **B:** following neuronal "excision," voltage response to depolarizing current pulses from the pre-excision depolarized holding potential (top) and a hyperpolarized holding potential (bottom) similar to the potential reached during the long hyperpolarizing pulse in the pre-excision panel. Note the absent Na<sup>+</sup>-spikes and a slightly reduced LTS. **C:** bar graphs showing tau (top), input resistance (middle), and capacitance (bottom) before (ctl) and after (exc) excision. Note that tau decreased and resistance increased following excision, yet capacitance decreased markedly ( $C = \tau/R$ ) consistent with a significant decrease in membrane surface area. **D:** following neuronal excision, voltage response to depolarizing current pulses from an imposed manual voltage-clamp before, during and after IFL 4%. Note that the IFL application changed input conductance and the LTS only slightly. All panels are from the same neuron.

IFL (4%) to the slice had increased membrane conductance by 42% before neuronal "excision."

Because isoflurane inhibits T-current in various neurons including hippocampal (Study 1994), investigations into the effects of IFL on T-currents were done using voltage-clamp analysis. Although the technique requires compact cell structure for biophysical interpretations of a voltage-gated conductance, voltage-clamp recordings may provide functional information about remote dendritic activities. During these experiments, the  $\text{Ca}^{2+}$  charge carrier was reduced to 1 mM and  $\text{Mg}^{2+}$  was increased to 3 mM in an attempt to stabilize the dendritic voltage during T-current activation. In addition, pharmacological blockers of voltage-gated  $\text{Na}^+$  and  $\text{K}^+$  conductances (TTX 300 nM, 4-AP 3 mM and TEA 10 mM) were used to better isolate the T-current. External  $\text{Cs}^+$  was not used routinely since  $I_{\text{H}}$  was not prominent during the blockade of  $I_{\text{Kir}}$  by TEA (sag current activated slightly only at hyperpolarizations  $> -90$  mV). When external  $\text{Cs}^+$  was applied with the other channel blockers, however, presumed high-threshold  $\text{Ca}^{2+}$ -currents were seen more frequently on top of the T-currents (cf. Tennigkeit, Schwarz and Puil 1996).

During voltage-clamp experiments, IFL (0.5, 1 and 2%) reversibly decreased T-current in a concentration-dependent manner (17 of 17 neurons). For example, from a holding voltage near rest, a short conditioning step to a hyperpolarized voltage followed by a depolarized test command elicited the T-current as a transient inward (downward) current (see Fig. 31B). Although this voltage-clamp protocol simulated the voltage changes during a rebound LTS, it controlled for the IFL-induced shunt of the hyperpolarizing pulse seen during current-clamp as well as IFL-induced changes in the membrane time constant. To further elucidate a possible shunt of dendritic T-current, the onset and recovery of the reduction in T-current were graphed using a time-series plot alongside the IFL-induced increase in leakage conductance during five changes in IFL concentration (see Fig. 31A; Ries and Puil 1993). From this analysis, the conductance increase and the T-current decrease occurred simultaneously, supporting the hypothesis that an increased conductance produced the decrease in the LTS. Application of  $\text{Ni}^{2+}$  (0.5 mM) blocked T-current without affecting leak conductance (see Fig. 31C).

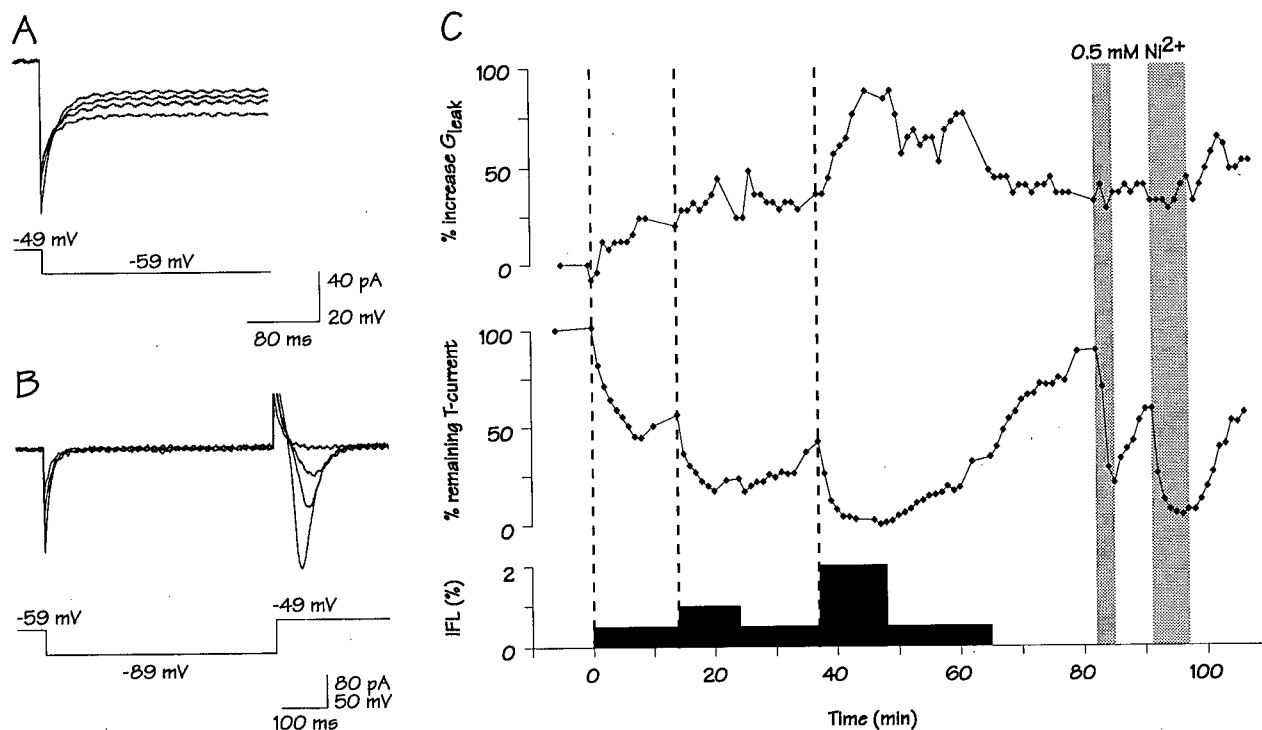


**Fig. 31. Effect of IFL washin and washout on leak conductance and T-current.**

**A:** voltage-clamp recordings showing IFL-induced increases in leak currents and concentration-dependence (from top to bottom; control, 0.5%, 1%, 2%). Leak currents were elicited with a hyperpolarizing voltage command (10 mV) from near RMP. **B:** leak-subtracted T-currents showing IFL-induced decreases and concentration-dependence (from bottom to top; control, 0.5%, 1%, 2%). T-currents were elicited with a 500 ms conditioning command to -89 mV and a test pulse to -49 mV. Leak currents were subtracted by computer. **C:** Time-series record of IFL-induced changes in leak currents ( $G_{\text{leak}}$ ; upper) and peak amplitudes of leak-subtracted T-currents (middle) with bar graph representing duration of application of IFL (bottom). Measurements were made at 1 min intervals; the total duration of IFL was 65 min with minimal rundown of T-current. Vertical dashed lines represent increases in [IFL]. Vertical dotted lines represent decreases in [IFL]. Note that the rates of induction and recovery for the IFL-induced increase in leak currents and the decrease in T-currents were similar. The  $\text{Ca}^{2+}$ -channel blocker  $\text{Ni}^{2+}$  (0.5 mM) was applied 2 times (vertical shaded bars). Note that  $\text{Ni}^{2+}$  application reversibly blocked the T-current, but did not change leak currents. All panels are from the same neuron with a solution containing TTX 300 nM and the  $\text{K}^{+}$  antagonists TEA 10 mM and 4-AP 3 mM.

### 3.5.2 IFL suppressed T-current by changing the spatial distribution of imposed voltages

Recognizing the limitations of voltage-clamp recordings from intact cells in slices, three T-current properties were investigated. First, the apparent voltage dependence of activation was compared before and during cumulative IFL concentrations. Next, the process of removal of inactivation of T-current, its voltage-dependence (steady-state inactivation) and its rate of recovery were examined. In these experiments, ohmic leakage currents were subtracted from voltage-clamp records. Peak T-currents then were used to construct I-V relationships. These relationships also were compared by plotting the normalized peak current *versus* potential before and during IFL application.

In the analysis of voltage-dependent activation, a long (>3s) hyperpolarized (~-110 mV) conditioning command was used to remove inactivation, followed by depolarized test commands of varying voltages (see Fig. 32A). Although tail-current protocols were not used to approximate maximum activation nor control for the driving force (Huguenard 1996), the normalized peak current was plotted to reflect an activation curve. During control conditions, the activation threshold for T-currents was ~-70 mV with a steep activation curve over only 5 to 10 mV (see Fig. 32A and B). Although similar to previously reported recordings in thalamic (Crunelli, Lightowler and Pollard 1989) and hippocampal (Karst, Joels and Wadman 1993) slices, the all-or-none manner of activation contrasted with reported graded recordings from dissociated neurons (Huguenard 1996). Presumably the steepness of activation reflected compromised voltage control as well as the rapid response from a large dendritic population of T-channels. Although the leak-subtracted T-current decreased during IFL, the all-or-none response changed to a graded one and shifted in a depolarized direction in a concentration-dependent manner (9 of 9 neurons; see Fig. 32B and C). The electrode voltage reflecting 50% "activation" changed as follows in mV: control,  $-68 \pm 2$  ( $n = 17$ ); IFL 0.5%,  $-60 \pm 3$  ( $n = 5$ ); IFL 1%,  $-55 \pm 10$  ( $n = 7$ ); and IFL 2%,  $-47 \pm 6$  ( $n = 5$ ; see Fig. 32D).

Steady-state inactivation was next tested as it determines the availability of T channels for activation from RMP during sleep. In contrast to the activation protocols, the voltage of the long and hyperpolarized conditioning command was varied and the depolarized test command was fixed, thereby controlling for the  $\text{Ca}^{2+}$  driving force (see Fig. 33A). During control testing, the

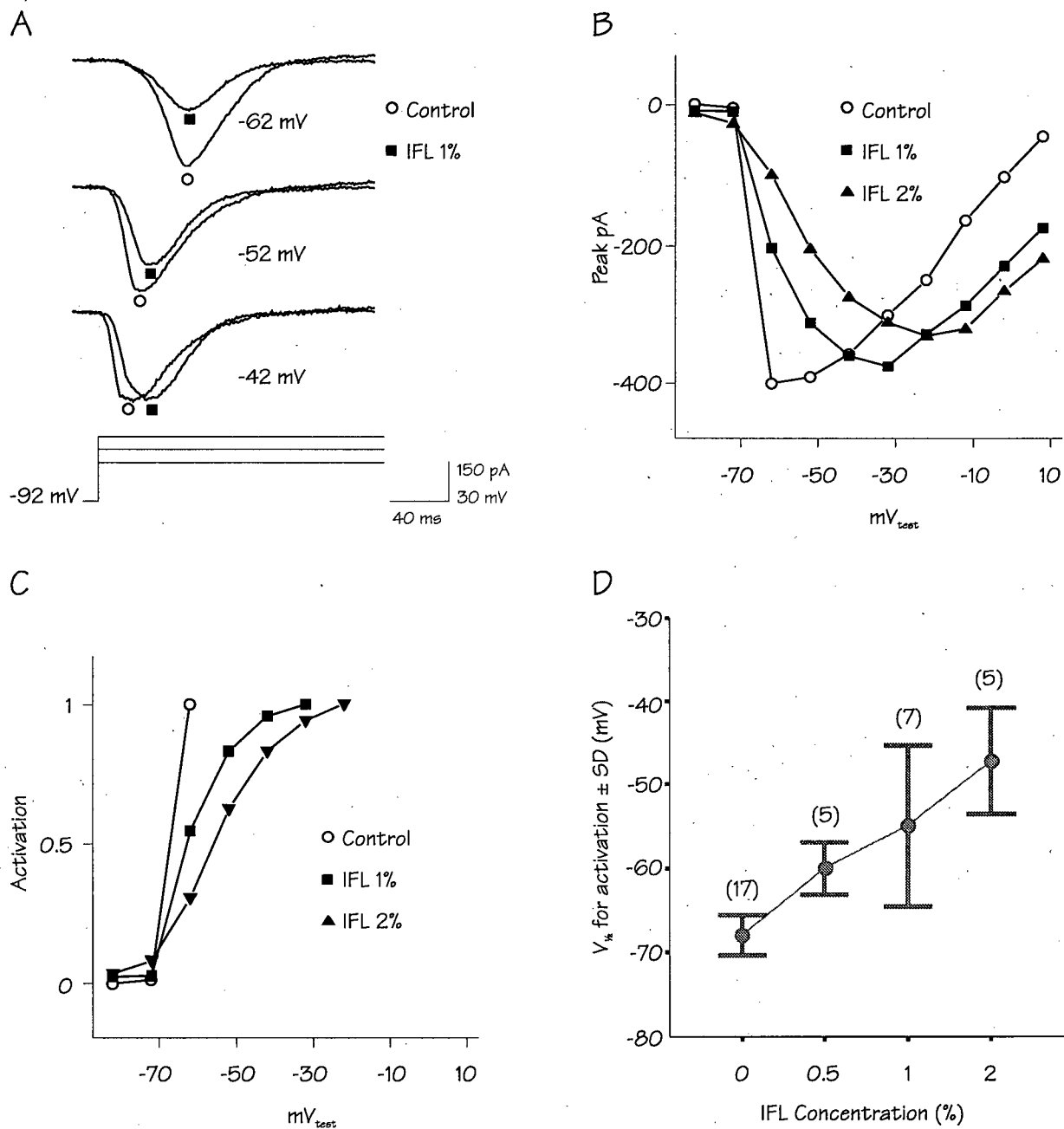


**Fig. 32. Effect of IFL on voltage-dependence of T-current activation.**

**A:** voltage-clamp recordings showing leak-subtracted T-currents elicited by 3 stepped voltage commands from a holding voltage of -92 mV. The control and IFL 1% responses are superimposed for each of the 3 test commands. Note the IFL-induced voltage-dependent decrease in T-current peak amplitude. **B:** I-V relationship for activation of peak T-current. Note the all-or-none response during control and the graded response with IFL. **C:** qualitative "activation" curve for T-current. Note the IFL-induced shift in the voltage-dependence of T-current activation. **D:** graph of the electrode voltage reflecting 50% activation *versus* IFL concentration for a series of neurons. Note that IFL shifted the activation curve in a depolarizing direction in a concentration-dependent manner. The numbers in parentheses represent *n*. A to C are from the same neuron. All responses were obtained in a solution containing TTX 300 nM, TEA 10 mM and 4-AP 3 mM.

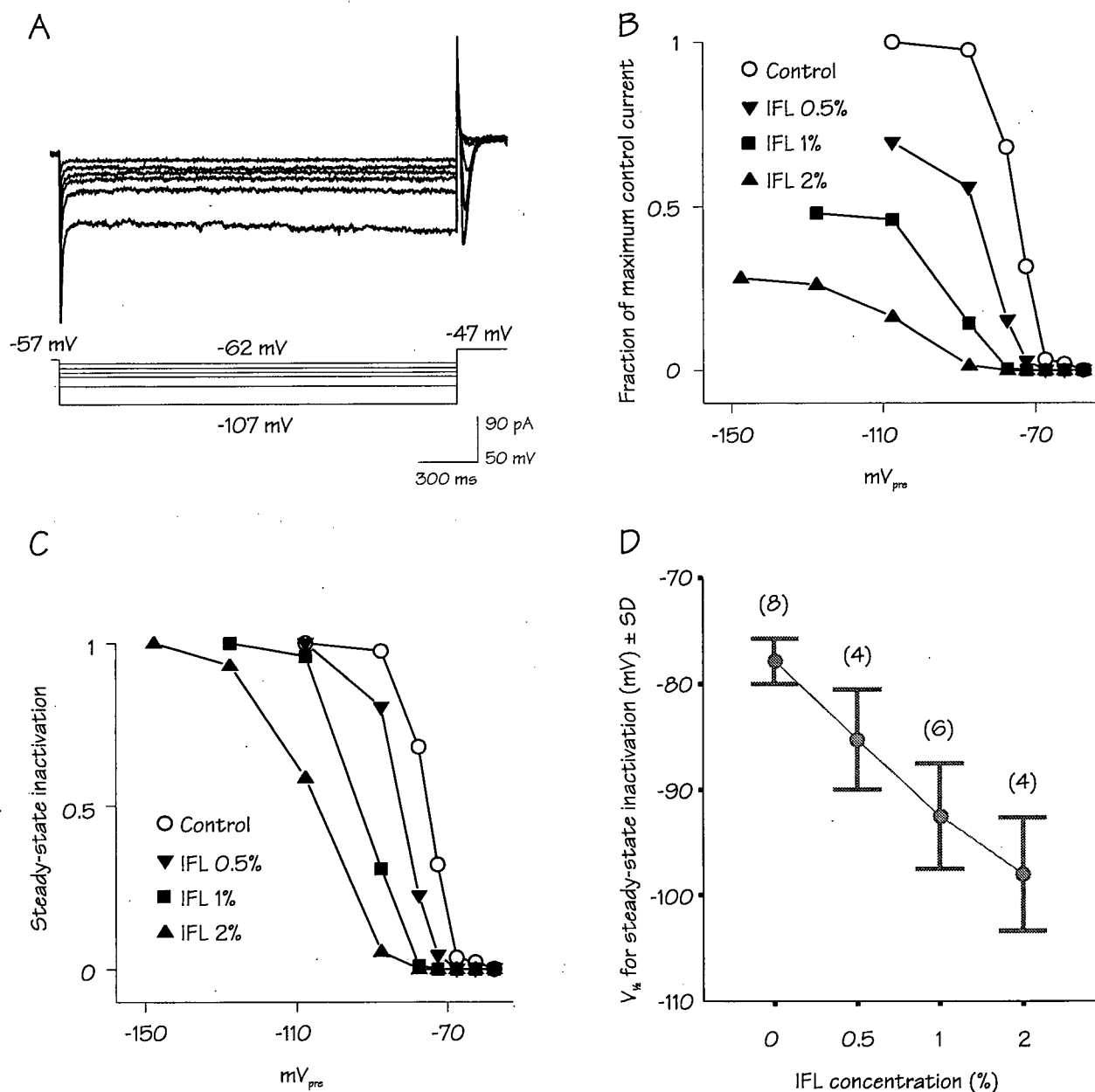


**Fig. 33. Effect of IFL on steady-state T-current inactivation.**

**A:** voltage-clamp recordings showing control T-currents elicited with a 2 s conditioning command at various hyperpolarized voltages and a fixed depolarized test command. **B:** graph of fraction of maximum control T-current *versus* the conditioning voltage ( $mV_{pre}$ ). Note that IFL decreased the peak T-current. **C:** inactivation curve for T-current. Note that IFL expanded and shifted the voltage-dependence in a hyperpolarizing direction. **D:** graph of averaged voltage midpoint for steady-state channel inactivation reflecting 50% inactivation *versus* IFL concentration for a series of neurons. Note that IFL shifted the inactivation curve in a concentration-dependent manner. The numbers in parentheses represent *n*. A to C are from the same neuron. All responses were obtained in a solution containing TTX 300 nM, TEA 10 mM and 4-AP 3 mM.

voltage-dependency was similar to reports on dissociated neurons (Hernández-Cruz and Pape 1989; Huguenard and McCormick 1992), with T-current becoming available from around RMP and increasing in a smoothly graded fashion with progressive hyperpolarization (see Fig. 33B). Under IFL application, the available T-current was decreased, but the voltage range expanded as well as shifted in a hyperpolarized direction in a concentration-dependent manner (7 of 7 neurons; see Fig. 33B and C). The electrode voltage reflecting 50% steady-state inactivation changed as follows in mV: control,  $-78 \pm 2$  ( $n = 8$ ); IFL 0.5%,  $-85 \pm 5$  ( $n = 4$ ); IFL 1%,  $-93 \pm 5$  ( $n = 6$ ); IFL 2%,  $-98 \pm 5$  ( $n = 4$ ; see Fig. 33D).

Finally, time-dependent removal of inactivation was investigated due to its importance in rhythmic burst firing and spindle oscillations. These experiments involved the same voltage protocol as steady-state inactivation, except that the duration of the hyperpolarizing conditioning command (rather than its voltage) was varied in order to assess the recovery of inactivation (see Fig. 34A). Instead of fitting time constants, the time to 50% recovery of peak T-current was measured at  $203 \pm 96$  ms in the control situation ( $n = 11$ ). During IFL, the available T-current was again reduced, but the recovery process became increasingly graded in a concentration-dependent manner (7 of 7 neurons; see Fig. 34B and C). The time for 50% recovery of peak T-current increased relative to the control value as follows: IFL 0.5%,  $72 \pm 35\%$  ( $n = 5$ ); IFL 1%,  $211 \pm 114\%$  ( $n = 3$ ); IFL 2%,  $333 \pm 153\%$  ( $n = 3$ ; see Fig. 34D).

The interpretation of these changes in voltage-clamp currents was complicated by a presumed inability to control dendritic membrane potential. For example, in contrast to dissociated neurons, a delay in the activation of T-current was observed (see Fig. 32A). This is consistent with spatially distant T-channels, according to mathematical models of voltage-dependent inward currents (Müller and Lux 1993). In these models of an active dendritic conductance, the I-V relations are steeply graded, yet become less steep with peak current attenuation when outward leakage currents are increased. In contrast to the presumed validity of voltage-ramp estimations of reversal potential for a steady-state conductance distributed throughout the soma and dendrites, a transient dendritic conductance is likely to be decreased by manipulations that increase membrane conductance (Spruston *et al.* 1993; Spruston, Jaffe and Johnston 1994).

When the increase in input conductance by IFL application was blocked by internal  $\text{Cs}^+$ ,

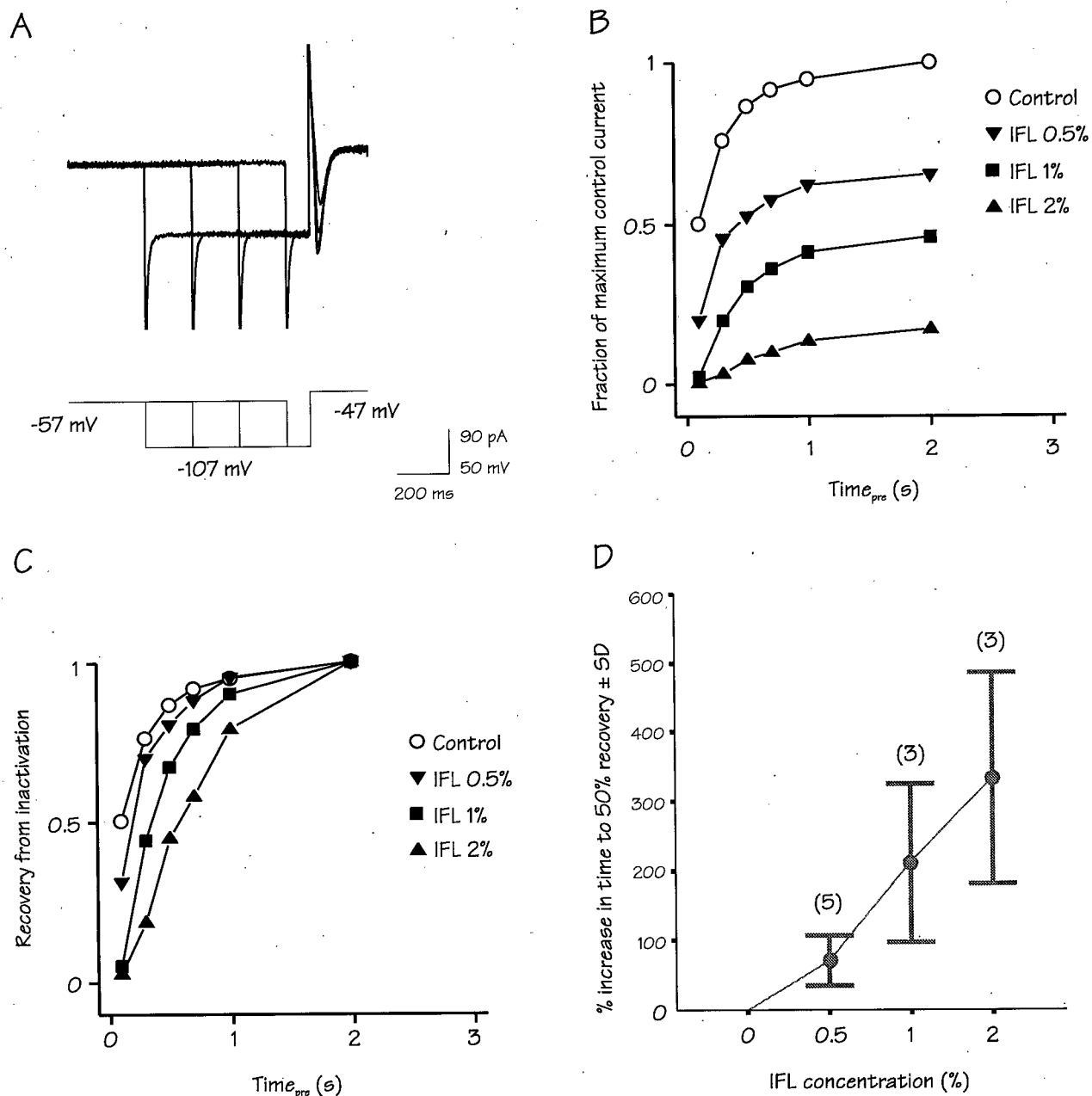


**Fig. 34. Effect of IFL on recovery from T-current inactivation.**

**A:** voltage-clamp recordings showing control T-currents elicited with a hyperpolarizing conditioning command of decreasing duration. The conditioning and test voltages were fixed.

**B:** graph of fraction of maximum control T-current versus the duration of the conditioning command ( $Time_{pre}$ ). Note that IFL decreased the peak T-current. **C:** inactivation recovery curves for T-current. Note that the recovery process became increasingly graded with IFL. **D:** graph of recovery midpoint versus IFL concentration for recovery from inactivation of T-current for a series of neurons. Note the concentration-dependent slowing of 50% recovery. The numbers in parentheses represent  $n$ . A to C are from the same neuron. All responses were obtained in a solution containing TTX 300 nM, TEA 10 mM and 4-AP 3 mM.

however, the peak T-current did not change (4 of 4 neurons; see Fig. 35A). In these experiments, when high concentrations of IFL (2 and 4%) induced an increase in membrane conductance, the voltage dependence for T-current expanded, but the maximum peak current still did not change. For example, IFL 4% shifted the hyperpolarizing voltage-dependency for steady-state inactivation in a hyperpolarized direction (see Fig. 35B). Furthermore, during 75 min of whole-cell recording, the peak amplitude of T-current steadily increased throughout the period, consistent with a progressive equilibration of internal  $\text{Cs}^+$  with the distal dendrites, a shortened length constant and therefore better voltage control (see Fig. 35B).

### 3.5.3 IFL-induced spatial block of T-window current did not affect $E_{\text{IFL}}$

Activation and inactivation curves for T-current reportedly overlap near RMP and result in a steady-state window conductance (Hutcheon *et al.* 1994; see Fig. 36A). In this analysis, only a qualitative representation is possible due to space-clamp errors and the less accurate activation protocol that was used. However, an attenuation of dendritic signal conduction by IFL could in effect separate the dendritic T-channels from the soma. As a functional reduction in this steady-state conductance would theoretically affect the reversal potential for the IFL-induced increase in membrane conductance,  $E_{\text{IFL}}$  was measured before and during blockade with nominally zero  $[\text{Ca}^{2+}]$  or  $\text{Ni}^{2+}$  (0.5 mM) in the external media (see Fig. 36B, C and D). During these experiments, however,  $E_{\text{IFL}}$  did not change (4 of 4 neurons).

### 3.5.4 Analysis of IFL-induced burst suppression

The IFL-induced burst suppression was largely due to the increase in  $\text{K}^+$ -conductance. As a result, a functional isolation of the dendritic T-current led to distorted voltage-dependencies in various properties of the T-current. For example, the IFL shunt restricted the spatial distribution of imposed somatic voltages in both depolarizing and hyperpolarizing directions away from RMP (see Fig. 36A). Since the voltages of T-current activation and steady-state inactivation were on either side of RMP, a presumed somatic electrode could not fully access either activation or steady-state inactivation during IFL.

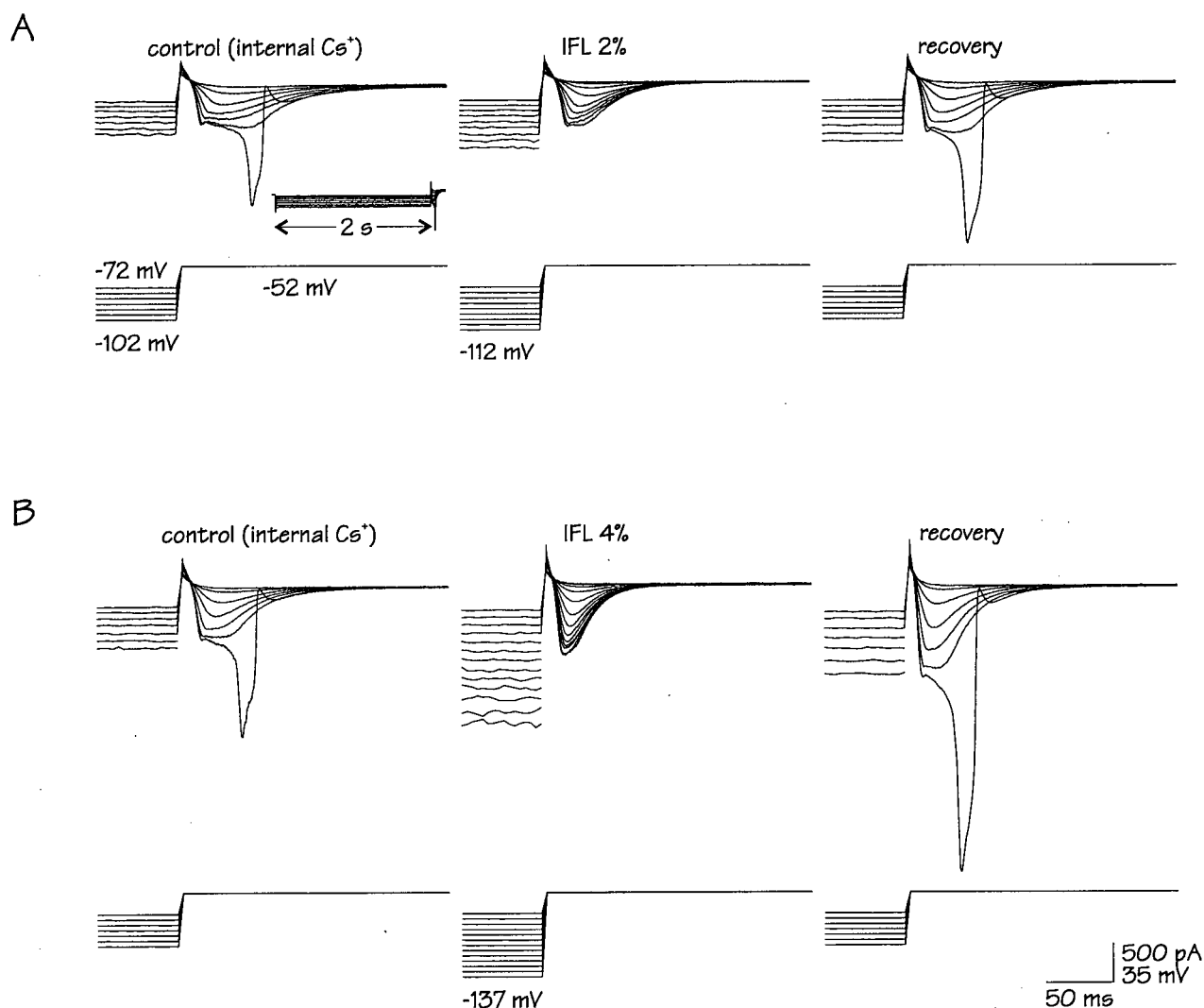


**Fig. 35. Effect of IFL on T-current in the presence of internal Cs<sup>+</sup>.**

**A and B:** voltage-clamp recordings showing T-currents in the presence of internal Cs<sup>+</sup> before, during and after IFL 2% and 4%, respectively in the same neuron. The inset trace in A shows the entire current response to a 2 s hyperpolarizing conditioning command of various voltages and a fixed test voltage (calibration bars for inset not shown). The faster transient was probably the high-voltage activated (HVA) current underlying the HTS. Note that the peak amplitude of T-current did not decrease with either application of IFL, but that the voltage-dependence expanded to a greater extent with the higher concentration of IFL. Note also that IFL still increased leak currents in the presence of intracellular Cs<sup>+</sup>. In addition, note that the peak amplitude of both the T-current and the transient HVA current steadily "ran up" during 75 min of whole-cell recording.

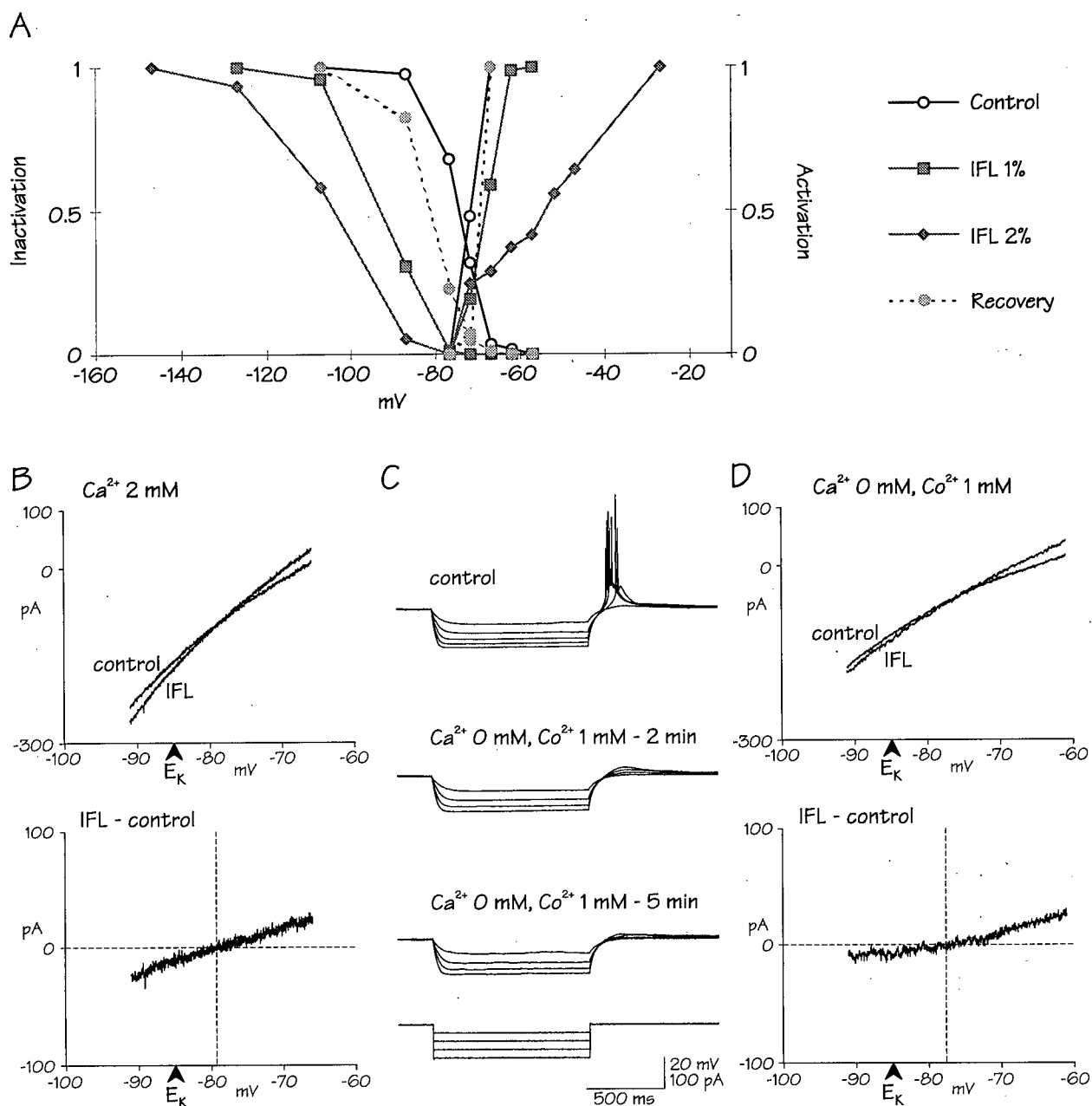


**Fig. 36. Effect of blocking T-window current on  $E_{IFL}$ .**

**A:** inactivation curve and qualitative activation curve for T-current during IFL 1% and 2% showing reasonable recovery. Note the presumed decrease in a T-window current with IFL. **B:** voltage-clamp recordings showing current response to voltage ramps before and during IFL (above) and current subtraction (below) in a different neuron. **C:** current-clamp recordings in the same neuron showing the reduction in LTS induced by nominally zero  $Ca^{2+}$  and the  $Ca^{2+}$ -blocker,  $Co^{2+}$  (1 mM). **D:** voltage-clamp recordings during zero  $Ca^{2+}$  in the same neuron showing approximately the same  $E_{IFL}$ . Note that presumed IFL blockade of an inward T-window current did not contribute to  $E_{IFL}$  for the increase in  $K^{+}$ -conductance.

### 3.6 Other inhalation anaesthetics

The IFL-induced increase in membrane conductance was compared with two other inhalational anaesthetics, halothane (2-bromo-2-chloro-1,1,1-trifluoroethane) and enflurane (2-chloro-1,1,2-trifluoroethyl difluoromethyl ether). Like IFL (1-chloro-2,2,2-trifluoroethyl difluoromethyl ether), these agents are halogenated hydrocarbons. Although enflurane and IFL are chemical isomers, there are important differences in their pharmacological properties. For example, enflurane concentrations that are >2 MAC can produce EEG seizure activity with tonic-clonic muscle twitching. In addition, differences exist between all three agents. For example, at equipotent concentrations, inhalational anaesthetics decrease the central control of breathing as follows: from greatest to least, enflurane > IFL > halothane. Cardiac contractility is decreased by halothane > enflurane > IFL, and systemic vascular resistance is decreased by IFL > enflurane > halothane. However, as these agents produce anaesthesia, the hypothesis was that they would produce thalamic inhibition at a concentration that was proportionate to *in vivo* anaesthetic concentrations.

Equipotent concentrations of halothane and enflurane were used in experiments in order to make comparisons with IFL 1% at room temperature. Halothane and enflurane MAC values in Sprague-Dawley rats are reported to be 1.03 and 2.21%, respectively, for adults (Mazze, Rice and Baden 1985), and 1.3 and 2.9%, respectively, when corrected for an age of 15 days (30% increase, Cook et al., 1981). Therefore, an anaesthetic potency ratio, based on the MAC values (at 37°C), of 1.3:1.9:2.9 for halothane, IFL and enflurane, compares well with experimental gas concentrations (at 22°C) of 0.5, 1 and 1.5%, respectively<sup>18</sup>.

Experiments with halothane and enflurane were performed during current-clamp recordings. From a depolarized holding potential of ~-60 mV during a manual voltage-clamp, both halothane 0.5% and enflurane 1.5% increased the required positive holding current, which implied an underlying hyperpolarization. In addition, these agents shunted tonic and burst firing. For

---

<sup>18</sup>To add to the difficulty in reconciling *in vitro* and *in vivo* results, these *in vitro* gas concentrations at room temperature may reflect *in vivo* anaesthesia, as aqueous solutions of halothane 0.54% and 1.1% are ED<sub>50</sub>'s for anaesthesia in goldfish at 20°C and 30°C, respectively (Cherkin and Catchpool 1964).

example, halothane and enflurane reversibly increased resting conductance by  $37 \pm 28\%$  (69, 26 and 16%,  $n = 3$ ) and  $30 \pm 5\%$  (4 of 4 neurons<sup>19</sup>) respectively. In addition, these agents induced a relative increase in current threshold for Na<sup>+</sup>-spike generation that was about twice the % increase in conductance. Although the small sample size limits a detailed comparative interpretation of the effects of the three anaesthetics, it at least suggests that a MAC value of either halothane or enflurane would significantly inhibit thalamic relay neurons *in vitro* at 37°C.

---

<sup>19</sup>Enflurane 1.5% reversibly hyperpolarized a fifth neuron during continuous intracellular injection of current to elicit tonic firing.

## 4 DISCUSSION

### 4.1 Summary of results

Whole-cell recordings were made from thalamic relay neurons that relay somatic sensation in a rodent thalamic slice preparation. Although intracellular staining was not performed, the LTS was evoked from every recorded neuron. The experiments were performed at either 22°C or 31°C.

At a concentration of IFL that was proportionate to *in vivo* anaesthetic concentrations, IFL decreased excitabilities of thalamic relay neurons by increasing resting conductance. This effect of IFL occurred in a reversible and concentration-dependent manner, as well as with equipotent concentrations of halothane and enflurane. The increased conductance produced by IFL had two consequences. By causing a hyperpolarization, the membrane potential moved away from the firing threshold and out of the mode for tonic Na<sup>+</sup>-spike firing which characterizes wakefulness. Secondly, the increased conductance shunted the effectiveness of injected depolarizing and hyperpolarizing currents, thereby suppressing the voltage-gated transitions to either the tonic or burst firing modes. This shunt mechanism was the more significant effect because the IFL-induced hyperpolarization did not convert tonic firing to burst firing. Indeed, the increased conductance decreased the firing of the LTS as well as its amplitude.

The burst suppression was largely secondary to the increase in resting conductance, which led to a functional disconnection of the dendrites from the soma. In the voltage-clamp studies, inadequate spatial distribution of imposed depolarizing and hyperpolarizing somatic step voltages shifted the voltage dependency for the underlying T-current. The increase in conductance produced by IFL was responsible for this voltage distortion, as it occurred in a concentration-dependent manner. In addition, the IFL-induced reduction in voltage transfer to different regions of the neuron was probably responsible for the elevation in the voltage threshold of the Na<sup>+</sup>-spike, the restriction in postspike repolarization and repetitive firing as well as the suppression of dendritic HTSs. The reduction in inward rectification during imposed

hyperpolarizations would likely reduce any tendency for oscillatory activity, which is dependent on an interaction of  $I_H$  and the T-current (McCormick and Pape 1990).

The increase in resting conductance was voltage-independent, sensitive to changes in external  $K^+$ , and suppressed by external  $Ba^{2+}$  and internal  $Cs^+$ .  $E_{IFL}$  for the IFL-evoked current was near the calculated  $E_K$ , but was consistently positive to  $E_K$ . This disparity suggested a minor role for another ion.  $E_K$  was verified by the action of baclofen and tacrine, as well as the inward rectification from  $I_{Kir}$ . Unfortunately, regular testing of  $E_K$  (e.g., with baclofen) was not carried out. Although a role for a second ion was not supported by external  $Na^+$ , external  $Ca^{2+}$  and both external and internal  $Cl^-$  substitutions, internal BAPTA decreased the disparity between  $E_K$  and  $E_{IFL}$ . Independent of the type of  $Ca^{2+}$  chelation, however,  $E_{IFL}$  correlated with the resting membrane potential. These results then are consistent with an increased  $K^+$  leak conductance, with or without an increased leak of other ions. The ATP-sensitive  $K^+$  channel that is suppressed by glibenclamide was not involved. Finally, IFL-evoked depolarizations in presumed glial cells suggested reversible increases in external  $[K^+]$  arising from thalamocortical neurons.

## 4.2 Comparison with other studies

### 4.2.1 $K^+$ -mediated anaesthetic-induced inhibition

A surprising finding was the  $K^+$ -efflux inhibitory activity instead of  $Cl^-$ -uptake in an area of the brain with significant  $GABA_A$ -related transmission (von Krosigk, Bal and McCormick 1993). Although a popular theory of anaesthesia involves enhanced  $GABA$ ergic activity by inhalational anaesthetics in non-thalamic brain regions, the lack of  $Cl^-$  involvement in IFL-actions in these experiments may relate to a higher concentration-dependence as well as conflicting reports of both IPSP or  $GABA$  potentiation (Mody *et al.* 1990; Sykes and Thomson 1989; Jones and Harrison 1992) and IPSP depression (Fujiwara *et al.* 1988; El-Beheiry and Puil 1989b). However, an IFL-evoked increase in  $GABA_A$ -mediated  $Cl^-$  and perhaps  $HCO_3^-$  conductance (Golan, Barkai and Grossman 1991) could explain the disparity between  $E_K$  and  $E_{IFL}$ . Indeed,  $Cl^-$  concentration gradients in thalamocortical neurons (El-Beheiry and Puil 1990; Staley, Soldo and Proctor 1995) may have been insensitive to the external and internal  $Cl^-$  substitutions tested here.

During the synchronized oscillations of sleep, thalamic reticular neurons inhibit thalamic relay neurons through fast GABA<sub>A</sub> and slow GABA<sub>B</sub> receptors (Crunelli and Leresche 1991; von Krosigk, Bal and McCormick 1993). Could inhalational anaesthetics be potentiating and/or activating thalamic GABA<sub>B</sub> receptors with or without GABA<sub>A</sub> receptor involvement? In thalamocortical (Sugiyama, Muteki, and Shimoji 1992) and hippocampal neurons (Pearce 1996), however, halothane blocks the postsynaptic GABA<sub>B</sub>-mediated K<sup>+</sup> conductance during exogenous GABA application. This observation needs to be duplicated along with experiments using IFL and GABA<sub>A</sub> and GABA<sub>B</sub> antagonists.

Consistent with the traditional viewpoint of nonspecific (i.e., non-receptor mediated) actions (Krnjević and Puil, in press), inhalational anaesthetics produce inhibition by increasing K<sup>+</sup> leakage in various mammalian neurons. For example, halothane hyperpolarizes 50% of intralaminar thalamic neurons by increasing a voltage-independent K<sup>+</sup> conductance (Sugiyama, Muteki, and Shimoji 1992). And, ether and halothane produce a hyperpolarization by increasing K<sup>+</sup> conductance in hippocampal neurons (Nicoll and Madison, 1982). Previous studies also revealed that IFL increases a voltage-independent K<sup>+</sup> conductance in hippocampal and neocortical neurons (Berg-Johnsen and Langmoen, 1987; Berg-Johnsen and Langmoen, 1990; El-Beheiry and Puil 1989a) and a nonspecified leak current in neocortical neurons (Puil, Hutcheon and Reiner 1994). Interestingly, the  $E_{IFL}$  obtained with an intracellular recording method (i.e., sharp electrodes) was reported to be 18 mV positive to a calculated  $E_K$  of -98 mV. When a comparison of the concentration-dependence (Sugiyama, Muteki and Shimoji 1992; Berg-Johnsen and Langmoen 1987; Berg-Johnsen and Langmoen 1990; Puil, Hutcheon and Reiner 1994) was made with the results described in this thesis, thalamocortical neurons may be more sensitive to inhalational anaesthetics. However, the studies using temperatures above the ambient temperature may have had significant evaporation of the volatile anaesthetic. In this regard, one investigation has reported that the measured concentration of anaesthetic was only 50% of the predicted concentration (Miu and Puil 1989), and another reported that the measured concentration declined along the length of the recording bath to approximately one-third at the site of the brain slice (Pearce 1996). Unfortunately, in studies at temperatures above the ambient temperature, the heating details and temperature measurements around the submerged slice are not mentioned.

In other hippocampal investigations, however, inhalational anaesthetics have either no effect on membrane potential (Fujiwara *et al.* 1988), mixed concentration-dependent effects on resting conductance (Krnjević and Puil, 1988), or mixed depolarizing and hyperpolarizing actions depending on the type of inhalational anaesthetic (MacIver and Kendig, 1991). For example, one study reported a hyperpolarization associated with a conductance increase by halothane, hyperpolarization associated with a conductance decrease by enflurane, and mixed effects due to IFL application (MacIver and Kendig, 1991). Although the ionic mechanism(s) of these changes was not reported, it would seem that hippocampal actions do not correlate with the *in vivo* anaesthetic state.

Do anaesthetics affect other voltage-independent  $K^+$  conductances, such as the  $Ca^{2+}$ -mediated and the ATP-sensitive  $K^+$  conductances (Krnjević 1974)? Like thalamocortical neurons, IFL and althesin block presumed  $Ca^{2+}$ -mediated slow AHPs and spike-train AHPs in neocortical neurons (El-Beheiry and Puil 1989a). A reduction in  $Ca^{2+}$ -mediated  $K^+$  conductance contrasts with a hippocampal and cerebellar report that ethanol, the benzodiazepines midazolam and clonazepam, and the barbiturate pentobarbital increase  $Ca^{2+}$ -mediated  $K^+$  conductances (Carlen *et al.* 1985). It is possible that a subtle enhancement of  $Ca^{2+}$ -mediated  $K^+$  conductance was outweighed in the present experiments by the IFL-induced shunt. Although glibenclamide inhibits IFL-induced coronary artery vasodilation (Cason, Shubayev and Hickey 1994) and myocardial protection (Kersten *et al.* 1996), ATP-sensitive  $K^+$ -channel agonists, like glibenclamide, do not change the MAC for IFL in rats (Zucker 1992). However, not all ATP-sensitive  $K^+$  channels are blocked by glibenclamide (Godfraind and Krnjević 1993). Future studies should be directed towards a possible anaesthetic action on ligand-gated voltage-independent  $K^+$  channels, especially the muscarine-sensitive  $K^+$ -leak conductance (El-Beheiry and Puil 1989c; cf. serotonin-sensitive  $K^+$  channel, Winegar *et al.* 1996, Winegar and Yost 1997).

Although very little is known to date about the structure of the non-ligand gated  $K^+$ -leak channel, the thalamic IFL-induced  $K^+$  efflux is consistent with the current molecular mechanism for inhalational anaesthetics. Originally, the Meyer-Overton rule (Meyer 1899; Overton 1901) was thought to imply that inhalational anaesthetics perturb the lipid structure of neuronal membranes. However, a popular theory says that inhalational anaesthetics act by binding directly to sensitive hydrophobic protein sites of ionic channels, perhaps from within the lipid membrane (Little

1996). Interestingly, the optical isomers for IFL disrupt lipid bilayers equally, yet increase a voltage-independent  $K^+$  conductance in molluscan central nervous neurons in a stereospecific manner (Franks and Lieb 1991). Similar experiments on thalamocortical neurons should be done with IFL's two stereoisomers.

#### 4.2.2 Anaesthetic reduction of $Ca^{2+}$ -current

Although the present thalamic investigations show that the  $K^+$ -mediated shunt was largely responsible for the IFL-induced reduction in T-current, numerous studies report that inhalational anaesthetics decrease  $Ca^{2+}$ -currents. For example, T-currents are suppressed by inhalational anaesthetics in dorsal root neurons (also high-voltage-activated  $Ca^{2+}$ -current or HVA-current, halothane and IFL, Takenoshita and Steinbach, 1991), in hippocampal neurons (IFL, Study 1994), as well as in cloned pituitary (also HVA-current, halothane, Herrington et al 1991) and cultured thyroid cells (IFL and enflurane, McDowell, Pancrazio and Lynch III 1996). In addition, other  $Ca^{2+}$ -currents are inhibited by volatile anaesthetics in hippocampal neurons (unspecified current, halothane and IFL, Krnjević and Puil 1988) and neocortical neurons (HVA-current, IFL, Puil, Hutcheon and Reiner 1994). In some of these investigations, however, either internal  $Cs^+$  was used for the recordings (Takenoshita and Steinbach 1991) or an increase in leak current was documented (Puil, Hutcheon and Reiner 1994; Study 1994). Therefore, since some HVA-currents, like T-current, are located in the dendrites (Kim and Connors, 1993; Hoehn, Watson and MacVicar 1993; Magee and Johnston 1995), some of the reported decrease in  $Ca^{2+}$ -current may be in fact due to a  $K^+$ -mediated conductance increase.

Although direct depression of HVA-currents by inhalational anaesthetics would presumably reduce memory-related long-term potentiation (MacIver, Tauck and Kendig 1989), the role of anaesthetic depression of  $Ca^{2+}$ -currents and  $Ca^{2+}$ -mediated transmitter release is being questioned in the literature. For example in the heart, equivalent MAC values of halothane, enflurane and IFL depress  $Ca^{2+}$ -currents equally, yet these anaesthetics have very different potencies as negative inotropes (Bosnjak, Supan and Rusch 1991). Similarly in the brain, P-type  $Ca^{2+}$ -channels are reported to be insensitive to inhalational anaesthetics, even though they may be critically involved in presynaptic transmitter release (Hall, Lieb and Franks 1994). If IFL's non-stereoselective L-type  $Ca^{2+}$ -channel depression (brain and heart, Moody et al. 1994; heart, Graf et

al. 1994) is shown also to occur with N-type  $\text{Ca}^{2+}$ -channels, then the mediation of anaesthesia by  $\text{Ca}^{2+}$  channels will be further brought into question as anaesthesia seems to be stereoselective (Harris, Moody and Skolnick 1992).

### 4.3 Functional significance

#### 4.3.1 Reconciling *in vitro* experimentation and *in vivo* MAC values

Many anaesthesiologists would argue that the physiological parameters measured in *in vitro* experiments must respond to the *in vivo* proportionate concentration range in order for the results to be considered relevant. However, to what extent must these concentrations overlap? In other words, does the inhibition of a given physiological parameter indicate an important mechanistic action only if the concentration-response curve is identical to the *in vivo* curve for MAC (Franks and Lieb 1994)? Although the former relationship is "graded" and the latter curve is "quantal" in nature, only a small perturbation may be required for a complex neuronal network (i.e., the brain) to stop functioning. Of course, consciousness and anaesthesia cannot be reflected by firing patterns in thalamocortical neurons. Yet nonlinear responses to IFL were seen in these experiments. For example, the relative increase in  $\text{K}^+$  conductance induced by IFL was always less than the relative increase in DC required to evoke tonic and especially burst firing, presumably because of reductions in the spatial and temporal distribution of imposed voltages. Considering then that spatial and temporal integration of neuronal activity in the thalamus is integral to both the transmission of pain impulses and the synchronous cortico-thalamo-cortical activity required to process and interpret pain, a 15 to 30% increase in resting conductance of individual thalamocortical neurons within an oscillating network may very well perturb the system sufficiently to create the anaesthetic state (Steriade, Curró Dossi and Contreras 1993).

#### 4.3.2 Anaesthetic-induced thalamic shunt

Could an increase in  $\text{K}^+$ -conductance explain the attenuation of 40 Hz brain activity with *in vivo* anaesthesia (Plourde and Villemure 1996) as well as its recovery during emergence from anaesthesia (Plourde *et al.* 1996)? Functionally, an anaesthetic-induced increase in voltage-independent conductance would inhibit the synaptic relay of voltage transfers through the

thalamus by reducing neuronal integration in the dendrites and  $\text{Na}^+$ -spike excitabilities in the axon, and by affecting transmitter release at thalamocortical-corticothalamic synapses. Concerning neuronal integration of incoming dendritic signals, an increase in conductance would both shunt the voltage response to current inputs and reduce the time-dependent voltage responses during electrotonic conduction. As a result, synaptic summation in both the spatial and temporal domain would be undermined, and many passive dendritic signals with or without the boosting assistance of HTSs and LTSs (Huguenard 1996) would decay before propagating to the soma and the axon hillock. Then, if large synaptic potentials actually arrive in the soma, the anaesthetic-induced increase in conductance and hyperpolarization of the soma would impair thalamic relay of sensory information by increasing the relative threshold for axonal  $\text{Na}^+$ -excitation. And finally at a third level of thalamic relay, anaesthetic-induced hyperpolarization of presynaptic terminals would suppress activation of HVA  $\text{Ca}^{2+}$ -currents and therefore decrease excitatory transmitter release in the neocortex.

As a result, anaesthetic action in the thalamus would suppress the excitabilities of neurons during both wakefulness and sleep. For example, inhalational anaesthetics would inhibit the relay of sensory impulses leading to analgesia and loss of awareness of the external environment. Neither the internal wakefulness characteristic of REM sleep nor nonREM sleep would result. Internal awareness, like consciousness, would be disrupted as the binding effect of 40-Hz oscillations would be shunted at a thalamic level (cf. Plourde 1993). In addition, an anaesthetic shunt of burst firing would decrease resonance (Tennigkeit *et al.* in press), inhibiting tendencies for the slow oscillations of sleep, and thereby producing the characteristic EEG pattern of anaesthetic associated burst-suppression (Steriade, Amzica and Contreras 1994; Akrawi *et al.* 1996). This would occur despite an anaesthetic-induced hyperpolarization. Finally, the anaesthetic induced increase in conductance would prevent both burst-related wakeup calls (Sherman 1996) to profound sensory stimulation, as well as the unknown unconscious process in which humans effect awakening from sleep.

## NOMENCLATURE

A	$K^+$ current that activates transiently in the subthreshold range; fast and slow types
BAPTA	1,2-bis(2-aminophenoxy)ethane N,N,N',N'-tetraacetic acid ( $Ca^{2+}$ chelator)
CNS	central nervous system
DAP	depolarizing afterpotential
E	equilibrium potential; e.g., $E_K$ for $K^+$ ; e.g., $E_{IFL}$ , reversal potential for IFL-actions
EEG	electroencephalogram
EGTA	ethylene glycol-bis( $\beta$ -aminoethylether) N,N,N',N'-tetraacetic acid ( $Ca^{2+}$ chelator)
EPSP	excitatory postsynaptic potential
GABA	$\gamma$ -aminobutyric acid, an inhibitory neurotransmitter
HTS	high-threshold spike
HVA	high-voltage activated
$I_H$	hyperpolarization-activated cation current
$I_{K(Ca)}$	$Ca^{2+}$ -dependent $K^+$ current
$I_{Kir}$	fast $K^+$ -mediated inward rectifier
IFL	isoflurane, an inhalational anaesthetic
IPSP	inhibitory postsynaptic potential
LTS	low-threshold $Ca^{2+}$ -spike
MAC	minimum alveolar concentration of an inhalational anaesthetic that in 50% of subjects prevents movement with a noxious stimuli, i.e., surgical incision
MLAEP	mid-latency auditory evoked potential
REM	rapid-eye-movement
RMP	resting membrane potential
T-current	"transient" T-type, low-threshold $Ca^{2+}$ -current
TEA	tetraethylammonium
TFF	tonic firing frequency
TTX	tetrodotoxin
4-AP	4-aminopyridine
40-Hz ASSR	40-Hz auditory steady state response

## BIBLIOGRAPHY

- Akil H, Mayer DJ, Liebeskind JC. Antagonism of stimulation-produced analgesia by naloxone, a narcotic antagonist. *Science* 1976; 191: 961-2
- Akrawi WP, Drummond JC, Kalkman CJ, Patel PM. A comparison of the electrophysiologic characteristics of EEG burst-suppression as produced by isoflurane, thiopental, etomidate, and propofol. *J Neurosurg Anesthesiol* 1996; 8: 40-6
- Allada R, Nash HA. *Drosophila melanogaster* as a model for study of general anesthesia: the quantitative response to clinical anesthetics and alkanes. *Anesth Analg* 1993; 77: 19-26
- Andrade J. Consciousness: current views. *International anesthesiology clinics* 1993; 31: 13-26
- Angel A. Adventures in anaesthesia. *Exp Physiol* 1991; 76: 1-38
- Anonymous. You won't feel a thing. *New Scientist* July 22, 1995; 29-31
- Antognini JF. Hypothermia eliminates isoflurane requirements at 20° C. *Anesthesiology* 1993; 78: 1152-6
- Antognini, JF, Kien ND. Cardiopulmonary bypass does not alter canine enflurane requirements. *Anesthesiology* 1992; 76: 953-7
- Antognini JF, Schwartz K. Exaggerated anesthetic requirements in the preferentially anesthetized brain. *Anesthesiology* 1993; 79: 1244-9
- Avramov MN, Murayama T, Shingu K, Mori K. Electroencephalographic changes during vital capacity breath induction with halothane. *Br J Anaesth* 1991; 66: 212-5
- Bassetti C, Mathis J, Gugger M, Lovblad KO, Hess CW. Hypersomnia following paramedian thalamic stroke: a report of 12 patients. *Ann Neurol* 1996; 39: 471-80
- Berg-Johnsen J, Langmoen IA. Isoflurane hyperpolarizes neurones in rat and human cerebral cortex. *Acta Physiol Scand* 1987; 130: 679-85
- Berg-Johnsen J, Langmoen IA. Mechanisms concerned in the direct effect of isoflurane on rat hippocampal and human neocortical neurons. *Brain Res* 1990; 507: 28-34
- Bevan JC, Veall GRQ, Macnab AJ, Ries CR, Marsland C. Midazolam premedication delays recovery after propofol in children without modifying involuntary movements. *Anesth Analg* 1997 (in press)
- Bogod DG, Orton JK, Yau HM, Oh TE. Detecting awareness during general anaesthetic

caesarean section. An evaluation of two methods. *Anaesthesia* 1990; 45: 279-84

Borges M, Antognini JF. Does the brain influence somatic responses to noxious stimuli during isoflurane anesthesia? *Anesthesiology* 1994; 81: 1511-5

Bosnjak ZJ, Supan FD, Rusch NJ. The effects of halothane, enflurane, and isoflurane on calcium current in isolated canine ventricular cells. *Anesthesiology* 1991; 74: 340-5

Bossu JL, Dupont JL, Feltz A. Calcium currents in rat cerebellar Purkinje cells maintained in culture. *Neuroscience* 1989; 30:605-17

Brown AM, Schwindt PC, Crill WE. Voltage dependence and activation kinetics of pharmacologically defined components of the high-threshold calcium current in rat neocortical neurons. *J Neurophysiol* 1993; 70: 1530-43

Carlen PL, Gurevich N, Davies MF, Blaxter TJ, O'Beirne M. Enhanced neuronal  $K^+$  conductance: a possible common mechanism for sedative-hypnotic drug action. *Can J Physiol Pharmacol* 1985; 63: 831-7

Cason BA, Shubayev I, Hickey RF. Blockade of adenosine triphosphate-sensitive potassium channels eliminates isoflurane-induced coronary artery vasodilation. *Anesthesiology* 1994; 81: 1245-55

Chalmers DJ. The puzzle of conscious experience. *Sci Am* 1995; 273: 80-6

Cherkin A, Catchpool JF. Temperature dependence of anesthesia in goldfish. *Science* 1964; 144: 1460-2

Christie BR, Eliot LS, Ito K-I, Miyakawa H, Johnston D. Different  $Ca^{2+}$  channels in soma and dendrites of hippocampal pyramidal neurons mediate spike-induced  $Ca^{2+}$  influx. *J Neurophysiol* 1995; 73: 2553-7

Clarke KA, Djourhi L. TRH analogue antagonizes anaesthetic induced depression of information transfer through the ventrobasal thalamus of the rat. *Neuropeptides* 1991; 18: 193-200

Collins JG, Kendig JJ, Mason P. Anesthetic actions within the spinal cord: contributions to the state of general anesthesia. *Trends Neurosci* 1995; 18: 549-53.

Contreras D, Steriade M. Spindle oscillation in cats: the role of corticothalamic feedback in a thalamically generated rhythm. *J Physiol (Lond)* 1996; 490: 159-79

Cook DR, Bandom BW, Shiu G, Wolfson B. The inspired median effective dose, brain concentration at anesthesia, and cardiovascular index for halothane in young rats. *Anesth Analg* 1981; 60: 182-5

Cormack RS. Conscious levels during anaesthesia. *Br J Anaesth* 1993; 71: 469-71

- Crick F. Function of the thalamic reticular complex: the searchlight hypothesis. *Proc Natl Acad Sci U S A* 1984; 81: 4586-90
- Crick F. *The astonishing hypothesis: the scientific search for the soul*. New York: Scribner: Maxwell Macmillan International 1993; 171-173 and 229-230
- Croning MDR, Zetterström TSC, Grahame-Smith DG, Newberry NR. Action of adenosine receptor antagonists on hypoxia-induced effects in the rat hippocampus *in vitro*. *Br J Pharmacol* 1995; 116: 2113-9
- Crunelli V, Haby M, Fassik-Gerschenfeld D, Leresche N, Pirchio M.  $Cl^-$  and  $K^+$ -dependent inhibitory postsynaptic potentials evoked by interneurons of the rat lateral geniculate nucleus. *J Physiol (Lond)* 1988; 399: 153-76
- Crunelli V, Leresche N. A role for  $GABA_B$  receptors in excitation and inhibition of thalamocortical cells. *Trends Neurosci* 1991; 14: 16-21
- Crunelli V, Lightowler S, Pollard CE. A T-type  $Ca^{2+}$  current underlies low-threshold  $Ca^{2+}$  potentials in cells of the cat and rat lateral geniculate nucleus. *J Physiol* 1989; 413: 543-61
- Deady JE, Koblin DD, Eger EI 2d, Heavner JE, D'Aoust B. Anesthetic potencies and the unitary theory of narcosis. *Anesth Analg* 1981; 60: 380-4
- Destexhe A, Contreras D, Steriade M, Sejnowski TJ, Huguenard JR. *In vivo*, *in vitro*, and computational analysis of dendritic calcium currents in thalamic reticular neurons. *J Neurosci* 1996; 16: 169-85
- Drummond JC. Use of neuromuscular blocking drugs in scientific investigations involving animal species: the benefit of the doubt goes to the animal. *Anesthesiology* 1996; 85: 697-9
- Dutton RC, Smith WD, Smith NT. Does the EEG predict anesthetic depth better than cardiovascular variables? *Anesthesiology* 1990; 73: A532
- Dwyer R, Bennett HL, Eger EI 2d, Heilbron D. Effects of isoflurane and nitrous oxide in subanesthetic concentrations on memory and responsiveness in volunteers. *Anesthesiology* 1992; 77: 888-98
- Dwyer RC, Rampil IJ, Eger EI 2d, Bennett HL. The electroencephalogram does not predict depth of isoflurane anesthesia. *Anesthesiology* 1994; 81: 403-9
- Eckhorn R, Bauer R, Jordan W, Brosch M, Kruse W, Munk M, Reitböck HJ. Coherent oscillations: a mechanism of feature linking in the visual cortex. *Biol Cybern* 1988; 60: 121-30
- Eger EI 2d. Concentration *versus* partial pressure: which is important? *Anesthesiology* 1986; 65: 122-3
- Eger EI 2d, Saidman LJ, Brandstater B. Minimum alveolar anesthetic concentration: a standard of anesthetic potency. *Anesthesiology* 1965; 26: 756-63

- El-Beheiry H, Puil E. Postsynaptic depression induced by isoflurane and althesin in neocortical neurons. *Exp Brain Res* 1989a; 75: 361-68
- El-Beheiry H, Puil E. Anaesthetic depression of excitatory synaptic transmission in neocortex. *Exp Brain Res* 1989b; 77: 87-93
- El-Beheiry H, Puil E. Anaesthetic depression of transmitter actions in neocortex. *Br J Pharmacol* 1989c; 101: 61-6
- El-Beheiry H, Puil E. Unusual features of GABA responses in layers IV-V neurons of neocortex. *Neurosci Lett* 1990; 119: 83-5
- Erdemli G, Krnjević K. Guanosine diphosphate is required for activation of a glyburide, ATP and cromakalim-sensitive outward current in rat hippocampal neurones. *Neuroreport* 1994; 5: 1362-4
- Firestone LL, Miller JC and Miller KW. Appendix: Tables of physical and pharmacological properties of anesthetics. In: Roth SH, Miller KW (Eds) *Molecular and cellular mechanisms of anesthetics*. New York: Plenum Medical Book Company 1986; 455-70
- Fox NJ. *The social meaning of surgery*. Philadelphia: Open University Press 1992; 46-76
- Franks NP, Lieb WR. Stereospecific effects of inhalational general anesthetic optical isomers on nerve ion channels. *Science* 1991; 254: 427-30
- Franks NP, Lieb WR. Molecular and cellular mechanisms of general anesthesia. *Nature* 1994; 367: 607-14
- Franks NP, Lieb WR. Temperature dependence of the potency of volatile general anesthetics: implications for *in vitro* experiments. *Anesthesiology* 1996; 84: 716-20
- Frith CD. Consciousness, information processing and the brain. *Journal of Psychopharmacology* 1992; 6: 436-40
- Fujiwara N, Higashi H, Nishi S, Shimoji K, Sugita S, Yoshimura M. Changes in spontaneous firing patterns of rat hippocampal neurons induced by volatile anaesthetics. *J Physiol* 1988; 402: 155-75
- Fujiwara N, Higashi H, Shimoji K, Yoshimura M. Effects of hypoxia on the rat hippocampal neurones *in vitro*. *J Physiol (Lond)* 1987; 384: 131-51
- Ghoneim MM, Block RI. Learning and consciousness during general anesthesia. *Anesthesiology* 1992; 76: 279-305
- Godfraind JM, Krnjević K. Tolbutamide suppresses anoxic outward current of hippocampal neurons. *Neurosci Lett* 1993; 162: 101-4
- Golan H, Barkai E, Grossman Y. High CO<sub>2</sub>-bicarbonate buffer modifies GABAergic inhibitory

effect at the crayfish neuromuscular synapse. *Brain Res* 1991; 567: 149-52

Graf BM, Boban M, Stowe DF, Kampine JP, Bosnjak ZJ. Lack of stereospecific effects of isoflurane and desflurane isomers in isolated guinea pig hearts. *Anesthesiology* 1994; 81: 129-36

Gray CM, Singer W. Stimulus-specific neuronal oscillations in orientation columns of cat visual cortex. *Proc Natl Acad Sci U S A* 1989; 86: 1698-702

Groenewegen HJ, Berendse HW. The specificity of the 'nonspecific' midline and intralaminar thalamic nuclei. *Trends Neurosci* 1994; 17: 52-7

Guilleminault C, Quera-Salva MA, Goldberg MP. Pseudo-hypersomnia and pre-sleep behaviour with bilateral paramedian thalamic lesions. *Brain* 1993; 116: 1549-63

Hagiwara N, Irisawa H. Modulation by intracellular  $Ca^{2+}$  of the hyperpolarization activated inward current in rabbit single sino-atrial node cells. *J Physiol (Lond)* 1989; 409: 121-41

Hall AC, Lieb WR, Franks NP. Insensitivity of P-type calcium channels to inhalational and intravenous general anesthetics. *Anesthesiology* 1994; 81: 117-23

Halsey MJ. Physicochemical properties of inhalational anaesthetics. In: Gray TC, Nunn JF, Utting JE (Eds). *General anaesthetics*; 4th ed. London: Butterworths & Co Ltd 1980; 45-65

Harada J, Aoyagi M, Suzuki T, Kiren T, Koike Y. A study on the phase spectral analysis of middle latency response and 40-Hz event-related potential in central nervous system disorders. *Acta Otolaryngol Suppl (Stockh)* 1994; 511: 34-9

Harris B, Moody EJ, Skolnick P. Isoflurane anesthesia is stereoselective. *Eur J Pharmacol* 1992; 217: 215-6

Haydon DA, Urban BW. The effects of some inhalation anesthetics on the sodium current of the squid giant axon. *J Physiol* 1983; 341: 429-39

Heneghan C. Clinical and medicolegal aspects of conscious awareness during anesthesia. *International anesthesiology clinics* 1993; 31: 1-12

Hernández-Cruz A, Pape H-C. Identification of two calcium currents in acutely dissociated neurons from the rat lateral geniculate nucleus. *J Neurophysiol* 1989; 61: 1270-83

Herrington J, Stern RC, Evers AS, Lingle CJ. Halothane inhibits two components of calcium current in clonal (GH<sub>3</sub>) pituitary cells. *J Neurosci* 1991; 11: 2226-40

Heyer CB, Lux HD. Control of the delayed outward potassium currents in bursting pace-maker neurones of the snail, *Helix pomatia*. *J Physiol (Lond)* 1976; 262: 349-82

Higashi H, Tanaka E, Inokuchi H, Nishi S. Ionic mechanisms underlying the depolarizing and hyperpolarizing afterpotentials of single spike in guinea-pig cingulate cortical neurons. *Neuroscience* 1993; 55: 129-38

- Hille B. Ionic channels of excitable membranes; 2nd ed. Sunderland: Sinauer Associates Inc. 1992; 315-36
- Hoehn K, Watson TWJ, MacVicar BA. Multiple types of calcium channels in acutely isolated rat neostriatal neurons. *J Neurosci* 1993; 13: 1244-57
- Horgan J. Can science explain consciousness? *Sci Am* 1994; 271; 88-94
- Huguenard JR. Low-threshold calcium currents in central nervous system neurons. *Annu Rev Physiol* 1996; 58: 329-48
- Huguenard JR, Coulter DA, Prince DA. A fast transient potassium current in thalamic relay neurons: kinetics of activation and inactivation. *J Neurophysiol* 1991; 66: 1304-15
- Huguenard JR, McCormick DA. Simulation of the currents involved in rhythmic oscillations in thalamic relay neurons. *J Neurophysiol* 1992; 68: 1373-83
- Huguenard JR, Prince DA. Slow inactivation of a TEA-sensitive K current in acutely isolated rat thalamic relay neurons. *J Neurophysiol* 1991; 66: 1316-28
- Hung OR, Varvel JR, Shafer SL, Stanski DR. Thiopental pharmacodynamics. II. Quantitation of clinical and electroencephalographic depth of anesthesia. *Anesthesiology* 1992; 77: 237-44
- Hutcheon B, Miura RM, Yarom Y, Puil E. Low-threshold calcium current and resonance in thalamic neurons: a model of frequency preference. *J Neurophysiol* 1994; 71: 583-94
- Jessop J, Jones JG. Conscious awareness during general anaesthesia -- what are we attempting to monitor? *Br J Anaesth* 1991; 66: 635-7
- Jiang C, Haddad GG. Effect of anoxia on intracellular and extracellular potassium activity in hypoglossal neurons *in vitro*. *J Neurophysiol* 1991; 66: 103-11
- Jones EG. The thalamus. New York: Plenum Press 1985; 325-75
- Jones MV, Brooks PA, Harrison NL. Enhancement of gamma-aminobutyric acid-activated Cl<sup>-</sup> currents in cultured rat hippocampal neurones by three volatile anaesthetics. *J Physiol (Lond)* 1992; 449: 279-93
- Karst H, Joëls M, Wadman WJ. Low-threshold calcium current in dendrites of the adult rat hippocampus. *Neuroscience Lett* 1993; 164: 154-8
- Keifer JC, Baghdoyan HA, Becker L, Lydic R. Halothane decreases pontine acetylcholine release and increases EEG spindles. *Neuroreport* 1991; 5: 577-80
- Kersten JR, Schmeling TJ, Hettrick DA, Pagel PS, Gross GJ, Warltier DC. Mechanism of myocardial protection by isoflurane: role of adenosine triphosphate-regulated potassium (K<sub>ATP</sub>) channels. *Anesthesiology* 1996; 85: 794-807

- Kihlstrom JF, Couture LJ. Awareness and information processing in general anesthesia. *Journal of Psychopharmacology* 1992; 6: 410-7
- Kim HG, Connors BW. Apical dendrites of the neocortex: correlation between sodium- and calcium-dependent spiking and pyramidal cell morphology. *J Neurosci* 1993; 13: 5301-11
- King EE, Naquet R, Magoun HW Alterations in somatic afferent transmission through the thalamus by central mechanisms and barbiturates. *J Pharmac Exp Ther* 1957; 119: 48-63
- Kinney HC, Korein J, Panigrahy A, Dikkes P, and Goode R. Neuropathological findings in the brain of Karen Ann Quinlan: the role of the thalamus in the persistent vegetative state. *N Engl J Med* 1994; 330: 1469-75
- Kissin I. General anesthetic action: an obsolete notion? *Anesth Analg* 1993; 76: 215-8.
- Kissin I, Morgan PL, Smith LR. Anesthetic potencies of isoflurane, halothane, and diethyl ether for various end points of anesthesia. *Anesthesiology* 1983; 58: 88-92
- Koch C. Computational approaches to cognition: the bottom-up view. *Curr Opin Neurobiol* 1993; 3: 203-8
- Koester J. Passive membrane properties of the neuron. In: Kandel ER, Schwartz JH, Jessell TM (Eds). *Principles of Neural Science*; 3rd ed. New York: Elsevier Science Publishing Co, Inc 1991; 81-94
- Komatsu Y, Iwakiri M. Low-threshold Ca<sup>2+</sup> channels mediate induction of long-term potentiation in kitten visual cortex. *J Neurophysiol* 1992; 67: 401-10
- Kress HG, Muller J, Eisert A, Gilge U, Tas PW, Koschel K. Effects of volatile anesthetics on cytoplasmic Ca<sup>2+</sup> signaling and transmitter release in a neural cell line. *Anesthesiology* 1991; 74: 309-19
- Krnjević K. Central actions of general anaesthetics. In: *Molecular Mechanisms in General Anaesthesia*. Halsey MJ, Millar R, Sutton JA (Eds). New York: Churchill Livingstone 1974; 65-89
- Krnjević K, Leblond J. Changes in membrane currents of hippocampal neurons evoked by brief anoxia. *J Neurophysiol* 1989; 62: 15-30
- Krnjević K, Puil E. Halothane suppresses slow inward currents in hippocampal slices. *Can J Physiol Pharmacol* 1988; 66: 1570-5
- Krnjević K, Puil E. Cellular mechanisms of general anesthesia. In: *Principles of medical biology, Molecular and cellular pharmacology (8A)*. Bittar EE (Ed.) Greenwich: JAI Press Inc (in press)
- Kulli J, Koch C. Does anesthesia cause loss of consciousness? *Trends Neurosci* 1991; 14: 6-10

- Leblond J, Krnjević K. Hypoxic changes in hippocampal neurons. *J Neurophysiol* 1989; 62: 1-14
- Lever MJ, Miller KW, Paton WD, Smith EB. Pressure reversal of anaesthesia. *Nature* 1971; 231: 368-71
- Little HJ. How has molecular pharmacology contributed to our understanding of the mechanism(s) of general anesthesia? *Pharmacol Ther* 1996; 69: 37-58
- Llinás R, Jahnsen H. Electrophysiology of mammalian thalamic neurones in vitro. *Nature* 1982; 297: 406-8
- Llinás RR, Paré D. Of dreaming and wakefulness. *Neuroscience* 1991; 44: 521-35
- Llinás R, Ribary U. Coherent 40-Hz oscillation characterizes dream state in humans. *Proc Natl Acad Sci U S A* 1993; 90: 2078-81
- Lydic R, Biebuyck JF. Sleep neurobiology: relevance for mechanistic studies of anaesthesia. *Br J Anaesth* 1994; 72: 506-8
- MacIver MB, Kendig JJ. Anesthetic effects on resting membrane potential are voltage-dependent and agent-specific. *Anesthesiology* 1991; 74: 83-8
- MacIver MB, Tauck DL, Kendig JJ. General anaesthetic modification of synaptic facilitation and long-term potentiation in hippocampus. *Br J Anaesth* 1989; 62: 301-10
- Magee JC, Johnston D. Characterization of single voltage-gated Na<sup>+</sup> and Ca<sup>2+</sup> channels in apical dendrites of rat CA1 pyramidal neurons. *J Physiol (Lond)* 1995; 487: 67-90
- Marrocco RT, Witte EA, Davidson MC. Arousal systems. *Curr Opin Neurobiol* 1994; 4: 166-70
- Marshall KC, Murray JS. Cholinergic facilitation of thalamic relay transmission in the cat. 1980 *Exp Neurol* 69: 318-33
- Mazze RI, Rice SA, Baden JM. Halothane, Isoflurane, and enflurane MAC in pregnant and nonpregnant female and male mice and rats. *Anesthesiology* 1985; 62: 339-41
- McCormick DA. Functional properties of a slowly inactivating potassium current  $I_{AS}$  in guinea pig dorsal lateral geniculate relay neurons. *J Neurophysiol* 1991; 66: 1176-89
- McCormick DA. Neurotransmitter actions in the thalamus and cerebral cortex and their role in neuromodulation of thalamocortical activity. *Prog Neurobiol* 1992; 39: 337-88
- McCormick DA, Bal T. Sensory gating mechanisms of the thalamus. *Curr Opin Neurobiol* 1994; 4: 550-6
- McCormick DA, and Pape H-C. Properties of a hyperpolarization-activated cation current and its role in rhythmic oscillation in thalamic relay neurons. *J Physiol (Lond)* 1990; 431: 291-318

- McCormick DA, von Krosigk M. Corticothalamic activation modulates thalamic firing through glutamate "metabotropic" receptors. *Proc Natl Acad Sci U S A* 1992; 89: 2774-8
- McDowell TS, Pancrazio JJ, Lynch 3rd C. Volatile anesthetics reduce low-voltage-activated calcium currents in a thyroid c-cell line. *Anesthesiology* 1996; 85: 1167-75
- Meyer HH. Welche Eigenschafte der Anästhetica bedingt ihre narkotische Wirkung? *Naunyn Schmeidebergs Arch exp Pathol Pharmacol* 1899; 42: 109-18
- Miller AH. The origin of the word 'anaesthesia.' *Boston Medical and Surgical Journal* 1927; 197: 1218-22
- Miu P, Puil E. Isoflurane-induced impairment of synaptic transmission in hippocampal neurons. *Exp Brain Res* 1989; 75: 354-60
- Mody I, Tanelian DL, MacIver MB. Halothane enhances tonic neuronal inhibition by elevating intracellular calcium. *Brain Res* 1991; 538: 319-23
- Moody EJ, Harris B, Hoehner P, Skolnick P. Inhibition of [<sup>3</sup>H]isradipine binding to L-type calcium channels by the optical isomers of isoflurane: lack of stereospecificity. *Anesthesiology* 1994; 81: 124-8
- Müller W, Lux HD. Analysis of voltage-dependent membrane currents in spatially extended neurons from point-clamp data. *J Neurophysiol* 1993; 69: 241-7
- Munglani R, Jones JG. Sleep and general anaesthesia as altered states of consciousness. *Journal of Psychopharmacology* 1992; 6: 399-409
- Nicoll RA, Madison DV. General anesthetics hyperpolarize neurons in the vertebrate central nervous system. *Science* 1982; 217: 1055-7
- Nisenbaum ES, Wilson CJ. Potassium currents responsible for inward and outward rectification in rat neostriatal spiny projection neurons. *J Neurosci* 1995; 15: 4449-63
- Ohara PT, Lieberman AR. Some aspects of the synaptic circuitry underlying inhibition in the ventrobasal thalamus. *J Neurocytol* 1993; 22: 815-25
- Overton E. Studien über die Narkose, zugleich ein Beitrag zur allgemeiner Pharmakologie. Gustav Fischer, Jena 1901
- Palkovits M, Brownstein MJ. Maps and guide to microdissection of the rat brain. New York: Elsevier Science Publishing Co., Inc. 1988
- Pape HC, McCormick DA. Electrophysiological and pharmacological properties of interneurons in the cat dorsal lateral geniculate nucleus. *Neuroscience* 1995; 68: 1105-25
- Pappas CA, Ransom BR. Depolarization-induced alkalinization (DIA) in rat hippocampal astrocytes. *J Neurophysiol* 1994; 72: 2816-26

- Pearce RA. Volatile anaesthetic enhancement of paired-pulse depression investigated in the rat hippocampus *in vitro*. *J Physiol (Lond)* 1996; 492: 823-40
- Picton TW, Stuss DT. Neurobiology of conscious experience. *Curr Opin Neurobiol* 1994; 4: 256-65
- Plourde G. Clinical use of the 40-Hz auditory steady state response. *International Anesthesiology Clinics* 1993; 31: 107-120
- Plourde G, Villemure C. Comparison of the effect of enflurane/N<sub>2</sub>O on the 40-Hz auditory steady-state response *versus* the auditory middle-latency response. *Anesth Analg* 1996; 82: 75-83
- Plourde G, Villemure C, Fiset P, Achim A, Backman S. Effects of the general anesthetic isoflurane on gamma rhythms and consciousness in humans. *Abstracts of the Society for Neuroscience* 1996; 22: 272.4
- Politi DM, Rogawski MA. Glyburide-sensitive K<sup>+</sup> channels in cultured rat hippocampal neurons: activation by cromakalim and energy-depleting conditions. *Mol Pharmacol* 1991; 40: 308-15
- Posner MI, Dehaene S. Attentional networks. *Trends Neurosci* 1994; 17: 75-9
- Prevett MC, Duncan JS, Jones T, Fish DR, Brooks DJ. Demonstration of thalamic activation during typical absence seizures using H<sub>2</sub><sup>(15)</sup>O and PET. *Neurology* 1995; 45: 1396-402
- Puil E, Hutcheon B, Reiner PB. Isoflurane inhibits calcium currents in neocortical neurons. *Neurosci Lett* 1994; 176: 63-6
- Puil E, Ries CR, Schwarz DWF, Tennigkeit T, Yarom Y. Sleep-inducing and anaesthetic actions of drugs on neurons of auditory thalamus. *International Symposium: Acoustical Signal Processing in the Central Nervous System*. Prague, Czech Republic, September 1996
- Ramoas AS, McCormick DA. Developmental changes in electrophysiological properties of LGNd neurons during reorganization of retinogeniculate connections. *J Neurosci* 1994; 14: 2089-97
- Rampil IJ. Anesthetic potency is not altered after hypothermic spinal cord transection in rats. *Anesthesiology* 1994; 80: 606-10
- Rampil IJ, Laster MJ. No correlation between quantitative electroencephalographic measurements and movement response to noxious stimuli during isoflurane anesthesia in rats. *Anesthesiology* 1992; 77: 920-5
- Rampil IJ, Mason P, Singh H. Anesthetic potency (MAC) is independent of forebrain structures in the rat. *Anesthesiology* 1993; 78: 707-12
- Ransom CB, Sontheimer H. Biophysical and pharmacological characterization of inwardly rectifying K<sup>+</sup> currents in rat spinal cord astrocytes. *J Neurophysiol* 1995; 73: 333-46

- Rehberg B, Xiao Y-H, Duch DS. Central nervous system sodium channels are significantly suppressed at clinical concentrations of volatile anesthetics. *Anesthesiology* 1996; 84: 1223-33
- Reichelt W, Pannicke T. Voltage-dependent K<sup>+</sup> currents in guinea pig Muller (glia) cells show different sensitivities to blockade by Ba<sup>2+</sup>. *Neurosci Lett* 1993; 155: 15-8
- Rhines R, Magoun HW. Brain stem facilitation of cortical motor response. *J Neurophysiol* 1946; 9: 219-29
- Ries CR, Sutter FM, Sutter MC. Drugs used in surgery. In: Page CP, Curtis MJ, Sutter MC, Walker MJA, Hoffman BB (Eds). *Integrated pharmacology*. London: Mosby International 1997; 399-410
- Ries CR, Puil E. Isoflurane prevents transitions to tonic and burst firing modes in thalamic neurons. *Neurosci Lett* 1993; 159: 91-4
- Ries CR, Scoates PJ, Puil E. Opisthotonos following propofol: a nonepileptic perspective and treatment strategy. *Can J Anaesth* 1994; 41: 414-9
- Russell IF. Midazolam-alfentanil: an anaesthetic? an investigation using the isolated forearm technique. *Br J Anaesth* 1993; 70: 42-6
- Schwender D, Kaiser A, Klasing KP, Pöppel E. Midlatency auditory evoked potentials and explicit and implicit memory in patients undergoing cardiac surgery. *Anesthesiology* 1994; 80: 493-501
- Schwender D, Klasing S, Madler C, Pöppel E, Peter K. Midlatency auditory evoked potentials and cognitive function during general anesthesia. *International anesthesiology clinics* 1993; 31: 89-106
- Schwender D, Madler C, Klasing S, Pöppel E, Peter K. Mid-latency auditory evoked potentials and wakefulness during caesarean section. *Eur J Anaesthesiol* 1995; 12: 171-9
- Scurr C, Feldman S. *Scientific foundations of anaesthesia*. Chicago: Year Book Medical Publishers, Inc. 1982; 544-57
- Shafer A. Metaphor and anesthesia. *Anesthesiology* 1995; 83: 1331-42
- Sherman SM. Dual response modes in lateral geniculate neurons: mechanisms and functions. *Vis Neurosci* 1996; 13: 205-13
- Sillito AM, Jones HE, Gerstein GL, West DC. Feature-linked synchronization of thalamic relay cell firing induced by feedback from the visual cortex. *Nature* 1994; 369: 479-82
- Singer W. Synchronization of cortical activity and its putative role in information processing and learning. *Annu Rev Physiol* 1993; 55: 349-74
- Singer W. A new job for the thalamus. *Nature* 1994; 369: 444-5

- Snead OC 3rd. Basic mechanisms of generalized absence seizures. *Ann Neurol* 1995; 37: 146-57
- Spruston N, Jaffe DB, Johnston D. Dendritic attenuation of synaptic potentials and currents: the role of passive membrane properties. *Trends Neurosci* 1994; 17: 161-6
- Spruston N, Jaffe DB, Williams SH, Johnston D. Voltage- and space-clamp errors associated with measurement of electrotonically remote synaptic events. *J Neurophysiol* 1993; 70: 781-02
- Stanski DR, Shafer SL. Quantifying anesthetic drug interaction: implications for drug dosing. *Anesthesiology* 1995; 83: 1-5
- Stark JA. Electroencephalogram and evoked potential analysis: a model-based approach. *International anesthesiology clinics* 1993; 31: 121-41
- Staley KJ, Soldo BL, Proctor WR. Ionic mechanisms of neuronal excitation by inhibitory GABA<sub>A</sub> receptors. *Science* 1995; 269: 977-81
- Steriade M. Central core modulation of spontaneous oscillations and sensory transmission in thalamocortical systems. *Curr Opin Neurobiol* 1993; 3: 619-25
- Steriade M, Amzica F, Contreras D. Cortical and thalamic cellular correlates of electroencephalographic burst-suppression. *Electroencephalogr Clin Neurophysiol* 1994; 90: 1-16
- Steriade M, Amzica F, Contreras D. Synchronization of fast (30-40 Hz) spontaneous cortical rhythms during brain activation. *J Neurosci* 1996; 16: 392-417
- Steriade M, Contreras D, Amzica F. Synchronized sleep oscillations and their paroxysmal developments. *Trends Neurosci* 1994; 17: 199-208
- Steriade M, Curró Dossi R, Contreras D. Electrophysiological properties of intralaminar thalamocortical cells discharging rhythmic (~40 Hz) spike-bursts at ~1000 Hz during waking and rapid eye movement sleep. *Neuroscience* 1993; 56: 1-9
- Steriade M, McCormick DA, Sejnowski TJ. Thalamocortical oscillations in the sleeping and aroused brain. *Science* 1993; 262: 679-85
- Stevens DR, Cotman CW. Excitatory actions of tetrahydro-9-aminoacridine (THA) on hippocampal pyramidal neurons. *Neurosci Lett* 1987; 79: 301-5
- Study RE. Isoflurane inhibits multiple voltage-gated calcium currents in hippocampal pyramidal neurons. *Anesthesiology* 1994; 81: 104-16
- Sugiyama K, Muteki T, Shimoji K. Halothane-induced hyperpolarization and depression of postsynaptic potentials of guinea pig thalamic neurons *in vitro*. *Brain Res* 1992; 576: 97-103
- Sutor B, Hablitz JJ. Influence of barium on rectification in rat neocortical neurons. *Neurosci*

Lett 1993 ; 157: 62-6

Sykes TCF, Thomson AM. Sodium pentobarbitone enhances responses of thalamic relay neurones to GABA in rat brain slices. *Br J Pharmacol* 1989; 97: 1059-66

Takenoshita M, Steinbach JH. Halothane blocks low-voltage-activated calcium current in rat sensory neurons. *J Neurosci* 1991; 11: 1404-12

Tennigkeit F, Ries CR, Schwarz DWF, Puil E. Isoflurane attenuates resonant responses of auditory thalamic neurons. *J Neurophysiol* (in press)

Tennigkeit F, Schwarz DWF, Puil E. Mechanisms for signal transformation in lemniscal auditory thalamus. *J Neurophysiol* 1996; 76: 3597-608

Thompson SM, Masukawa LM, Prince DA. Temperature dependence of intrinsic membrane properties and synaptic potentials in hippocampal CA1 neurons *in vitro*. *J Neurosci* 1985; 5: 817-24

Todd MM, Weeks JB, Warner DS. A focal cryogenic brain lesion does not reduce the minimum alveolar concentration for halothane in rats. *Anesthesiology* 1993; 79: 139-43

Tokimasa T, Sugiyama K, Akasu T, Muteki T. Volatile-anaesthetics inhibit a cyclic AMP-dependent sodium-potassium current in cultured sensory neurones of bullfrog. *Br J Pharmacol* 1990; 101: 190-2

Tunstall ME. The reduction of amnesic wakefulness during caesarean section. *Anaesthesia* 1979; 34: 316-9

von Krosigk M, Bal T, McCormick DA. Cellular mechanisms of a synchronized oscillation in the thalamus. *Science* 1993; 261: 361-4

Wang ZX, Ryan AF, Woolf NK. Pentobarbital and ketamine alter the pattern of 2-deoxyglucose uptake in the central auditory system of the gerbil. *Hear Res* 1987; 27: 145-55

Williams SR, Turner JP, Anderson CM, Crunelli V. Electrophysiological and morphological properties of interneurons in the rat dorsal lateral geniculate nucleus *in vitro*. *J Physiol (Lond)* 1996; 490: 129-47

Winegar BD, Owen DF, Yost S, Forsayeth JR, Mayeri E. Volatile general anesthetics produce hyperpolarization of *Aplysia* neurons by activation of a discrete population of baseline potassium channels. *Anesthesiology* 1996; 85: 889-900

Winegar BD, Yost CS. Halothane directly activates potassium channels in *Aplysia* neurons. *Anesth Analg* 1997; 84: S567

Winson J. The biology and function of rapid eye movement sleep. *Curr Opin Neurobiol* 1993; 3: 243-8

- Wolfson B, Hetrick WD, Lake CL, Siker ES. Anesthetic indices--further data. *Anesthesiology* 1978; 48:187-90
- Woodbridge PD. Changing concepts concerning depth of anesthesia. *Anesthesiology* 1957; 18: 536-41
- Zhang L, Krnjević K. Whole-cell recording of anoxic effects on hippocampal neurons in slices. *J Neurophysiol* 1993; 69: 118-27
- Zhang L, Valiante TA, Carlen PL. Contribution of the low-threshold T-type calcium current in generating the post-spike depolarizing afterpotential in dentate granule neurons of immature rats. *J Neurophysiol* 1993; 70: 223-31
- Zucker JR. ATP-sensitive potassium channel agonists do not alter MAC for isoflurane in rats. *Anesthesiology* 1992; 76: 560-3
- Zurita P, Villa AEP, de Ribaupierere Y, Rouiller EM. Changes of single unit activity in the cat's auditory thalamus and cortex associated to different anesthetic conditions. *Neurosci Res* 1994; 19: 303-16